Detecting Water Loss Leaks in Large Shallow Reservoirs Using Tracers: Laboratory Experiments

Vukušić, Toni

Supplement / Prilog

Publication year / Godina izdavanja: **2022**

Permanent link / Trajna poveznica: https://urn.nsk.hr/urn:nbn:hr:123:433827

Rights / Prava: In copyright/Zaštićeno autorskim pravom.

Download date / Datum preuzimanja: **2025-03-24**

UNIVERSITY OF SPLIT

dabar
DIGITALNI AKADEMSKI ARHIVI I REPOZITORIJI

SVEUČILIŠTE U SPLITU
FAKULTET GRAĐEVINARSTVA ARHITEKTURE I GEODEZIJE

MASTER THESIS

Toni Vukušić

Split, 2022.

SVEUČILIŠTE U SPLITU
FAKULTET GRAĐEVINARSTVA, ARHITEKTURE I GEODEZIJE

Toni Vukušić

Detecting water loss leaks in large shallow reservoirs using tracers: laboratory experiment

Acad. year: 2021./2022.
Student: Toni Vukušić

Registo de Tema de Dissertação de Mestrado

Mestrado em Engenharia Civil (MEC) Ano Letivo _2021/2022 Semestre _2º

Nome do Aluno: Toni Vukusic Nº 2021263701

Email: tonivukusic998@gmail.com Telefone: +385 99 335 7776

Título da Dissertação: **Detecting water loss leaks in large shallow reservoirs using tracers: laboratory experiments**

Orientador: Prof. Dr. João L.M. Pedroso de Lima Instituição: UC/MARE Assinatura:

Orientador: Prof. Dr. Isabel Pedroso de Lima Instituição: UC/MARE Assinatura:

Resumo (300 palavras)

Sustainable water management demands that losses are reduced. However, although the problem of water losses is found in many situations, their nature often makes the identification of losses a difficult task. In large reservoirs water losses are mostly from evaporation, percolation on bottom and ditches and underground leaks. To reduce those losses we need leak detection techniques.

The main objective of this dissertation is to explore techniques for the estimation of the location of possible water loss sinks in large shallow reservoirs using tracers, using physical laboratory scale model.

The study will be based on laboratory experiments conducted at the Laboratory of Hydraulics, Water Resources and Environment of the University of Coimbra (Portugal). The experimental set-up includes a squared soil flume (2×2 m2) with a horizontal soil surface. The soil placed in the flume will be of very low permeability. After flooding the flume (simulating a large shallow reservoir), sinks will be created in the physical model. The following tracers will be tested: thermal, dye and fluorescent. Various sink locations should be studied, for various hydraulic conditions (e.g., discharge, depth, tracer volume).

Parecer do Coordenador da Área Científica DEC ☐ / Representante do Departamento ☐

Favorável ☐ Desfavorável ☐ Assinatura _____

Justificação (em caso de parecer desfavorável)

Parecer do Coordenador do Mestrado

Favorável ☐ Desfavorável ☐ Assinatura _____

Justificação (em caso de parecer desfavorável)

Assinatura do aluno _____ Data 12/03/2022

Erasmus+

University of Split
International Relations Office
Erasmus coordinator
Ruđera Boškovića 31
21000 Split

Letter of Confirmation

This is to confirm that student **Toni Vukušić** from the **University of Split** spent 5 months at

the University of Coimbra, Faculty of Science and Technology, Department of Civil

Engineering, within the framework of the Erasmus + Programme, for the purpose of research

for his Master thesis entitled: *Detecting water loss leaks in large shallow reservoirs using*

tracers: laboratory experiments. He conducted all the experimental work proposed and

treated and analysed the laboratory data resulting in a compreensive draft version of his

master thesis. He performed the experiments together with a Ph.D student (Soheil Zehsaz).

This Letter must be signed and notarized either by host Professor/Mentor, Dean, or Erasmus coordinator of the abovementioned Institution and serves as proof of fulfilled obligations stated in the Learning agreement.

Prof. Dr. João Pedroso de Lima   Prof. Dr. M. Isabel Pedroso de Lima

Full Professor   Assistant Professor

Coimbra, 19/07/2022

Stamp of the Institution:

Faculdade de Ciências e Tecnologia
UNIVERSIDADE DE COIMBRA
Depart.º de Engenharia Civil
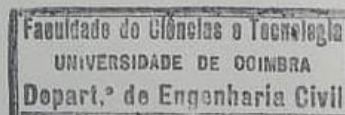
SVEUČILIŠTE U SPLITU

FAKULTET GRAĐEVINARSTVA, ARHITEKTURE I GEODEZIJE

Split, Matice hrvatske 15

STUDIJ: DIPLOMSKI SVEUČILIŠNI STUDIJ GRAĐEVINARSTVA

KANDIDAT: Toni Vukušić

BROJ INDEKSA: 0083215042

KATEDRA: Katedra za gospodarenje vodama i zaštita voda

PREDMET: Hidrotehnički sustavi

ZADATAK ZA DIPLOMSKI RAD

Tema: Detekcija točaka gubitka vode u velikim plitkim rezervoarima korištenjem trasera: laboratorijski eksperimenti

Opis zadatka: Održivo upravljanje vodom zahtijeva da se gubici vode reduciraju. Međutim, iako se problem gubitka vode pojavljuje u mnogim situacijama, zbog njihove prirode često identifikacija samih gubitaka predstavlja zahtjevan pothvat. U velikim rezervoarima gubitci vode uglavnom potječu od isparavanja, procjeđivanja na dnu i jarcima, te podzemnog curenja. Da bismo reducirali te gubitke, potrebne su nam tehnike detektiranja curenja. Glavni cilj ovoga diplomskog rada je istražiti tehnike za procjenu mogućeg mjesta gubitka vode u velikim plitkim rezervoarima koristeći trasere i fizički model na laboratorijskoj skali. Studija će se temeljiti na laboratorijskim eksperimentima provedenim u Laboratoriju Hidraulike, Vodenih Resursa i Okoliša, Sveučilišta Coimbra (Portugal). Eksperimentalna postava uključuje kvadratni zemljani žlijeb(2×2 m^2) s vodoravnom površinom tla. Tlo smješteno u kvadratni žlijeb, imat će vrlo nisku propusnost. Nakon poplave zemljanog žlijeba (simulirajući veliki plitki rezervoar), drenažne točke će se iskopati u fizičkom modelu. Ispitat će se sljedeći traseri: termalni, obojeni i fluorescentni. Različite lokacije drenažnih točaka trebaju se proučiti, za različite hidrauličke uvjete (npr. protok istjecanja, dubinu, volumen trasera).

U Splitu, 20. rujna, 2022.

Voditelj diplomskog rada: Predsjednik povjerenstva za završne i
                                              diplomske ispite:

Doc. dr. sc. Katarina Rogulj   Izv. prof. dr.sc. Ivo Andrić

Detekcija točaka gubitka vode u velikim plitkim rezervoarima korištenjem trasera: laboratorijski eksperimenti

Sažetak: *Prioritet ovog rada je evaluacija metoda praćenja koje se koriste u svrhu otkrivanja točke propusnosti u plitkim rezervoarima vode. Gubitak vode koji se pokazuje na velikoj prostornoj razini kroz istjecanje, curenje ili duboku perkolaciju, treba istražiti simulacijom okoliša i uvjeta koji dovode do toga. U opisu procesa i tehnika praćenja uključenih u eksperiment korištena je literatura o metodologijama i strujanju plitkih voda od raznih autora značajnih za naš rad. Fizikalni model postavljen je u laboratoriju, a sastoji se od sustava za unos vode i zemljanog kanala s površinom od 2x2 m. Ciljevi obuhvaćaju kvalitativnu i kvantitativnu procjenu plitkog toka površinske vode i kretanja trasera prema točki propusnosti, kao rezultat korištenja određene tehnike praćenja. S obzirom na ciljeve, eksperimentalni postupak je podijeljen na fazu navodnjavanja i detekciju. Konstantno ravnomjerno pražnjenje korišteno je za pretapanje kanala, za rekonstrukciju prirodnih uvjeta plitkog protoka, a dvostruki traser toplinske boje ubrizgan je kroz čaše za procjenu brzina protoka. Definirana su i modificirana tri parametra za način istraživanja detekcije točke propusnosti kroz više eksperimentalnih pokusa. Toplinski traser odabran je kao predstavnik za sve pokuse zbog raspoložive opreme i kvalitete slike. Rezultati prikupljeni eksperimentalnom analizom pomogli su u raspravi o prednostima i slabostima ove vrste eksperimentalnog pristupa. U slučaju poplave, empirijski podaci poslužili su kao sredstvo za istraživanje kretanja plitke vode preko gole površine koja služi kao pozadina za tehnike praćenja. Uspoređeni su različiti rezultati detekcije točke propusnosti, a najpovoljniji i najnepovoljniji rezultati uzeti su kao reprezentativni za termalnu tehniku praćenja*

Ključne riječi: *plitki, traser, tehnika praćenja, detekcija, točka propusnosti*

Detecting water loss leaks in large shallow reservoirs using tracers: laboratory experiments

Abstract: *This work is prioritized on evaluating tracer methods that are used for the purpose of detecting the drainage point in shallow water reservoirs. Water loss exhibited on a large spatial scale through leakage, seepage, or deep percolation, needs to be researched by simulating the environment and conditions that lead up to it. Literature on methodologies and shallow water flow from various authors significant to our work was used in the description of the processes and tracing techniques involved in our experiment. A physical-based model was set up in a laboratory setting, consisting of a water input system and a soil flume with a 2x2 m area space. Objectives comprise a qualitative and quantitative evaluation of the shallow surface water flow and tracer movement towards the sink point, as a result of using an appointed tracing technique. In regards to the goals, the experimental proceeding was divided into the flooding and detection phases. A constant steady discharge was used to flood the flume, for the reenactment of natural shallow flow conditions, and a dual thermal-dye tracer was injected through cups for estimating flow velocities. Three parameters were defined and modified, for the means of investigating the detection of the sink point, through multiple experimental trials. Thermal tracer was chosen as a representative for all of the experiments due to the available equipment and image quality. Results gathered from the experimental analysis helped discuss the merits and weaknesses of this kind of experimental approach. In the case of flooding, the empirical data served as a means to investigate the shallow water movement across the barren surface that serves as a background for tracer techniques. Various results from the detection of the sink point were compared, and the most favorable and unfavorable results were taken as representative of the thermal tracing technique*

Keywords: *shallow water, tracer, tracing technique, detection, sink point*

INDEX

1. INTRODUCTION

1.1. Framework and motivation

In the context of spatial water distribution, there is one factor that can't be overlooked, whether we are talking about agriculturally cultivated flood areas or artificially confined water bodies, water loss presents a threat to long-lasting water management and sustainability Governing bodies are in constant motion of gaining more knowledge on water audits and implementing loss control programs (e.g improving water holding capacity, leak assessment, discourage plant growth, flow conditioning), to preserve the biogeochemical cycle which is in correlation with the hydrological system. On a global scale, water losses vary by spatial and temporal conditions, although the main types that influence the hydraulic hemisphere can be observed through the outdoor water retention systems[2,3,15,16]. Water loss in its conservative form(be it leaks, spills, or runoff) presents a barrier in the field of hydrology, hence we can deduce that stable shallow water flow presents a way of observing this problem closer. Usually, in enclosed structures, there are set measures to detect any damages, from which water may flow out, though, in soils, the places of larger water absorption are more difficult to estimate. As such it is vital to understand the input and output of the system that makes water-based transport processes possible in the rural setting. Staying ahead and observing the natural phenomena within our hydrological cycle will help us in detecting the patterns from which we can allocate deterrents for countering our problems. The narrative that we will be discussing through this work, deals with laminar water flow and comprehending its way of movement among the surface and partly sub-surface areas, for the sake of water loss investigation. Digitalization has made it easier to assess the situation of water movement by simulating the system and forces that contributed to the observing predicament, so a proper solution can be found. [2,3,4,6]

Sustainability is a general postulate in many fields of work, and so water management, holds it mandatory, to uphold all the necessary rules and regulations, which lead to a productive managing practice (evaluate all the parameters, because the performances under which a system operates are relative through time). The amount of water that escapes its designated position in our naturally or artificially segregated environment, has an adverse impact on the economical sphere and water balance (the law of water balance) [9,32]. One of the most concerning topics, that holds the scientific community's interest, is how to decrease water scarcity during this day and age, where accountability is being placed on monitoring(so we have a sufficient to cover all consumption areas). It is an engineering accountability to detect and restore, any areas that could provide long-term repercussions on sustainability and finance. In that sense, we have to gather knowledge about constant water outflow and the behavior exhibited in uncontrolled water environments. The notion of knowing how much of the water volume is lost as a product of evaporation, runoff, deep percolation, seepage, and leakage due to inefficiency in construction or terrain permeability, etc., depends mainly on the accuracy of measuring equipment and quality of data that we are working with. By that statement, it is in the interest of the whole world to find new methods of detecting(that don't affect the environment), points of drainage, so that we can develop our knowledge and optimize our approach. We can deduce a lot of different scenarios that

can forgo water depletion and on that basis, we can do equivalent experimental work in combination with numerical modeling. [9,14,16,17,].

Generally, we are working with low velocities that occur in the spatial setting that we will be observing through this work. Particle tracking and imaging will be needed in the experimental proceedings, so that we can extract adequate data, for further statistical treatment. Proper investigation using leak detection techniques rests on the knowledge of overland flow distribution and hydrological processes. More precisely we need to have insight into surface flow velocities and discharge rates so that we can form adequate hydrodynamic models and mathematical equations representing the spatial nonuniformity of water courses [1,7,24,61]. Flow tracing techniques play an integral role in the detection and visualization of flow velocities and transport processes; for example, the usage of artificial tracers to measure runoff volume. Tracers give us an insight into the dynamics and phase changes of activities that occur in nature (surface water–groundwater interactions, paleohydrology, water movement in very low permeable rock compositions, calibrating and validating numerical flow and transport models), by the method of point injecting tracers at different time intervals along the flooded surface. A noticeable distinction lies among the tracer practices which are dependent on the time and space variable, and that is the concentration, and runoff volume of the diluted medium. In the investigation of sink point water loss, we will be dealing with shallow water surface runoff, along which we will be using a variety of different tracers, such as dye, fluorescent and thermal tracers[7,37,60,68]. Whether we are talking about evaporation, absorption, or seepage, every loss of water has to be attended to, so it doesn't affect the procured volume and future use. All of the mentioned processes can be observed in large reservoirs, differing in displacement and size. Due to the fine nature of water coursing at the bottom, we have to recreate these scenarios through laboratory proceedings. For that need, we will be testing tracers in shallow overland flows, under varying conditions that represent real possibilities. So that at the end we could compare the results of each test and determine the relevant arrangement[7,14,18]

1.2. Objectives

This work is aimed at studying the shallow overland water flow, more precisely its movement towards the sink point. For that need, we will put together a flume with experimental equipment for testing as well as implementing a tracking methodology.

The experiment will be held in the Department of Civil Engineering, Sciences, and Technologies, University of Coimbra (DEC/FTUC). In our experimental proceeding, we used a variation of 3 different tracer samples, under specified hydraulic and geological conditions, to investigate the trajectory of the tracing material towards the sinking point in the testing area. Objectives comprise:

(i)   collecting information on previous studies relating to the topic of assessment

(ii)   examining the qualitative feature of the waterfront movement through real-time
         images, as well as determining shallow surface flow velocities and area of spread

(iii)   to try out the most suitable tracing techniques for the detection of the seepage point by changing up the parameters(discharge rate, tracer type, material for sink hole, sink point displacement) under which the experiment is being carried out

(iv)   to compare the results presented in statistical and graphic form, then underline the most optimal approach.

1.3. Structure of the thesis

The reviewing dissertation that is under elaboration is divided into 5 chapters:

Chapter 1 – this segment describes the basis of our work through an introduction review, as well as the idea, motivation, and objectives that will be explored
Chapter 2- this segment encompasses the bibliographical review of the scenery that exhibits water loss, the impacts of such kind of a problem, and techniques to detect water movement
Chapter 3- this segment entails the methodology and laboratory setup, for the experimental proceeding
Chapter 4- this segment consists of statistical comparisons of the given results, through graphs, charts, and tables
Chapter 5- this segment surmises the conclusions around the analyzed results and gives suggestions for improvements
Chapter 6- Literature

2. BIBLIOGRAPHIC REVIEW

This chapter gives us an insight into the background of the importance of water conservation, the characteristics behind laminar water movement, and techniques for detecting water loss in a natural and artificial water encasement. It is important to know different views of understanding water loss so we can have a firm grasp on the experimental procedure and analysis of the problem.

2.1. Sustainable water management

Water as a basis of day-to-day life has a role in many different ways, such as existential and hygienical needs in daily foregoing and industrial development, hydropower generation, navigation, and ecosystem conservation. In that sense, it is important to distinguish that all water bodies can be conceptualized and investigated through studies in 3 major fields: hydrology, physical chemistry, and biology. As the human population keeps growing, the demand for larger freshwater quantities and proper water management becomes a priority. The elimination of the policy 'use and discard becomes switched with the norm of sustainable management of resources. Concerning to the previous statement scientists, today have to deal with the pressing issue of food shortage due to the increase of the population as well as the impacts of climate change. In that sense water for irrigation becomes a staple in using the right amount of water at the right time and place, which is essential for the ecosystem and ecology. A lot of funding has been invested to promote water conservation in irrigated agriculture, knowing it carries heavy political weight because the outcomes of water conservation programs oftentimes don't present sufficient results. In the agricultural domain, irrigation systems provide a surface conveyance mechanism with a focus on maximization of farm profit or water productivity, and minimization of waterlogging, groundwater depletion, or transpiration[10,11,12,16].

The terminology changes in the case of reservoirs with the present large storage of water used for multitudes of purposes like storage of drinking and irrigation water, recreation, flood protection, navigation, and hydropower production. For those needs, it is important to manage demands and interests, in a way where we take in the negative and positive aspects conceived on a local, regional and global scale and surmise them through a management framework, so we can easily mitigate negative impacts and make demands more accessible through systematization. This prospect is explained through the concept of Sustainable Development which has been on the discussion board for over a decade. It is defined as "development that meets the needs of the present without compromising the ability of the future generations to meet their own needs" (by the World Commission on Environment and Development). For the water-based development projects, the concept of sustainable development includes determination and planning of the demands for the water through the project region, rational water use, participation of the stakeholders, equitable development for human development, achievement of the environmental and social protection by a sensible economic growth, comprehensive observation and assessment, effective supervision and provision of the necessary conditions for the protection of water-related structures. Sustainable development ensures the stable improvement of the state in which water management is being conducted by facilitating the many needs that need to be reached, in the proper function of the hydrological system. In sustainability lies the balance of the three main legs: economic, social, and environmental by which all acts in the observed hydrological system all facilitated[9,15,18].

To have a firmer grasp of sustainable water management and its practices, we have to count on all the associated impacts that are presented on a global scale. One thing that needs to be recognized is that any adjustments made to the water cycle will leave large and complex effects

on the ecological and economic system because natural ecosystems have accepted the phenomenons and changes that shape that domain. A holistic approach is needed in managing resources due to the negative implications that arise from utilization, like technical, legal, and environmental, to social values, norms, and habits. Also, many countries struggle with water supplies needed to satisfy their urban, environmental, and agricultural needs. Unproductive water uses, including evaporation, runoff, weed growth, and deep percolation are the main perpetrators of reducing budget when talking about water supply. In regards to those consequences, engineers and operators need to be aware of the spatial and technical troubles, that may come up over time, so our project can adhere to the overall sustainable frame. The challenge of the sustainability practice becomes growing out of old habits that leave an adverse mark on water conservation, structural durability, irrigation effectiveness, and ecological compliance. Loss percentage accumulates itself through a variety of contexts, starting from the effects of natural processes to the inadequate maintenance of structural encasements. For example, declination of the water quality in a certain maintained area does not only affect the economic substrate but the environmental balance of the aquatic life in its proximity. Social parameters are usually the decisive ones that shape the political sphere around conclusions and implementations incorporated in the development and treatment stages. Social impacts of reservoirs are segmented, based on the processes that happen inside and around them, connected to the land use, the social fabric, and the governance. Technical flaws in the case of inadequate discharge requirements and pass-through mechanisms can leave a negative ecological impact. Impacts on the agricultural domain can be seen through the growing water scarcity momentum that affects the industrial and economical lifeline, and in regards to that, it needs to be rehabilitated. Equal distribution of water in agricultural practices, with a focus on retaining the necessary volume, will lead to a decrease in net losses and management development[4,17,32].

2.1.1. Artificial and natural water bodies

Certain creations during human history have revolutionized the domain of Science, Technology, and Mathematics, but the most prevalent invention in civil engineering history is the first wall ever built. They have served a multitude of purposes from support, enclosure, and shelter but mainly for separation and conservation. Also, they serve as a vital aspect that determines water confinement practices and enables the sustainable functioning of water dependent structures. Apart from man-made structures, there are examples in nature that have resulted in certain areas capturing volumes of water and retaining them, due to the topographic position and geological formation. Agricultural workers have relied on using open spaces to help them with crop management, so through excavation and dilatations, they created canal routes for water distribution. Ideas such as rectangular prisms have evolved out of water retaining practices, as well as higher development in dam structures for water flow regulation. From a technological perspective, all these operations are working on keeping the basin water storage at its original level, through different means[11,18,64].

Natural catchments

Wetlands represent a natural display of a flooded area permanently or seasonally, which include coastal lowlands, topographic depressions, broad flats on instream divides, the base of slopes, and topographic highs with little slope. All of these landscapes make for good observation of surface flows of water, due to the fact that location influences geological characteristics such as; slope, thickness, and permeability of soils; and the composition, stratigraphy, and hydraulic properties of the underlying strata. Waterways, groundwater, soil, and lakes are common water

capacity supplies, and their levels can alter quickly in reaction to human and natural variables. For that reason accessibility of water resources presents an important matter mostly in water supply and irrigation schemes. The 3 factors that influence the accessibility of water: are (i) request; (ii) climate designs; and (iii) quality[1,9,22].

Ditches and ponds

Ditches and ponds represent natural depressions, made from human activity with the purpose of detaining water. Water gathered in these confinements is usually brought through storm rain runoff and, excessive saturation of the top layer of soil due to the rise in groundwater level. Both nature storage elements can be used in the practices of water diversion when it is necessary to have a fixed holding unit, to regulate the peak discharge of water during flood events, that may obstruct the river system. Ponds can vary dependent on their size and not always be fit for storing water, but they are still considered hydrological modifications. Their use is determined by their size and position, for maintenance or management, and they are usually detention-based storage units[9,16]. Ditches uphold the role of drainage in the process of intaking any excess water runoff by minimizing turbulence and diffusing dead areas. Ditches in conjunction with detention basins can be used for roadside or urban collection system improvement. When designing an urban system, through the approximation of the drainage area we can determine the runoff patterns. And for that,s ake we use ditches and detention basins that keep the peak discharge contained at predetermined conditions. On a watershed scale, basins can contribute to the increase in water flow velocity, by which the damaging erosive energy exerting forces increase their presence in the downstream network[5,9,14].

Floodplain

Floodplains are the longest stretch of wetland that we can be observed in a usually riparian setting, consisting of the main channel of rivers and streams that are surrounded by geologically formed plains. Preserving the ecosystems of this kind in a healthy and pure matter encapsulates the importance of the natural system, because of the co-dependency of all of the elements in the system. As we already know wetlands in general are preserved by precipitation events, springs, or floodplain flow. Floodplains make a crucial role in maintaining the stability of the stream by achieving low-velocity flow and providing sediment deposits for the land around the stream. Drainage design in the early days consisted of floodplains, steams, and natural channels, which relied on surface runoff. The undeveloped watershed provides the perfect background for creating stream channels through runoff events over geological time. This fluvial landscape provides a multitude of uses and has an immediate part in the hydrological cycle. In case of large precipitation events and consequently runoff, incisions are created on the surface of the natural environment, this isn't the case when there is an even distribution of sediments across the area during rainfall. An increase in the impervious surface is a qualifying factor that influences hydrological response characteristics of the watershed unit, causing erosion and lowering aquatic health[1,5,22].

Lake

Lake is a part of a natural system, usually characterized as a basin, whose water level is dependent on the natural flow regime. Conventional sources of fresh water can be found in lakes, as natural water storage reservoirs, where human and environmental factors contribute to the shift in water level. Depending on its size it can serve as a part of the stream or be governed by it through the condition of its: size, location, and position in relation to the stream network.

Lakes have undismissive ecological importance, which is why we have to eliminate the threats like eutrophication and choking by algae to preserve them in a sustainable sense. In relation to streams, these catchment sites experience low velocities, significant temperature stratification towards the bottom, turnover regime cycles and alternation in regards to seasons, winds, and other forces. Water storage of this unit has an environmental cost on natural flows and altering stream corridors through a change in water flow, water quality, and alternation in habitat. Irrigation practices throughout the years have mostly depleted the resources that these confinements have to offer. That in combination with the annual losses can administer a problem on the regional scale if the balance of inflow and outflow is not maintained[1,9,23,14].

Irrigation fields

Irrigation processes depend on extracting water from a reservoir or underground well and distributing it across a given area of land. There is a mechanism behind the action of flooding, during which the operator controls the outflow of the water. Water moves, usually directed from a higher elevation in regards to the field, and when flooded the water volume decreases during the coming days, because of the drying and infiltration. Regarding irrigation techniques, these two are nonindependent around the world.

Bassin irrigation as a simple form of surface irrigation consists of flooding an area constructed of basins in a grid formation, in which the water is accumulated and slowly infiltrates the soil. The main channel for irrigation is placed in one direction and together with permanent or seasonal bunds on each side, they outline each sunken basin area. The shape and size of the basin is determined by the land slope, soil type, available stream, required depth of irrigation, and farming practices. Basins can be round, square, and aligned across the contour, with a constant zero radian angle. One of the attributes of this type of irrigation system is that it produces high uniformity across the area since it reduces runoff. In the case of the 'closed basin' water is driven into an individual basin and the whole volume is allowed to infiltrate. In contrast 'sequential basins' are irrigated separately by a supply channel, which lets out water onto adjacent basins and is regulated by the water level elevation[8,11,12,16]. Furrow irrigation is a kind of surface irrigation that involves flooding a series of narrow channels, that has the role of simultaneously transporting and infiltrating water into the ground. The usual depth of furrows is between 20-30 cm and the water coursing through the channel doesn't exceed two-thirds of its depth. Depending on the soil and the adjustment of the slope we may have long or short furrows, and on the front side of the channel, we have the main pipe for water discharge. One of the characteristics of this kind of irrigation is that we get 'downfield' disuniformity (which is inherent) and 'inter-row' diss-uniformity which is a consequence of the infiltration capabilities of the soil. Management of furrow plays a big role in the efficiency of its use, as well as the density of the soil, where very clayey and sandy soils are favorable[16,49].

Artificial structures

Impoundment structures contributed greatly to water conveyance and storage disciplines, so the occurring theme is furthering its utilization in the natural system. Whether we are draining an existing water body, stopping the flow of the stream with embankments, or harvesting rainwater, data of the observed area needs to be collected. That entails physical data through topographical displays and geological examinations, hydrological dana extracted through collective sources, and also photographic records that determine the conditions for the engineering work. Industrial water supply, flood control, and reservoir design represent interventions in the natural system which are derived from the need to allocate water resources

to maintain quality and quantity. There should be a clear distinction between the type of structure we are using in the project area. Wheater we are working with temporary structures that require inexpensive labor and material for e.g. modification, or permanent structures that require hard materials for dissipating energy and endurance[1,14,19].

Reservoirs

Water reservoirs play an integral role in our society through the storage of water, flood protection, establishment of an aquatic environment, and conversion of water properties. For these undertakings either a wall is created across a valley or stream, or depression is made through excavation work, and it is described best through 3 parameters: (i)volume (ii)inundated area (iii) spread of the water oscillations. It is through the process of backing upstream flow, supplying from an external source, and collecting runoff or rainwater that we get water storage units. The use of water that these structures provide is versatile, like for irrigation, domestic, and hydropower purposes, so any damages, that can cause the decrease in the water level must be dealt with immediately[13,18,19].

Artificial reservoirs are independent of nature in the sense that they can change the flow of the stream or preserve water for productive use, by controlling the natural flow regime.

Nature and the reservoirs are in a codependent relationship that is administered in the qualitative and quantitative aspects of water, for example, how can reservoir water influence the quality downstream of the dam, and how human activities affect different properties of water in a reservoir. The construction of dams or reservoir leaves negative consequences in the catchment, such as a shift in flow and sediment regime and an increase of nutrients containing harmful chemicals. If there is only one reservoir in the system 'water storage unit and consumer' then it is an independent unit, but it can also be a part of a system of reservoirs, which have a mutual cooperative function. Hydraulic structures distinguish themselves by their inlet, conduit and outlet, as well as wall or steel formations surrounding the encasement, so by that notion, we can have different structural types of reservoirs, like bank-side reservoirs, detention reservoirs or service reservoirs. There is a variety of purposes for a reservoir among which the following are most applied:

1)active storage reservoirs that help overcome the dependency on natural sources during droughts

2)flood control reservoirs that function through bank-full discharge or increase in acceptable volume to hold the water surplus

3)impounding reservoirs which are placed on streams, usually serve to satisfy water supply demands and for flood protection

4)conservation reservoirs are meant to be used to withdraw water for irrigation, industrial, agricultural and domestic purposes as well as power generation and maintenance. [9,11,15,19]

Water storage tank

Water tanks are storage facilities that are used for short-term water discharges in excess rates, which is drawn from natural resources. They can be situated in the ground, elevated, or on the surface, with a built-in pump system, and are mostly used for irrigation and domestic activities. Different materials can be used for the construction of these storage tanks depending on the nature of their application. These units have to be regulated daily on their release power because they have a periodically repeating cycle that lasts one day. Parameters of the water tank, such as storage space, are determined on the basis of demand from the public and yield from the water resources[16,19]. Among different practices, storage tanks are vital for rainwater harvesting for the purpose of irrigation. They are a very costly investment, but carry a large

benefit from an environmental point of view, because of the large set of energy and life cycle impacts. Water that will be collected depends on the size of the tank, which is influenced by the rain capacity and daily demand for outflow, so a maximum increase has to be determined. Each periodical controlled release of water makes room for the coming storm event which will fill the capacity of the tank, so in that sense, it is recommended to pick the optimal size of the tank through economic and environmental benefits. Materials used for the tank, play a part in the water quality, where cement serves well for neutralizing acidity, but mostly used materials are polyethylene and fiberglass[17,19,70]

Water holding capacity

The existing concern that surrounds most agricultural projects is 'how to deal with physical and biological soil degradation, during shifting climate periods'. Because during most conventional agricultural practices, the soil is not regenerated so it degrades in health during ongoing crop-yielding periods. A large number of soils are heterogeneous and anisotropic and they act as dynamic storage for water, continued through the intake of rainwater and irrigation water, so it could be used for plant growth. Furthermore, there are two parameters that could leave a negative impact on the vertically and laterally uniform widespread soil parameters (even in well-defined soil layers), which are: the amount of pore compared to solid particles and hydraulic conductivity. Despite that, the aforementioned parameters are bound to decrease with the depth from the soil surface, because of the natural effect of consolidation, which leads to the decrease in permeability. Soil water content is defined as a volume of water contained in a volume of water at any given moment, and in contrast, the maximum amount of water that could be contained is known as water holding capacity[16]. There are different ways to measure soil water capacity, either through soil moisture sensors, time-domain reflectometry probes or if we are lacking equipment through the gravitational method. The SWC index is shown as a relation of wet to dry content
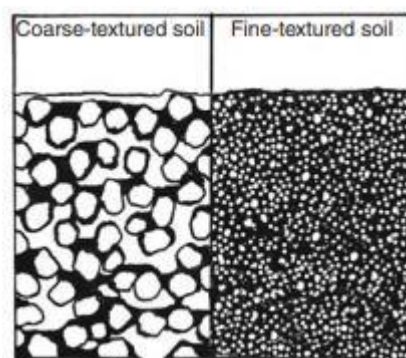
Figure2.1 Water retention in coarse and fine-textured soils (adapted from[16])

$$WHC(\%wt) = \frac{(wet\ sample\ weight - dry\ sample\ weight)}{(dry\ sample\ weight - container\ weight)} x100\%$$

The real value of water holding capacity can be seen through the capability of the soil to preserve water in its pores during natural drainage due to gravity. Of course, the soil has a limit to how much water it can absorb and that is above the water holding capacity, which is mostly characterized by the soil texture and organic matter content. Size, structure, and spread of soil particles speak directly to the amount and size of pores that can accumulate water, so for

reference clay soil will have a bigger volume of smaller pores than the volume of large pores in sandy soils. And with that, it is clear to conclude that larger pores will have increased drainage of water under the infulence of gravity, which decreases their water holding capacity. Organic matter particles increase the water holding capacity of soil because of their affinity to water, and the various shapes and sizes they confrom to. In contrast to that compaction has a negative impact on water holding capacity because it pushes the particles together. Improvement of soil water holding capacity is favorable in cases when we are experiencing a lack of water inputs, which can then bring about resilience through dry spells and reduce water loss to deep percolation and evaporation. The end result is beneficial to the crop yield with more healthier and robust plants and all-around green water storage. So the improvements in soil holding capacity can be achieved by mixing in finer soil particles with organic matter which clumps the particles together providing enough room for pores and lowering compaction, especially around the surface level[16,71].

Residence time of water inside large retention sites

If we are looking at a large aquatic system, the hydraulic residence time is an important parameter by which we can follow different processes contributing to the reduction of quality and quantity of the water volume, for example, eutrophication processes, thermal stratification, isotopic composition, etc. There have been made, numerous experimental studies on measuring the transfer and retention of scalar quantities or water inside a liquid recipient. Considering that the lake size, water source, and watershed are the key segments that define the residence time, we can propose that it's a good tool for defining the structure and external influences on the observed system. Impoundments, small drainage lakes, and lakes with large volumes of groundwater inflow and stream outlets have rapid water exchange rates which contribute to short residence time, the opposite is true for seepage lakes with no surface outlets. For large seepage lakes, average residence time takes many years, and in the case of small impoundments around several days[1,28]. Flood-control reservoirs give a good insight into the fluctuation of water volume retention time. Such impoundments leave sufficient space, that has been predetermined or emptied, for the intake of water during a flood event. And so the flood control effect needs to be properly predicted so that we don't end up with extensive storage capacity, or unbearable discharges for the downstream part of the stream. A good way to mitigate these intakes is by releasing water according to the rule curve which foresees that the storage volume is kept at a reasonable level through spill-out, during a certain period of the year, or by short-term discharge forecasts[19].

This equation indicates the increase and intake mechanism in a reservoir:

$P - O = R$ →inflow-outflow=retention

P>O, R is positive, and the water level increases
P<O ,R is negative and the water level decreases

2.1.2. Water loss control

Although we can observe different kinds of water loss occurrences in a natural setting, or a confined environment, we will be focusing our attention on water depletion which is most pronounced in a static water body. Furthermore, we have to study the hydrological cycle to gain knowledge about water loss prevention, so we can generate an experimental model to help us in solving our problem. Hydraulic systems as well as natural water systems, have always been subject to some form of water loss. Water used for domestic purposes, experiences daily net

loss, because of improper management or unforeseen circumstances. Since the days of the Roman Empire, this problem has been present in water distribution systems but neglected because of existing quantities and no ramifications on the budget. Today governing bodies and International Water Organisation is calling for the mandatory application of water audits and practices to counter the problem of water loss, so as to maintain a level of economic relief[2,4].

Water loss and gains in the hydrological cycle

If we explore the global hydrological cycle, we gain insight on various physical water transformation processes, that can help us better understand the movement of water in different aggregate states and indicate water loss behavior patterns. In regards to that, the system can be divided into three subsystems: the atmospheric water system, containing the processes of precipitation, evaporation, interception, and transpiration; the surface water system containing the processes of overland flow, surface runoff, subsurface and groundwater outflow, and runoff to streams and the ocean; and the subsurface water system containing the processes of infiltration, groundwater recharge, subsurface flow, and groundwater flow[6,16]. The hydrological cycle represents the continuous movement of water above and below the Earth's surface. Water kept on a surface level is depleted through the process of evaporation which consumes the water from open surfaces and transpiration which consumes the water kept in plants and leaves. The accumulated mass of vapor then moves towards the atmosphere, where under the right conditions it creates precipitation events. Water that falls to the ground may be intercepted by solid or liquid terrain, such as latching onto vegetation, falling into surface water bodies, becoming overland flow over the ground surface, infiltrating into the ground, and flow through the soil. A large amount of intercepted water returns to the atmosphere through the already mentioned processes, and the rest percolates deeper into the soil strata. This water can be carried through canals as runoff and emerge in springs or seep through cracks and fissures in the watershed and make its way to the basin, or the sea. Also, another significant factor that influences infiltration, runoff, and evapotranspiration is land cover, since the type, density and uniformity of the vegetation, influence the soil moisture change on a spatial and temporal scale[1,5,6].

Description of the three most significant water loss initiators

Open surface water storage spaces, such as reservoirs, lakes, irrigation fields, etc. make for perfect candidates to explain the core processes which cause water loss.

Evaporation

Evaporation is a process of transforming water from a solid or liquid state to water vapor, which condenses in the atmosphere. This process is the most prevalent water loss that is exhibited in a lake or reservoir. Globally evaporation is the main consumer of precipitation detained on or in land, averaging a total of 60-70% with the remaining percentage serving as runoff across the watershed to the sea. However, it experiences variations due to effects of solar input, location of mountains and proximity to oceans. Arid regions are most susceptible to evaporation due to the increased temperature and humidity. Runoff generation can be decreased due to evaporation reducing the rates of water input in the catchment are, which results in smaller amounts of runoff water. The nature of impoundments makes them retention storage units, that experience long-term interferences of evaporation on the water balance, which hence calls for water resource planning and water supply studies. In the case of surface lakes, water loss is a function

11

of solar radiation, the temperature of the water and air, the difference in vapor pressure between water and the overlying air, and wind speed across the lake. Evaporation is usually measured with a class A pan filled to 8 inches, with a rainfall gauge that can be adjusted and observed daily[1,5,6,14].

Infiltration

The process of water entering the soil profile through the surface is known as infiltration and the dynamics of that movement are dependent on the size and formation of soil pores. It is a property of soil responsible for the retention of surface irrigation, because of the control over the amount of water that gets absorbed and overland flow. There a different scales of infiltration dependent: (i) soil properties (ii)initial soil moisture content (iii)previous wetting history (iv)permeability and its changes due to the surface water movement (v)cultivation practices (vi)type of crop being sown (vii)climate effects. At the beginning of a rain, event infiltration is initially high, but through time it straightens out to a fairly steady state of infiltration. This state, also called the basic infiltration rate defines the permeability of the soil. The texture pattern of the soil determines the time during which water will be coursing downwards as a result of gravitational pull. So in the case of coarse-textured soils(sand and sandy loam mixture), that time is smaller, in comparison to fine-textured soils(clay mixtures) which have a longer residence time due to the small size of the pores. However the clay-based soils are less susceptible to gravity, so the spread of the water droplets is more pronounced laterally, resulting in a larger soil moisture volume. With that being said a mixture of coarse and fine soil makes for the most effective water infiltration. Sandy soils have a big tendency for surface sealing and compaction, because they absorb water quickly. Infiltration can be measured by driving a ring infiltrometer into the soil, where water is placed in a ring and the infiltration rate is being measured by the drop of water level over time. Infiltration is one of the most difficult hydrological parameters to measure, because of the sudden shifts in soil and water conditions and it demands a precise controlled experimental environment. In watersheds the difference between gross rainfall and direct runoff taken from a hydrograph represents infiltration[1,6,14,16].

Leakage and seepage

Hydraulic structures that are carrying a water load will always experience deterioration, after a given period time, and the magnitude of leakage depends on the condition of the infrastructure and the value of the constant load. Leaks, bursts, and overflows are responsible for tremendous damage that can be inflicted without proper maintenance, or as a result of poor construction. That is usually the case of insufficiently-compacted or pervious-layered impoundments, poor adhesive properties of the concrete outlet pipes or other structures, or loose bonds between the impoundment and the foundation or abutments. In some cases, the banks of reservoirs may be built out of heavily damaged materials, or have continuous intersections that bind porous strata. Old underground brick or masonry reservoirs usually experience leaks through the joints and linings which were not properly composed. Leaks are best detected at night when we have isolated the system by closing the inlet and outlet valve and then we perform the depth test over time by measuring the drop in water level. Then we proceed to calculate the reservoir area, volume per area times the drop measurment and calculate the volume that's lost. The difficulty of the calculations depends on the form of the structure, because we experience a change in volume depending on the area segment the water level drops to[3,19]. Besides leaks water can escape through the bottom of the reservoir, or bad sealings on the functional structure through the act to seepage. Losses of water to the soil under the reservoir are difficult to quantify and

usually, losses to infiltration or seepage are considered negligible and ignored in reservoir system analysis studies. In the initial period of using the resevoir, seepage losses are rather extensive but decrease over time, hence why the reservoir shouldn't be placed on excessively leaky formations[1].

Reduction tactics for the 3 main water loss initiators

Irrigation practices that are set up for agronomy purposes, experience the overarching effects of water loss through deep percolation, evaporation and runoff. Resolutions can be found through water management practices, like, enhancing water holding capacity, improve infiltration, cover and protect the soil. These methods also bring about the resistence of soil to erosion and other forms of land degradation. One of the main tasks straining the farmer comunity is preserving the water in the root soil level without encouraging any movement downwards. For this reason it is prefered to increase the water holding capacity which is dependent on:
-soil particle size(fine particles like clay increase the lateral volume of the moisture spread, keeping the water in place under the force of gravity)
-organic matter content(benefits the soil by enhancing the clumping of the soil particles and makes room for pores for water retention)
-compaction(this process lower the retention capability of soil especially in the root zone, so it is beneficial to have loose uncompacted soils)
There are a number of practices put in place to extend the soil water holding capacity, these include cover cropping, fallow, sediment recycling, agroforestry and conservation agriculture[16,71]. On the watershed scale reducing evaporation from the soil surface, storage reservoirs and conveyance system will increase water productivity. Therefore we have to have a reliable net of system operators that are willing to act upon finding a problem. This introduces a water loss optimization program ,which entails the improvement of technical and financial performance of water systems and efficient use of nature water resources. The basic premise behind eliminating water loss from reservoirs is:
-reducing deep percolation by building soil water holding capacity
-reduce water lost through evaporation
-discourage weed(unproductive plant) growth[16,22]
The reservoir bottom is preserved over time by the act of sedimentation, which decreases the permeability of that layer. In the case the reservoir is found leaking a diver is sent into the reservoir to spread the fine sand over the walls and the base ,which becomes drawn into patterns where the suction of the leak takes place. In case of a significant leak external part of the reservoir is programmed to be lined. The logitudinal componenet of the reinforcement in concrete linings varies from 0,1% to 0,4% and 0,1% to 0,2% for the transverse componente. This prevents prevents serious cracks in the lining and ties neighbour sections of lining together to provide additional strenght in case of settlement damage in the case of subgrade soils or some others factors. One of the more important factor in dam structures is to achieve a monolithical composit of blocks in a transverse direction by grouting longitudinal contraction joints. The openings of transverse joints between adjacent blocks makes room for leaks ,so to prevent this seals are placed on joints adjacent to the upstream face of the dam. The act of clearing foresets reduces the infiltration capacity of the soil and evapotranspiration and increases surface runoff and streamflow[1,3,11]

2.2. Movement of shallow surface flows

Water movement on a solid surface can be gneerated through various means like gravitational forces, external influences(wind, snow melt,etc.) and mechanical pressure-induced transport. The movement of the waterfront in a certain direction depends on the wetting properties of the soil (hydrophilic and hydrophobic) as well as molecular interaction amongst the same and opposite charged particles. Water thats maintaining its flow in a certain direction, will be under the influence of adhesive forces, connecting the water and soil particle, that have good hydrophilic qualities. And also cohesive forces among water particles which bind together water particles in all directions, though the surface water layer is susceptible to imbalance because of the air being on the other side. And so depending on the energy of water flow in a certain direction we have a large amount of imbalanced water particles from the surface layer and in general the force causing the sliding of the layers is bigger than the force trying to keep them in place or surface tension. From then on depending on the soil type the slid layers get adsorbed or adsorbed to the surface providing a base for the incoming water particles.

2.2.1. Overland flow

The entire natural watershed is set in motion by the events of water input and water distribution networks. Among which surface runoff is the conduit function that ties together the actions of the water inlet (rainfall, snow, thaw of frozen soils and irrigation) and water outlet (streamflow, infiltration, interflow, and throughflow). Overland flow is created through a mechanism of ponding on the surface terrain and with time(until a certain depth) achieving resistance to the retention forces trying to keep the water in place. In a natural setting, it is created through rainfall events or snow melt, with a goal of feeding the drainage systems, driven by its high spatial and temporal variability[1,5,6,54]. Surface water doesn't maintain its hold long on the surface, as a result of gravitational forces, accumulation, and surface topography, with a nonunifrom movement patterns, though more organized behavior is examined at a hillslope scale. Mainly overland flow persists for a short distance until compromising a net of tortuous channels on the watershed surface, being fractionally small in-depth, which increases with advancement and later contributes to the widespread stream channel flow. In the engineering and hydrological sphere, runoff is a good tool for predicting hydrological responses in an area and flow routing plots. The flow of water over a watershed surface is complicated in nature, both spatially and temporally. In that environment surface flow takes two forms: overland flow that covers a wider space, through diffusive sheet spreading and channel flow, contained inside rills and gullies moving with turbulent motion[6,14].
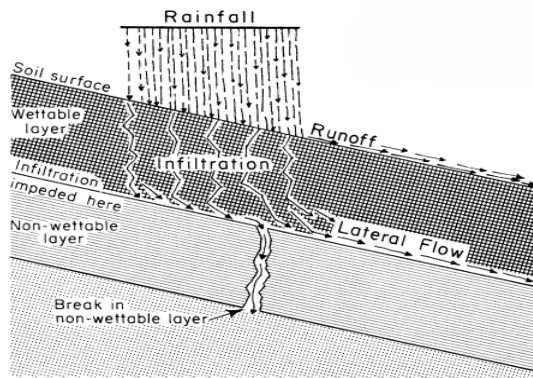
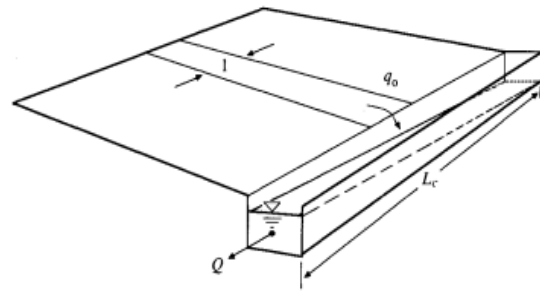*Figure.2.2 Water movment throught the soil and the surface during precepitation* (adapted from[67])

Figure.2.3. Overland flow from a plane into a channel (adapted from[6])

Overland flow ,usually flows in patterns decribed as anastomosing pathways, which concentrate water in rivulets rather in a thin sheet spread across the land canvas, by the definition of Abrahams ,,overland flow is as a shallow sheet of water with threads of deeper, faster flow diverging and converging around surface protuberances, rocks and vegetation''. The repeated movement of water can cause the development of rills ,which then influence further movement of fluid, depending on the variables of their geometry, flow hydraulics and sediment concentrations, that change with time[1,59,23]. Runoff generation as a root cause of erosion is highly dependent on the intensity of precipitation, vegetation cover and the amount of organic matter in the soil. Regardless of their high local variablity, one of the main exhibitors of control over overland flow depth and velocity is the shape of the hillslope. When disscusing excess runoff generation, soil water content means lot, during the duration of the precipitation event. Coarse soil tend to have a higher water tabel due to the smaller pore space ,which results in a biger soil water content that causes increased runoff. In which case we can make a prediction of the rate of runoff by comparing the soil moisture storage in the previous month (ST) and soil moisture capacity (STC). Where runoff genertion is a fraction of surplus that becomes runoff for the ongoing month and the rest is carried into the next month.

There are two main mechanisms that determine the generation of overland flow: infiltration excess(Horton) and saturation excess(Dunne) [1,30,23,17,54]

Saturation-excess overland flow

One way saturation-excess overland flow can transpire is as 'return flow' which occurs when interflow entering the saturated area exceeds the capacity of interflow through the soil profile and has to exit on the surface. This kind of runoff event lasts as long as the seepage from the soil layer allows it, also it is highly dependent on the capillary fringe that allows for groundwater to enter pores in the subsurface layer. Another term in which saturation-excess overland flow is shown is through the cause of direct precipitation falling on an already saturated area, it is also known as the Dunne mechanism or 'saturation from below'. It is explained as the incoming capacity of water from the surface infiltrating the soil profile to the limit where maximum saturation has been achieved, which results in the rising water table. This kind of runoff-generation mechanism is most common in humid regions with soils that have quality water retention properties and dense vegetation accompanied by a shallow water table. When an area reaches its potential for 'saturation form below' all incoming water input gets immersed in the overland flow runoff. The disposition of the groundwater table in relation to the stream, especially in flat terrains, is a good initiator for saturation from below. The variable source area concept which depicts the extent of the saturation from below a certain area can realize is

dependent on the fluctuation of the depth of the water table through seasonal and event defined time scales. When talking about the extent of the saturated areas, geometrical predispositions play a big role, where near stream areas in a concave hillslope arrangement and wide flat valleys are prime examples. Except for these two situations, saturation from below happens also in areas where subsurface flow lines converge in slope concavities or where soil layers conducting subsurface flow are really locally thin, etc.[30,54,59].

Infiltration-excess overland flow

Infiltration-excess overland flow is created when the rate of water input on the land surface is higher than the infiltration rate of the soil, which brings about accumulation of water in small deperessions on the surface. Water that makes its way from the surface, to the soil doesn't immediately get delivered out, because part of it infiltrates and the other part evaporates. Only when the storage limit has been reached does water spills out in an irregular sheet or converges into rivulets. There is a delay in letting water out of the depression storage onto different surface detention areas, because of varying soil water storage levels. Places with intensive rainfall events, low permeability of soils, and barren surface area condition infiltration-excess runoff. During a storm event, not all of the basin area will achieve the same level of infiltration, considering that some areas of the soil will have a stronger resistance to water intake due to unresponsive capillary forces of saturated pores. Spatial variabillity of the soil properties affecting infiltration and spatial variability of surface water input dictates the runoff-generation mechanism, during a storm event. As Betson (1964) pointed out only a partial part of the watershed area brings about infiltration excess runoff, and those are areas without proper vegetation or with a thin cover. That being said infiltration-excess overland flow is especially pronounced in areas, which promote the development of crust, compaction and sealing, which all decrase permeability. Semi-arid rangelands with a high rate of rainfall, as well as areas with compact soil structure, and paved urban areas are good for examining infiltration-excess progression[1,30,59].

Water movement through floodplains

The transport of water and sediment over floodplain areas is tough to predict, and isn't always accurately modeled due to the transient nature of floods, variable floodplain width, surface topography, land cover, and other structure produced by humans and animals. In conditions where steady flow is exhibited during the rising of the water level in a floodplain environment, the fastest flow is present in the main channel with velocities and bed shear stress decreasing with distancing from the channel margins.
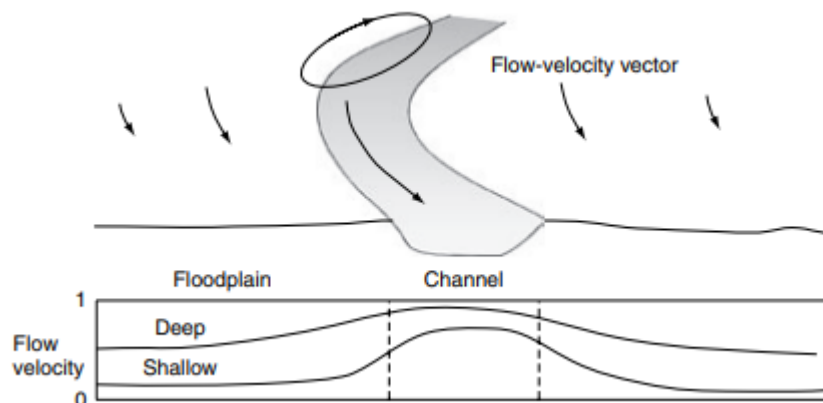

Figure.2.4 Water flow over the floodplain, with a display of down valley variability of flow with relation to the distance from the main channel (adapted from[23])

Water flow on floodplains is complicated by its transient nature, variable floodplain width and surface topography (channels, depressions, mounds of sediment such as levees and crevasse splays), vegetation, and structures produced by humans and other animals[1,5]. Therefore, flow and sediment-transport patterns on natural floodplains are not well known, and numerical models of water flow and sediment transport are poorly developed. However, many laboratory experimental studies of overbank flow adjacent to river channels have been undertaken, mostly with steady flows over the simple channel–floodplain geometry, and with immobile boundaries without sediment movement. Despite these simplifications, the experiments have elucidated some important features of floodplain flows when water covers the floodplain and flow is steady and mainly down the valley. The fastest flow in simple channel–floodplain models is in the main channels, and the flow velocity and bed shear stress on the floodplain diminish away from channel margins. Vortices created at the, channelfloodplain margin, because of the shifting currents, cause an abrupt decrease in flow velocity. With distancing from the main channel the depth of the flow in the floodplain increases in correlation with the flow velocity, with no ramifications on the velocity from the channel margin. Shallow floodplains mainly experiences big losses in velocity due to the hydraulic jump on the margin, and wide floodplains only feel the loss a short distance away from the channel margin. Flow convergence in floodplains contributes to the increase in flow velocity, which can change depending on the bed roughness, and the expansion of the flow zone. These changes in flow and transport of sediment over time control the spatial erosion and deposition on floodplains. The rise of the water level in the main channel can be caused by water feeding from crevasse channels, overland flow carried through rills, and precipitation. Over that this causes overspilling onto the flood basin, where the water gains acceleration, garnered by erosive flows. At the time of the peak flood water completely cover the flood plain and continues its movement onward with a decrease in velocity at the leading edge water wave. At the end of the floodplain water coverage, the water level subsides making its way to the drainage channels and groundwater, and with that floodplain lakes diminish over time[1,23]

2.2.2. Shallow water flow dynamics and kinematics

The characteristics of the shallow water bodies are difficult to measure and quantify, because of their accessibility and characteristics, however, they are important for determining surface runoff, erosion control, and water quality modeling. For the analysis of this kind of flows that are governed by principles of continuity and momentum, usually use one or two-dimensional flow models, because of the restrictions given by 3d modeling.
Velocity components in the x and y direction, in the case of shallow surface flow, are derived from the free surface profile excitation and go as follows:

$$u(x,y,t) = a\omega \left[\frac{\cosh[k(y+ho)]}{\sin(kho)}\right] \cos(kx - \omega t)$$
$$v(x,y,t) = a\omega \left[\frac{\sinh[k(y+ho)]}{\sin(kho)}\right] \sin(kx - \omega t)$$

When we are talking about depth in relation to velocity, we can see that fluid particles, in deeper water follow a clockwise circular rhythm pattern due to the magnitudes of component velocity being the same. For shallow water depths, this motion is contorted into an ellipticalshaped paths or flattened lines, because the v velocity component diminishes when approaching the bottom

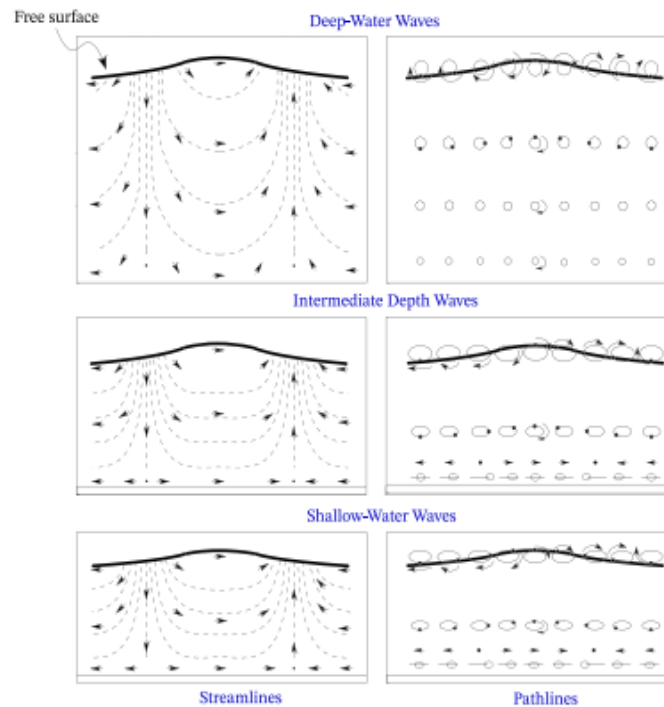and the free surface leaves no space for evolving in regards to the bottom.

Figure.2.5 Particle rotation under gravity wave propagation (adapted from[26])

We can conclude that the amplitude of horizontal motion in shallow water flows has more importance than the amplitude of vertical fluid motion, due to its value approaching 0 towards the bottom. Shallow water is represented by the relative magnitude of ho and L, and due to the small values of h_0/L , wave speed taken from the graph below achieves nearly asymptotical constant values given by : $c = \sqrt{gh_0}$, hence the horizontal velocity components become practically uniform across the entire depth, not dependent on the wave length[26,63].
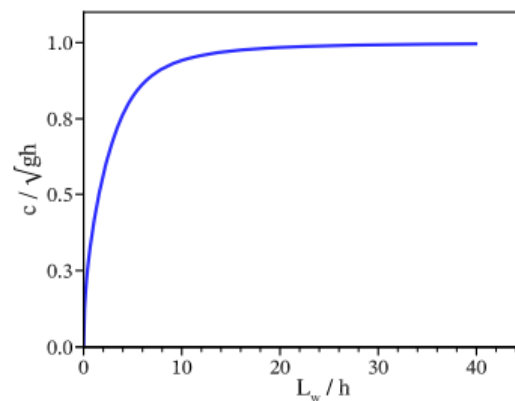
Slika.2.6 Graf ovisnosti valne brzine o valnoj duljini i dubini (adaptirano iz [26])

This conclusion about the independence of horizontal velocity in regards to the vertical velocity can be projected onto the pressure distribution in shallow water depths. Pressure variations are normally exhibited due to the accelerations in the vertical direction, conceived by curvatures of the water surface. This is not the case in shallows depths where kh_0 has a very small value, there the pressure distribution is considered to be hydrostatic. The pressure equation can be gained by modifying the velocity potential of a free surface equation:

$$p = po + \gamma \left[\tau \frac{\cos k(y+ho)}{\cos kho} - y \right]$$

Coming back to the earlier explanations, we can explain turbulence that is mostly pronounced in the horizontal lenghtscale, due to the restriction of depth. Examination of turbulent motions such as the creation of vortices, drag due to friction and resisting the viscosity influence, leads to the separation of large-scale two dimensional turbulence(L_{2D}>H) and small-scale threedimensional turbulence(L_{3D}<H). Realization of the natural seeting depicts a thin water layer bounded by the frictional bottom and free surface, where large-scale and small-scale turbulant distortions of the fluid mass work separately and in relation.

Instability caused in flowing shallow water is a product of the ratio between drivign force and dissipative force. The fundamental driving force behind horizontal turbulence, on a large 2D scale, is shear pressure, which increases with acceleration through the bottom and depends on the he viscosity of the fluid. Topography also plays a big part in the formation of the flow layers, which are led by the change in velocity due to the bed roughness, this creates turbulence on a large-scale[21,63].

Reynolds number flow clasification

One of the key factors in determening the flow regime in open channels and natural streams, is by calculatin the Reynolds number which signifies the ratio of inertia forces to fluids viscosity. High values of Reynolds number ,are presented in free-surface gravity flow that exhibit high resistence to the flow due to inertia ,opposite of stable discharges where viscous stresses between adjacent layers control the uniform flow. Increase of the Shallow overland flow as an example of external viscous flow, has to be cathegorized on the basis of its longitudinal component, as laminar or turbulent flow. Reynolds number defined through uniform depth (h_0) and depth-avareged uniform flow velocity (u_0): $Re = \frac{uo \times ho}{v}$ [6,24]

Diffuse sheet overland flow moving very slowly thorugh the vegetation layer and under high infiltration can be experimentaly evaluated as laminar flow when $R_e \leq 500$, which corresponds to the discharge per unit widht of the order of 10^{-6} m^3/s/m, through the value of kinematic viscosity. In cases where we have a very thin layer(milimeter scale) of water flowing downhill under gravitational pull, Reynolds number can be approximated as $R_e \leq 350$, though open channel flow is mostly depicted by turbulent flow conditions. Another alternative to defining the Reynolds number is using the perpendicular distance from the wall, which helps us scale the velocity gradient: $R_{el} = \frac{uy}{v}$. Through this we determine that the flow close to the wall, under constant kinematic viscosity, is laminar due to the no-slip condition, regardless of the mean flow. Turbulent conditions dissipate with flow expanding closer to the wall, and takes form as of a very viscous fluid. In between the two flow layers a transient zone is formed, acting as a buffer for the conversion of turbulent flow into laminar[24,26].

Saint-Venant equations

Overland flow is a prime example of shallow water distribution, which can be undertaken by depth avareged Sain-Vennant equations. This kind of water movement is a couple of deegres more difficult to analyze in relation to open channel flow which gets feed by overland sources. As disscused in the previous section there are two acts of motion that stem from overland flow that is the laminar regime, influenced by the parametes of steady flow distribution and turbulent regime, which is realized through rainfall impact, highly relative roughness, and channelezation. These aspects complicate the evaluation of flow hydraulics on a spatial and temporal scale, however in a general watershed model these parameters get molded into the

turbulent flow analysis. Because of the temporal and spatial discontinuity, stemming from external sources, overland flow has a vaguely defined area of spread, which makes it difficult to do a numerical simulation[6,8,26].

Saint-Venant equations or one of its approximations are used in simulating 1D unsteady flow in natural and non-natural channel, which can be simplified through calibration. Often termed shallow water equations they can also be dispalyed in 2D form, which is frequent in watershed applications.

$$\frac{\partial A}{\partial t} + \frac{\partial Q}{\partial x} = q \qquad Sf = So - \frac{\partial y}{\partial x} - \frac{v}{g}\frac{\partial v}{\partial x} - \frac{1}{g}\frac{\partial v}{\partial t}$$

Equation above represent the full dynamic wave equation(Sain Venant equations), compromised out of the continuity equation(to the left) and momentum equation(to the right).In the presented equations Q represents the discharge, A is the area of cross section, v is the velocity, S_f is the friction slope, S_0 is the bed slope, y is the water depth in realtion to the bottom, and x and t are the independent variables representing spatial and temporal flow attribute . These equations require eligible measured hydraulic data ,numerical techniques and cross-sectional stream geometry to determine a solution. So in regards to overland flow, the equation to the right can be simplified, for example in shallow streams if the bed slope stay fixed after the appropriate duration of time, the rate of change in water depth $(\frac{dy}{dx})$ will only slightly deviate from the usual value ,as well as the temporal velocity change term$\left(\frac{1}{g}\right)\left(\frac{\partial v}{\partial t}\right)$ and the longitudinal velocity gradient term$\left(\frac{v}{g}\right)\left(\frac{\partial v}{\partial x}\right)$. So in these cases these terms, on the right side of the equation can be ignored. One of the simplified versions of the Saint-Vennant equations is the Kinematic wave equation, which is assorted without inertial and pressure terms. It is used for the study of undteady flow, which in this version is most applicable for overland flow modeling.

The momentum equation goes as follows: $S_f=S_0$,which can present complications by defining friction slope as the bed slope and assuming uniformity over the distribution net, if not for its use in unsteady flow continuity. Adjusting the momentum equation to the unsteady discharge equation, creates alterantive solutions for the momentum equation:

$$\frac{\partial Q}{\partial x} = c\frac{\partial A}{\partial x} \qquad\qquad \frac{\partial Q}{\partial t} = c\frac{\partial A}{\partial t} \quad [1,6,26]$$

NRCS –Velocity method

The NRCS velocity Method, is the most commonly used method, for estimating the concentration-time(T_C), which is the sum of travel times, for each flow segment that occurs from the beginning of the surface runoff event unit it reaches the watershed outlet.

The movement of water through the watershed can be approximated as sheet flow, shallow concentrated flow, and channel flow. They are a part of the drainage conveyance system and are crucial in calculating peak discharge from an area, which happens when all of the flow segments are involved in runoff from the site. Urbanization usually decreases the concentration-time and hence increasing the peak discharge velocity[56,57].

Travel time is the ratio of length of flow to flow velocity: $T_t=\frac{L}{3600V}$

T_t-travel time (hr)
L-flow lenght (ft)

V-average velocity (ft/s)

Time of concentration T_c consist of adding up consecutive flow segment, that are attributed to the drainage area: $T_c = T_{t1} + T_{t2} + \dots + T_{tm}$

T_c-time fo concentration
m-number of flow segments

Time of concentration is dependents on the following factors:

1. Surface roughness -urban area development has affected the increase of flow velocity, through lowering the retardance of flow.
2. Channel shape -designed hydraulic characteristics of the channel system, promote faster runoff velocities and shorter travel times
3. Slope -can be increased or decreased by urban intervention, so we can enhance water management and conveyence activites

Sheet flow is the first segment of analysis and represents flow over a surface plane. It usually spread to a distance of about 100ft, and we use Manning's kinematic solution, which incorporates all the flow obstruction factors(raindrop impact, drag, transport of sediment), for computing T_t:

$$T_t = \frac{0,007(nL)^{0,8}}{(P_2)^{0,5} s^{0,4}}$$

Surface Description	n
Smooth Surface (concrete, asphalt, gravel, or bare soil)	0.011
Fallow (no residue)	0.05
Cultivated Soils:	
Residue cover $\leq$ 20%	0.06
Residue cover > 20%	0.17
Grass:	
Short grass prairie	0.15
Dense grasses[1]	0.24
Bermudagrass	0.41
Range (natural)	0.13
Woods:[2]	
Light underbrush	0.40
Dense underbrush	0.80

Figure.2.7 Manning's roughness coefficient for sheet flow (adapted from[57])

Shallow concentrated flow develops after a maximum of 100 feet, which usually develops in rills, gullies and swalles. Channel type and slope roughness determine the transient nature of these flows, above which tillage can also affect the direction of the flow. This flow can be determined from the table below based on the environmental scheme. [56,57]

Flow Type	Depth (feet)	Manning's n	Velocity Equation (ft/s)
Pavement and small upland gullies	0.2	0.025	$V = 20.238(s)^{0.5}$
Grassed waterways (and unpaved urban areas)	0.4	0.050	$V = 16.135(s)^{0.5}$
Nearly bare and untilled (overland flow); and alluvial fans	0.2	0.051	$V = 9.965(s)^{0.5}$
Cultivated straight row crops	0.2	0.058	$V = 8.762(s)^{0.5}$
Short-grass prairie	0.2	0.073	$V = 6.962(s)^{0.5}$
Minimum tillage cultivation, contour or strip-cropped, and woodlands	0.2	0.101	$V = 5.032(s)^{0.5}$
Forest with heavy ground litter and hay meadows	0.2	0.202	$V = 2.516(s)^{0.5}$

Figure.2.8 Equations and assumptions developed from the speed/slope chart for shallow concentrated flow (adapted from[57])

Open channel flow is the most distinguishable out of the mentioned, because of their accesibility for cross-sectional surveys, visibility in aerial photographs and marked lines on maps and plans. Manning's equation or water surface profile information can be used to estimate average flow velocity:

$$V = \frac{1,49 \left(r^{\frac{2}{3}} \right) \left(s^{\frac{1}{2}} \right)}{n}$$

V-average velocity (ft/s)   s-slope of hydraulic grade line

R-hydraulic radius   n-Manning's value for open channels flow
  -A/P
  A-cross sectional area of flow
  P-wetted perimeter, ft.

Type of Channel and Description	n
A. Closed Conduits Flowing Partly Full	
1. Steel - Riveted and Spiral	0.016
2. Cast Iron - Coated	0.013
3. Cast Iron - Uncoated	0.014
4. Corrugated Metal - Subdrain	0.019
5. Corrugated Metal - Storm Drain	0.024
6. Concrete Culvert, straight and fee of debris	0.011
7. Concrete Culvert, with bends, connections, and some debris	0.013
8. Concrete Sewer with manholes, inlet, etc., straight	0.015
9. Concrete, Unfinished, steel form	0.013
10. Concrete, Unfinished, smooth wood form	0.014
11. Wood - Stave	0.012
12. Clay - Vitrified sewer	0.014
13. Clay - Vitrified sewer with manholes, inlet, etc.	0.015
14. Clay - Vitrified subdrain with open joints	0.016
15. Brick - Glazed	0.013
16. Brick - Lined with cement mortar	0.015
B. Lined or Built-Up Channels	
1. Corrugated Metal	0.025
2. Wood - Planed	0.012
3. Wood - Unplaned	0.013
5. Concrete - Trowel finish	0.013
6. Concrete - Float finish	0.015
7. Concrete - Finished, with gravel on bottom	0.017
8. Concrete - Unfinished	0.017
9. Concrete Bottom Float Finished with sides of:	
a. Random stone in mortar	0.020
b. Cement rubble masonry	0.025
c. Dry ruble or rip rap	0.030
10. Gravel Bottom with sides of:	
a. Formed concrete	0.020
b. Dry rubble or rip rap	0.033
11. Brick - Glazed	0.013
12. Brick - In cement mortar	0.015
13. Masonry Cemented Rubble	0.025
14. Dry Rubble	0.032
15. Smooth Asphalt	0.013
16. Rough Asphalt	0.016
C. Excavated or Dredged Channel	
1. Earth, straight and uniform	
a. Clean, after weather	0.022
b. Gravel, uniform section, clean	0.025
c. With short grass, few weeds	0.027
2. Earth, winding and sluggish	
a. No vegetation	0.025
b. Grass, some weeds	0.030
c. Dense weeds or aquatic plants in deep channels	0.035
d. Earth bottom and rubble sides	0.030
e. Stony bottom and weedy banks	0.040
3. Channels not maintained, weeds and brush uncut	
a. Dense weeds, high as flow depth	0.080
b. Clean bottom, brush on sides	0.050
D. Natural Streams	
1. Clean, straight bank, full stage, no rifts or deep pools	0.030
2. As D.1 above, but some weeds and stones	0.035
3. Winding, some pools and shoals, clean	0.040
4. As D.3 above, but lower stages, more ineffective slope and sections	0.045
5. As D.3 above, but some weeds and stones	0.048
6. As D.4 above, but with stony sections	0.050
7. Sluggish river reaches, rather weedy or with very deep pools	0.070
8. Very weedy reaches	0.100

Figure.2.9 Mannings roughness coefficient for open channel flow (adapted from[57])

2.3. Soil-water interactions

Sediment transfer and deposition

Water and soil relations may be explained through the formations of rivers, rills, gullies, and other surface formations as a result of water distribution activities. The hydrological cycle triggers the dynamics of soil moisture extent variations and circling of bio matter and chemicals, such as runoff carrying phosphorous and organic carbon. A mass of certain organic or inorganic matter moving through the observed volume of moving water is called transport. Among this flow, mass changes in its amount, as a cause of reactions exhibited either in decrease because of the change in structure of the compound or some substance reforming its affinity, to adhere to the predominant matter[1,23]. Also the addition to the transporting mass could be given through external deposits. For reference, grains of gravel or sand submerged in the water will be under the impact of buoyancy and dependent on its density will either sink or stay afloat. This is also further influenced by the turbulence of the water flow, some portion of sediments

can get left behind over a bed of retained sediment due to viscous shear stress and dynamic pressure. This relative motion is called drag, displayed from friction-induced restraint(surface drag) or resistance due to dynamic pressure(form drag). Form drag has a bigger role in sediment deposition because of the influence on individual grains and bed form arrangement. Suspended solids in natural water flow undergo various transformations of their base composition and settled down at certain points differentially, determined by their density and volume. Although a certain amount of solid mass will keep its hold permanently, others enter back into the water course through turbulence this occurs in shallow areas with strong currents and rushes of wind[1,23,27]. Dependent on the granular size and flow condition, certain patterns can be discerned. Low energy areas such as pools in rivers and null zones in estuaries area a harbor for sediment deposition and particle magnification. In lakes coarse sediments are scattered around shallow regions and finner particles in the middle of the flooded area, as a result of wind and current encouraged turbulence. Human interactions can alter the deposition patterns, as well as intense natural events, these include dam construction, mounding the river bed and floods. Conservation of the sediment load in dams structure can lead to degradations of the downstream end as a result of insufficient sediment yield, erosion impact, etc. Agreddation can be achieved through various activities in which it provides excessive deposits in a certain area, as a consequence of excavation work ,sea-level rise or above average sediment supply. This shifts the sediment equilibrium through time-based erosion acts and overall deposition [1,20,66].
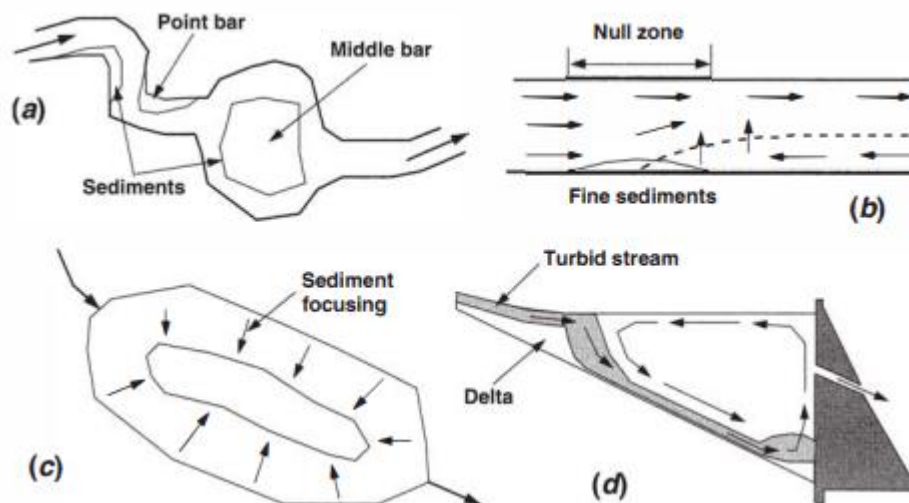

Figure.2.10 Deposition routes of fine sediment in natural water bodies
a)top vies of river   b)side view of estuary
c)top view of lake   d) side view of impoundment (adapted from[20])

Wettability

One of the most commonly established dynamic properties, that shows its effect in contact between fluid and soil particles is the wettability of the soil plane. During the intersection of the two-dimensional differing state mediums, water accumulates on the surface of the soil, as a consequence of surface tension and prevailing attributes of the soil. During this exchange, various member cell sizes and discharge faults affect the formation of the first water layer more specifically the structure and longevity of the hydrogen-bond grid. In case of small ratios of faults existing in the two-dimensional hydrogen bond grid, irregular droplet profiles form in part incompletely, which prologues the time residence on the surface, before the complete adsorption[67,72]. This is presented through water droplets 'balling up' on the surface, through the mutual bonds achieved by attraction forces between water particles. Continuing layers decrease in residence time on the surface before getting absorbed into the soil. We can conclude that the degree of wettability is determined by the reaction forces that attract soil particles to water particles in comparison to the repelancy of that unity through binding of water particles. Another important factor in discerning hydrophobic from hydrophilic surfaces is the wetting angle of the water droplet in relation to the plane surface. In the case of hydrophilic surface mediums, the water bubble is more squashed due to the porosity structure of the soil, adsorbring the partial volume. The wetting angle defines the magnitude of attraction between soil and water particles, from which we can deduce that hydrophobic surfaces have decreased rate of flow due to the coupling of the water particles.
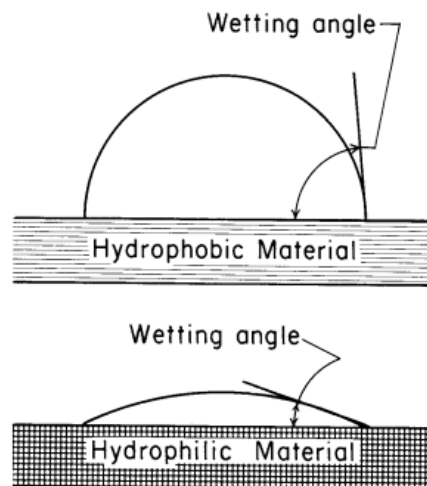

Figure.2.11 Wetting angle under hydrophlic and hydrophobic surface textures (adapted from[67])

In the case of unsaturated soil, water can follow the pattern of movement through the passage of energy, in which attractive forces are guided by the thermodynamical transition from high energy region to low energy. Water repellent(non-wettable) soil layers, that form mostly in humid areas due to drying effects, or places exposed to high temperature, consist of waxed layers in sequences or unevenly, due to the degradation of organic composition. These soils reside mainly on chaparral brushland or scorched and sandy loam wetlands, where the pedigree of wettability is based on: vegetation effectiveness, fire history, soil attributes and numerous collaborative external factors. Water repellency is a key initiator of, runoff succession and modified evaporation, which directly corresponds to its prevalence in the hydrological cycle. The relationship between infiltration and water resistance depends on the texture of the soil profile and its wetting properties, where slightly non-wettable soils recieve water quicker than exceedingly wettable soils preserving water on the surface until it evaporates[26,67].

2.4 Integrated water tracing methods

Tracer application in today's day and age is embued through various sciences, for the detection of certain properties, defining fluid kinematic transition patterns, or investigation of inaccessible areas. Their use in hydrological science and in investigating the water cycle has contributed to further development of segments that make water movement possible, as well as finessing the modeling behind ongoing systematic research dilemmas. (Infiltration limits ,groundwater movement shifts, erosion propagation ,deposition displacement).There are different variations of tracers recognized as stable isotopic or radioactive-based properties, or artificial or natural tracers viewed as substances with chemical or physical properties. In the words or Flury and Wair(2003); citing: "an ideal tracer for hydro-environmental research should: i) have movement similar to water; ii) be conservative, i.e. without degradation during the measurement time; iii) not show sorption to other environment components (e.g. soil, sediments, rocks); iv) be visibly distinguishable from the background of the system; v) be detectable either by chemical analysis or by visualization; vi) low toxicological impact on the study environment"[7,37]. The field of use of this kind of compact matter is widespread, from investigating infiltration limits, tracing groundwater movement, characterization of erosion propagation, or following deposition displacement. When used in their field of practice there are 3 parts of the hydrological systematic approach that stay immutable. First is the input into the environment that can be achieved through concentrating or injecting the tracer, the second is the potency of the natural or artificial tracers as it moves through the foreign medium, and the third which signifies the output from the system is described as the derived volume and concentration of the tracer. Tracer techniques represent the experimental domain of gathering empirical data, that is later used for calibration and validation of certain(kinematic, dynamic, hydrological) models, or processed quantitatively and qualitatively. Tracer techniques have a big relevance in water resource management, where they contribute to the promotion of certain studies inside the water conservation policy and upgrading certain implementation project, through further discoveries about the natural system. For the purpose of this work the further review will mainly focus on artificial tracers used in investigating natural phenomenoms and their comprehension[7,27,73].

2.4.1. Artificial tracers

Before using tracers in natural and laboratory experiments, we have to get familiar with the 'ins and outs' of their use. Artificial tracers provide clearer insight into the latent and active processes that occur around the hydrological system and mechanics of the water distribution network. Their feature is restricted both spatially and temporally, therefore, their application must be exercised safely and controllably. Apart from that, their sustainable properties, allow for instruments to observe them clearly in the natural setting, which contributes to quantitative assesment of flow velocities, flux, residence time, dispersion, etc.[7,62]. A system with restricted timelines is usually in the focus of their discussion such as surface runoff, which can't be relied on measurement instruments to provide an accurate analysis. This is an issue because of the thin layer of water, coursing through a plane of scattered residue disrupting the flow, as well as various surface conditions. Hence for the matter of assessing velocity fields, flow trajectories, and direction in shallow water flows, karst aquifers, and a plethora of different varients of tracers stand at the disposal. Among these groups the most traditionally used are the dye and salt tracer, although different occasions, requests tracers, that may have a more pronounced conservative nature. Solubility determines the longevity of the tracer material inside the medium, on par with sorption which can be damaging for the flow. The chemical footprint

of certain tracers, makes them reliable candidates, for undertaking a certain task, like fluorescent tracers, which are mostly used in any scenario. Mainly artificial tracers are injected into the body of water, where they adapt to their surrounding, providing a signal for the motion displayed in the volume. Based on the physicochemical state of drifting particles ,they are used for assortment of special problems[7,36,60,61]

Salt tracers

In efforts to avoid issues that may arise with heterogeneity and anisotropy of the hydraulic regime and unfamiliar causes of velocity and movement shift, we use salt tracers as monitoring units in various scenarios. The mechanism behind the application of salt tracers relies on electrical probes which are placed in the subsurface and transmit a signal to the transitioning saltwater edge, which in turn transmits a signal. These tracers work as both environmental and artificial tracers due to their chemical background. Their non-reactive nature has made them suitable for a load of applications in karst systems, groundwater passages, porous geological strata, and seepages from rivers and pipes[73]. Regardless of the quality that salt tracers, when placed in water coursing areas, they are transported through the influence of a mass transport mechanism, so they have to be carefully chosen. Because of their strong ion base and positive solubility properties they have been involved all around the hydrological system until fluorescent tracers made their way to the tracer sphere. Shallow overland flows make the perfect examples of small-scale ventures, which work for the amount of the tracer that needs to be used for it to be effective. When mixing salt into the water volume we need to make sure to appoint a favorable ratio, so it doesn't affect the solubility. The quality of response of the measuring equipment depends on the frequency of the salt wave passage, which depends on the concentration of salt in the appointed time at the section of the stream. The chemical and physical properties of salt in water consist of kations and anions which separate during dissolution, with a high electrical conductivity as a product of chaotic ions. When applying these tracers in soil profiles conceived out of fine soil, the mineral and organic particles attract ions contained in salt, through ion exchange. Sorption in the view of cations has a bigger adsorption rate than in regards to anions, which reflects low sorption conditions. Factors that influence cation and anion exchange volume, towards soil particles, are the potential of ions in the view of charge, and ion radius. Negative consequences of using salt tracers include sizeable degrees of pollution, transition issues, difficult processing, and excessive substance injections. Although regardless of the mentioned setbacks, these tracers are favored in practices, because of their low maintenance, large quantities, and quality recording features[7,62,65].]

Fluorescent tracers

Due to their virtuous capabilities in artificial tracing disciplines, these tracers have become renowned among their preceding beneficiaries, with the highest rate of efficiency and use. Boundaries set by traditional methods of tracing the water-based movement are circumvented through their innate characteristics. Such as insoluble demeanor, which works well for preventing adhesion on passing layers of material, which reduces the volume of the tracers sample, opposite to the effect of dye tracers. Also, the expressed luminosity in an indistinct setting, which enhances the quality of the imaging techniques and eases the process without interference. They are especially beneficial for describing unrestricted flow margins, wash load flow, and heavy floods through 2D and 3D flow assessment, flow vortex, and bathymetric features of materials. Clearance on toxicity levels is much higher in concern to other chemical compounds, as well as uniformity in regards to concentration on the calibration curve. Concise analysis and small quantities of material used, benefit the cost

margin of this tracer, and diverse ways of tracing water flow, are a product of pronounced sensitivity, easy handling, and simple detection terms[7,39,40,64]. There have been numerous investigations done to define the applicable kind of fluorescent tracers, which are fixed in a small number for today's use in tracing. Even among the prospective candidates, there aren't enough conditions to expand their use, mostly due to the manufacturing process. Some of these tracers include Rhodamine WTS for exploring drainage, Uranine and Deuterium for testing fissured aquifers and Pyranine for macropore water transition. Fluorescence functions from luminescence source energy as a cause of electromagnetic radiation, and transmits an light impulse of very short lenght 10-18. The energy source entices the atoms from lower energy ends and kicks them up to a higher energy state, where they let out energy thorugh a flash of light.

The intensity of fluorescence emission is proportional to the intensity of incident light and the concentration of tracer:

$$Ie = A * Io * \varepsilon(\lambda ex) * \emptyset(\lambda em) * c * d28$$

Ie = fluorescence intensity

A = instrumental constant

I_0 = incident light intensity

$\varepsilon(\lambda ex)$ = molecular extinction coefficient at wavelength λex

c = tracer concentration

$\Phi(\lambda em)$ = quantum yield

d = sample layer thickness

A trace substance's fluorescence intensity is determined by its physical parameters, such as quantum yield, extinction coefficient, and tracer concentration. This property is important since the detection limit is determined by the fluorescence intensity with which it is positively associated in one sense and in the other with the sample background[7,27].

Dye	Relative fluorescence intensity [Uranine = 100%]	Detection limit [mg/m^3]	Excitation/ emission [nm]
Naphthionate	18	0.2	325/420
Pyranine	18	0.06	455/510
Uranine	100	0.001	491/516
Eosine	11.4	0.01	515/540
Amidorhodamine G	32	0.005	530/555
Rhodamine B	9.5	0.02	555/575
Rhodamine WT	10	0.02	560/585
Sulforhodamine B	7	0.03	561/586

Figure.2.12 Table of values among the dye compounds, dispalying their relative fluorescence and detection limit (adapted from[7])

Dye tracers

As an artificial tracer with long use of tracing transport processes, dye tracers lack the inherent potential to be anything more than products for staining experiments. This is represented in their defected spatial and temporal reenactment of water behavior, which makes them perfect candidates for representing haphazard and unsteady flow in soil. These tracers provide good insight into the mean flow velocity of shallow overland flow, by following the leading dye edge after the injection has taken place. Once inside the recipient, the colored chemical compound undergoes a reaction in which the particles of the injected mass get spread around by water particles, which explains high solubility. In such concentrated conditions, dye particles can get separated from the reactive balance, while moving through water parcels, as a product of hydrogen bonding, ion exchange, and solidliquid contact angle principle, which are all preliminary factors of sorption[7,27,37]. Dye tracers experience negative effects through the chemical reaction of dissolution, which decreases the brightness factor, and oxidation which slowly degrades the dissolved constituent. Therefore mobility and visibility are the main acts that make a qualifying factor, for the kind of tracer material that is going to get picked to draw out flow patterns through stained patches in the water profile. Nonflourescent and fluorescent dyes have prevalent physical and chemical properties, which come to light under low pH levels, which induce hydrogen bonding. Methylene blue is a dye tracer with excellent luminosity features but has a dominant trend of adsorbing to approaching the surface, which has a backlash on flow tracking. In that sense the use of acid dyes has shown the best result both in their decent movement speed and the quality of the captured image. The dye front exhibits higher rates of retardance in relation to controlled tracers and the wetting front and is navigated through space, by the fluctuation of sorption, physical and chemical restrictions of soil, and variations in contact time. Image processing is a necessity if there is a need for deeper insight into the patterns and characteristics that were observed through dye tracing methods[7,38,45,52].

2.4.2. Solute transport characteristics

Solute transport

Whenever we are talking about the movement of foreign substances in a controled volume, whether that be the coursing of the pollutant in the wastewater network, or tracking material that's entered the streamline, properties of mass transport are important for processes that affect the balance of flow. In these circumstances, it is important to have a good understanding of the molecular reactions, depending on the ratio of the solute mass in the solvent volume. Where the dilution of the concentrate initiates ion or molecule separation, that is further led by collision with water particles in the longitudinal and lateral direction, following meandering pathways. This collision is a product of hydration in which the water particles latch onto oppositely charged ions preventing them from rearranging and shifting their motion to match the flow of the solution[74]. The process continues until the compound has achieved an equilibrium state, having reached the threshold of energy-induced water flux(created through chemical reactions). Before the timeline of solute parcel spreading, a few other processes contribute to the change in form and shift of hydrodynamical and kinematical properties of the solution. A big part in determining the initial processes, leading the solution onward, is determined by the type of distribution flow and surface characteristics[25,74,75].

Advection paired with diffusion

The ongoing involvement of the two elements comprises a time-sensitive medium, which displays various chemical-physical and microbiological processes. Observing this environment we can discern the transport mechanism based on the influence of the relative motion of the whole system, and the transport conceived from the 'reflexive' nature of particles to react to each other[25,75].
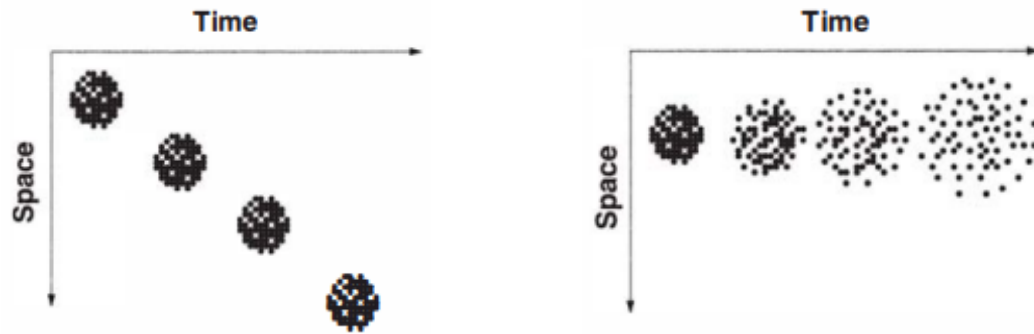

Figure.2.13 a)transport of a dye particle through,   b)transport of a dye particle through, initiated
initiated by advection   by diffusion(adapted from[20])

Advection represents the behavior, of a single unit inside the union, moving from one place to another, as a consequence of the set motion. This physical phenomenon depends on the reactive forces of individual particles, and other elements, providing resistance to the kinematic force. Wind energy and gravity are usually the driving forces that initiate the movement of the water, where advection constitutes the velocity fields developed from that disturbance of the static form. The dissolved compound functions passively inside the solution, as a result of flux, attained through energy coursing between the ions and water particles. In which case, this flux can increase or decrease depending on the time and place, and the energy potential. Enhancing the solute concentration, by adding to the solution, will not result in immediate change in velocity and sorption direction, uniformly over the spread area. But will have a gradual distortion pattern over the concentrated plane, which is responsible for the dispersive solute flux(uneven distribution of the solute parcels). Lakes with natural drainage spots and downstream transport in natural conduits make for good examples of the advection process [20,25]. Diffusion is a tendency of sporadically charged particles, or molecules to move around the space, or the movement of mass due to the intermolecular reactions. Through this inverse process, tightly bonded molecules of the solute material get spread out and dilute the solution gradually. This transfer starts from the areas of higher concentration and simmer down in lower concentration areas, of the bulk formation. The presence of a solute agent in dilute solutions doesn't affect the overall dynamics of the water body if it is limited to the right amount. In turn it offers a smooth progression of the concentration decrease all the way to the bottom end of the volume. There are various ways to modify the transport rate of the allocated particles in the concentrated solution due to: temperature increase, electromagnetic charge, and pressure. The magnitude of diffusion is approximated by these three factors:

1)Area of spread- the larger the volume the larger the network of the diluted substance
2)Mixing capability- which can be enhanced under conditions that give energy supplies
3)Concentration gradient- which emphasizes that bulk content moves from areas of high mass to areas of limited mass, in favor of achieving the network balance[20,25,29].

Fix's law represents the realized concentration and flux of the solute mass, of a certain unit area, gained by, oriented diffusion feeding.

$$qs = \frac{\Delta M}{\Delta A \Delta t}$$

In regards to the external starting mechanism of the solvent and internal igniting mechanism of the solute, we can define that motion through a differential equation, that ties them together. It can be said that the solute inside the recipient volume, moves by the joint effort of the volumetric flux of the solvent and Fickian flux of the solute. This notion leads to the determination for superimposing the two separated mass fluxes into gaining one predominant mass flux needed for advective diffusion.

The constructed equation is: $\frac{\partial C}{\partial t} + V * \nabla C = D\nabla^2 C$, which can be simplified by implementing a constant advection velocity: $\frac{\partial C}{\partial t} + u\frac{\partial C}{\partial x} = D\frac{\partial^2 C}{\partial x^2}$. In the case when advection dominates, solute particles move at a velocity of u, and in the case when diffusion dominates, particles travel infinitley fast. [25,29,75]

Dispersion

Another important quality of water turbulence, when examining the amount of soluble content, is the component that allows mixing on a larger scale. As soon as the soluble matter gets submerged into the receiving volume, hydrogen bonding initiation begins, which highly affects solubility. This component works along with other solute transport mechanisms, and it is determined by the kinematic properties of water flow. In relation to diffusion, dispersion spread uniformly through the control volume, dependent mainly on the velocity gradient. At the scale of typical molecular disruption as an effect of diffusion, the dispersion can be regarded as a Fickian diffusion process, when the two are collaborating. Due to the limitations set by the surrounding and dynamic nature of water, this process doesn't show as much promise as it does with smaller spaces and confined domains. Diffusion and dispersion are two overarching processes in which their effectiveness is determined by the force behind the shifts in velocity that causes mixing. In static natural water bodies, dispersion leaves the most impact as it is influenced by external forces, spontaneously breaking the molecular tension and promoting turbulent diffusion[20,25,29]. Another type of dispersion is necessary, to explain diffusion distributed concentrated layers formed during long and intense network mass transport events. Since this process is connected to diffusion, through the conversion and adaption to turbulence, by the agitation of particles, it introduces an adjacent mixing practice shown in unsteady natural streams. Dilution of highly suspended solids can be achieved through turbulent diffusion which realizes its potential through the inner wroking of eddies. In shallow streams, longitudinal dispersion has contributed to the development of heat, through longitudinal shear flow, as well as mass molding, through transverse diffusion and longitudinal solute parcel transport[25,29,55].
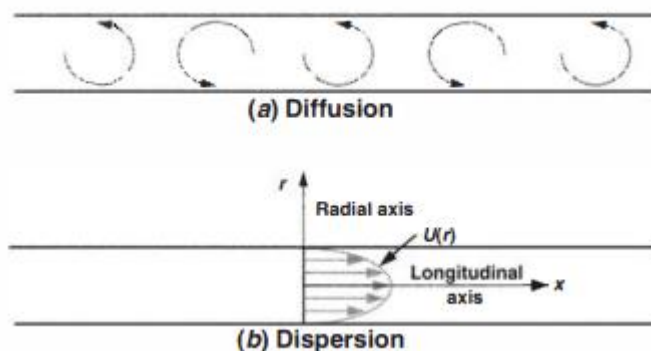

Figure.2.14 Contrast between diffusion and dispersion (adapted from[20])

3.METHODS AND MATERIALS:CASE STUDY

The following chapter of this thesis work describes the environment and procedures, involved in a streak of experiments done on a physical model. Firstly, the beginning sections provide a description of the laboratory setup and the needed materials. Thereafter, the last section describes the structure of the experimental methodology, used for investigating the nature of sink point water loss.

3.1. Laboratory setup

The experimental work was done at the hydraulic laboratory, water resources and Environment (LHRHA) of the Department of Civil Engineering (DEC) of the Faculty of Science and Technology of the University of Coimbra (FCTUC), with the purpose of investigating flow dynamics and tracer leading-edge movement[44,47] towards the sink point. A 3D representation of the comprised physical model is shown in Figure 3.1. The area of examination is comprised of a soil flume 2 x 2 m, with an attached pinned grid formation, visible on the top of the surface area. A characteristic spot was left for the sinkhole, which was dug up and covered until a certain time it was needed for the experiment. The constant flow was applied through the feeder box, on the downstream side of the flume which is a part of the water supply system, that provides water through the constant head tank placed at a higher elevation. The constant head tank was filled with tap water from the laboratory supply system (Conductivity: 75.9–150 µS/cm at 20 ∘C; pH: 6.5–7.3; Turbidity: < 1.1 NTU; O2: 1.0–3.7 mg/L; Total hardness: 21.4–33.3 mg CaCO3/L; [87], which was also used to prepare the tracers. Monitoring of the experimental proceeding was done using a GoPro camera and an Infra-red camera, during the entirety of the held tests. The described setup wasn't changed, in any way, during the time it was used, with the only difference among tracer materials and fillings for the sink hole, being used at determined times.
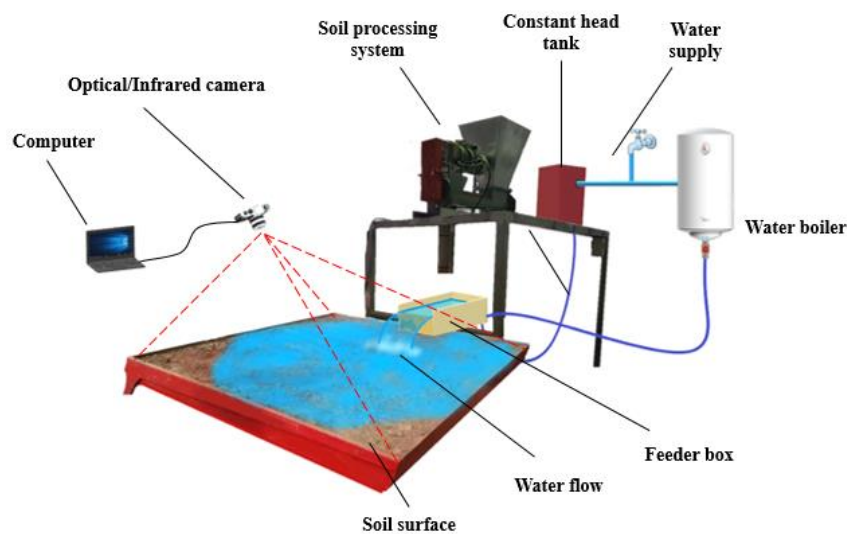

Figure 3.1 Schematic representation of the laboratory setup using the infrared camera

3.1.1. Soil and surface morphology

The experimental ground consisted of a 0.1m deep soil layer, which consisted of sandy loam, collected from fluvial deposits from the right bank of river Mondego, near the vicinity of Coimbra, Portugal, as used in other studies [47,88]. The key physical characteristics of the soil used in the soil flume experiments are: -Sand content: 79%; -Silt content: 10%; -Clay content: 11%; -Bulk density: 1100 kg/m3; -Soil depth: 62 mm; -Colour: brownish. In between the experiments we weren't looking to preserve the state of surface skin that had suffered local sediment scattering and deformations caused by rills and fissures. This serves as a representation of the natural topographic display usually formed after runoff events[23,89]. Interventions on the experimental surface were made, only in the case of excessive buildup of soil in one place, so that we can don't deviate from a somewhat straight surface plane. Due to the heterogeneous texture of the sandy loam, during the spread of water on the soil surface, different spots of the area will have inputs of preferential flow into the subsurface [88]. This influences the runoff speed, which results in a longer recording time during the flooding of the soil flume. Experiments were conducted under different moistures of the soil morphology(dry, wet, saturated), for the sake of procuring more results for assessment.

3.1.2. Video recording system

Recording of the soil flume was done, with a Samsung Galaxy S8 optical camera (Resolution 1080p at 120/90/60/50/48/30/25/24fps; 1920 × 1080 video frames) placed on the upstream end of the flume and the FLIR DUO PRO R infrared video camera(Resolution (number of pixels): 336 × 256; Accuracy: +/- 5 ∘C or 5% of readings in the −25 ∘C to +135 ∘C range; Spectral range: 7.5–13.5 μm), placed on the right side of the flume. Both of the cameras were fixed in a position above the flume(0,65m for the GoPro camera and 3,1m for the infrared camera) and supported by a metal structure, in order to obtain the optimal camera angle. The optical camera records the propagation of the leading edge dye plume movement, providing images for examining the geometry and dynamics of the flooded area [37]. Due to the dispersion rate of the dye material, it is in our interest to work with equipment, which provides better rendering resolution. Some of the setbacks that need to be dealt with before recording include, providing good lighting conditions, which improve the image of the diluted dye plume, and the soil flume needs to be positioned to minimize the reflection of the light. An infrared camera works on the principle of reading electromagnetic waves transmitted, because of the thermal emissivity coefficient of water and constructing a 2D image[44,45]. Since the water and wetted soil emissivity coefficients are very similar (maximum of 15%), for the working spectral range of the infrared camera (7.5–13.5 μm) the associated errors can be ignored. During the experiment, the leading edge of the thermal tracer was captured in a time-lapse of snapshots taken at each 1-second interval. The luminance of the heated water provides a distinctive spectral range which contributes to clearer visualization of the heat movement[86]. Sensing technology of this kind makes it easier to extract empirical data needed for quantitative and qualitative analysis of shallow surface flows.

Figure 3.2 Point of view from the infrared camera of the experimental setup

3.2. Tracers
3.2.1. Thermal tracers

This tracer will be used in the experimental trials, to record water movement through a bulk motion of hot water, following spatial and temporal temperature trend changes. Heat is usually a reliable source for gathering information on discharge rate, changes in flux, and shallow water kinematics because it offers mathematical, economic, and visual viability. In the present case, that refers to qualitative and quantitative assessments, of flow properties and patterns, achieved through thermal image processing[80,88]. Hot water works well with the recipient, adapting to the flow velocity, through the cooling process and only contributing to minor disturbances caused by the change in density. In this sense, it is less intrusive than other chemical and solid tracers. Temperature distributions of the tracer in the area of equal specific heat capacity highlight the cohesion process(mixing, diffusion, dispersion) over time in small-scale spatial applications[42]. Also due to the prominent characteristic of heat radiation, they are noticeable through infrared thermography in in-caved streams and enclosed systems not exposed to light. The movement of thermal tracers(heat transport) injected into the water medium, is governed by three mechanisms: conduction, radiation, and convection. Heat transport can be approximated by Fourier's law (analogous to Fick's law in the 2nd chapter), which states that heat moves from regions of high energy to low energy [20]. An appropriate volume of thermal tracer needs to be used so that we don't disrupt the energy of the flow and to achieve an adequate concentration of the thermal plume. Mainly through the processes of thermal dispersion, the molecular state of the water environment is disrupted by lateral and longitudinal engagement of the thermal parcel in the mixing properties of the fluid, and in that free convection and thermal diffusion mostly contribute to the wide spread of heat. Richmann's law of mixing in the heat-exposed environment equates that two identical mediums will have the same final temperature after achieving thermodynamic equilibrium, which is achieved by the conduction

of heat. Heat preferentially infiltrates the soil at higher permeability spots due to the thermal conductivity of soil(0.37 to 1.42 W/(cm K)), which increases the heat emissivity factor in those areas[42,80]. For the thermal tracer experiments, water was heated in a kettle to a temperature of approximately 80°C and injected through cups(~ 20mL) and syringes at measured points. In the experiments, the average overland flow temperature was in the range of 18.0–20.0 °C. The temperature of water in the sink point detection phase was approximately 75-85°C distributed through a slug injection.

3.2.2. Dye tracers

Enrollment of this tracer during the experimental proceeding is concentrated on enhancing the qualitative state of the images, for the goal of defining surface flow velocities. The volume of the solute compound was produced by adding a red food coloring (10mL carmoisine dye (E122)) into a 200ml cup and diluting it with tap water. The mixture was then heated up and divided into tracer dosages of 20mL. Solute particles are governed by the advectiondispersion transport mechanism, which is more pronounced in these conditions due to the higher kinetic energy [37]. The double tracer is under the effect of hydrodynamic and thermal dispersion, which exhibits variability in space and time due to the surface roughness.

3.3. Experimental methodology

This section gives a summary of experimental trials performed for the purpose of investigating the issue of water loss, through the determination of following water movement towards the sink point. For the purpose of executing the planned methods, we will need to present input data and parameters, relevant to the problem we are trying to examine. Following that, an integrative approach was defined, which divides the experiment into two phases. The first phase consists of flooding through which we will examine the behavior of the natural water movement(runoff, shallow streams, etc.). And in the second phase, we will couple the flooding with an application of a thermal tracer, with means of tracing the leading edge of the tracer.

3.3.1. Laboratory conditions

Defining logistics for the experimental method of investigating water loss at a certain surface point, is important for correctly depicting the natural conditions, so parameters need to be defined. The case of study involves an adjustable shallow water discharge, across a plane soil surface, with single or multiple planned drainage spots, consisting of a coarse type of granular filling. Hence in order to perform a concise evaluation of the experimental findings, we must determine the conditions under which each experiment will be carried out. In regards to this, the following parameters are important:

Discharge rate

This is one of the prime initiators for achieving the laminar water flow state, which depicts the setting we are trying to simulate. Before starting the flooding process we need to determine the appropriate discharge rate, that will suffice the means of the experimental trial, due to the restricted geometry of the soil surface. Discharge has to be set up so that there is enough time to evaluate the hydrological conditions before water covers the experimental ground. This equates to smaller Reynolds numbers dictating streamlined flow conditions, that aren't achieved in the experiment due to nonuniform velocities and water depths[90]. If the rate of discharge approaches turbulent flow conditions, this might disrupt the investigation of the experiment, and in the case of very low stationary flow, the time of the whole experiment is notably extended(which is unfavorable in time-restricted circumstances). Maintaining the appointed flow rate is imperative for us to qualitatively and quantitatively frame the hydrological model's behavior[8]. After the injection of the dye tracer, hydrodynamic dispersion is governed by the flow velocity, so the discharge needs to be regulated so it doesn't cause irregularities in the spread of the solute parcel[37]. For that purpose, the constant discharge applied for the flooding is a result of a water tank standing at a fixed height difference of 1.5 meters in relation to the feeder box. And for the implementation of the second phase of the experiment, the discharge velocity of the thermal tracer needed to be calibrated, to make it applicable in the flooded environment. Applying thermal tracers changes the dynamic properties of water, so caution is set in choosing the favorable discharge rate, which should be a couple of magnitudes lower than the administered flow for flooding.

Sinkhole filling

The permeability will be the leading factor in determining the progression curve of our experiments. A porous medium is intended to be placed inside the sinkhole, that will mediate the extraction of the surface water. The seepage rate at the sinkhole will depend on the granulometry of the materials used for filling the hole. In that regard to that, coarse granular material will be used in the experiments, which presents a contrast to the fine-texture surrounding, and it will be categorized into groups depending on the grain size. This included coarse gravel and coarse sand, to establish the variations in time between accessing and exiting the sinkhole. The sinkhole diameter has to be picked according to the capacity of the sinkhole in the most pervious state because intake volume is limited depending on the space between the grains[85]. The layer of soil around the filling material, as well as the filtering medium, had to be well compacted, so as to prevent sagging of the soil edges or collapse of the grainy structure, as a result of the accelerated flow at that point or water pressure. Grainy materials make the best filtering solution for laminar flow rates, because of their high drainage properties[23]. Due to the gravitational pull near the edges of the sinkhole, the fluid's speed rate increases exponentially, causing an increase in the energy gradient from movement between the crudely shaped grains. Due to turbulence or generally, water rapidly flowing into the sinkhole, the top layer of grains is elevated and experiences drag on its way down. In case the filling isn't compacted well, more water gets into the sinkhole, albeit depending on the viscosity of water, as well as, the size and density of the grains, which impacts the settling speed of the grains[66].

Sinkhole displacement

This parameter is important for expanding the water diversion network and allowing for simultaneous observation of different hydrodynamic and property changes happening at, the individual sinkholes or between them. Depending on the number of sinkholes we choose we decrease the detection time, because of the increase in accessible pathways towards the sink point. That is represented through the flowlength, which corresponds to the level of hydraulic connectivity in the soil flume and is mostly influenced by topographic factors of the soil[84]. Due to the fact that we have no vegetation cover, and microtopographic features aren't pronounced because of the straightened and unfractured surface, this contributes to the overall connectivity of potential runoff paths. Flow connectivity works well in increasing velocities around the surface area and overall flux of the system[1,84]. The number of sinkholes will be increased sequentially after a set of experiments and also keep the diameter of the sinkholes the same so that the geometric conditions under which the experiment is done stay continuous.

3.3.2 Flooding phase

After the introduction of parameters described in '*Section 3.3.1*', they are implemented in the flooding phase of our experiment. A physical model stationed in the Hydraulics laboratory was established, over a couple of weeks for experimental trials involving arial flooding of the soil surface. To describe the temporal and spatial variability of water movement through the surface, we needed to capture the ongoing process in real-time and after that determine the viable representative time increments. The flooding was mostly done during the later morning, due to the better lighting in the laboratory. The sinkhole either hadn't been constructed during the flooding phase or it was covered up. Specific points on the soil surface had been marked with 16 pins, placed at an equal distance of 40cm from each other and the edges of the flume, as shown in *Figure.3.3*. This formation represented a grid with each pin being a source point for injecting the double tracer, sometime after the waterfront has passed the marked point. The output of water was initiated by turning the valve of the water tank, which started filling up the feeder box to a certain level. At that point water started flowing out on the downstream end of the flume under a constant discharge of Q_F= 0,145 L/s, presented in *Figure.3.4*. The GoPro camera started filming, following the progression of the wavefront across the soil surface. Water slowly started covering the marked point on the surface, through lateral and medial spreading, and as mentioned the double tracer was injected following the expansion of the water cover. The spreading of the solute plume in the water was recorded for estimating overland flow velocities at different points, by following the movement of the tracer leading edge. Tracer injections were repeated at the same spots so that the velocity estimation could be done, with minimal marginal error. The flooding process lasted until the water covered the whole surface area and the average depth of around 1-2cm was achieved. At that point, the inflow of water would be stopped and a sinkhole would be excavated using a 5 cm cylinder, so the flooded surface can be used in the second phase of the experiment. The flooded area serves as a plot for visualizing hydraulic processes through tracer applications. The flooding period would vary depending on the soil moisture content, for example, if the soil was saturated then water would achieve a specific depth uniformly in a shorter period of time, as a result of saturation and infiltration excess(discussed in the *2. Chapter*). In that case, saturated or wet soil is more preferable from a time-saving standpoint, than the dry soil layer.
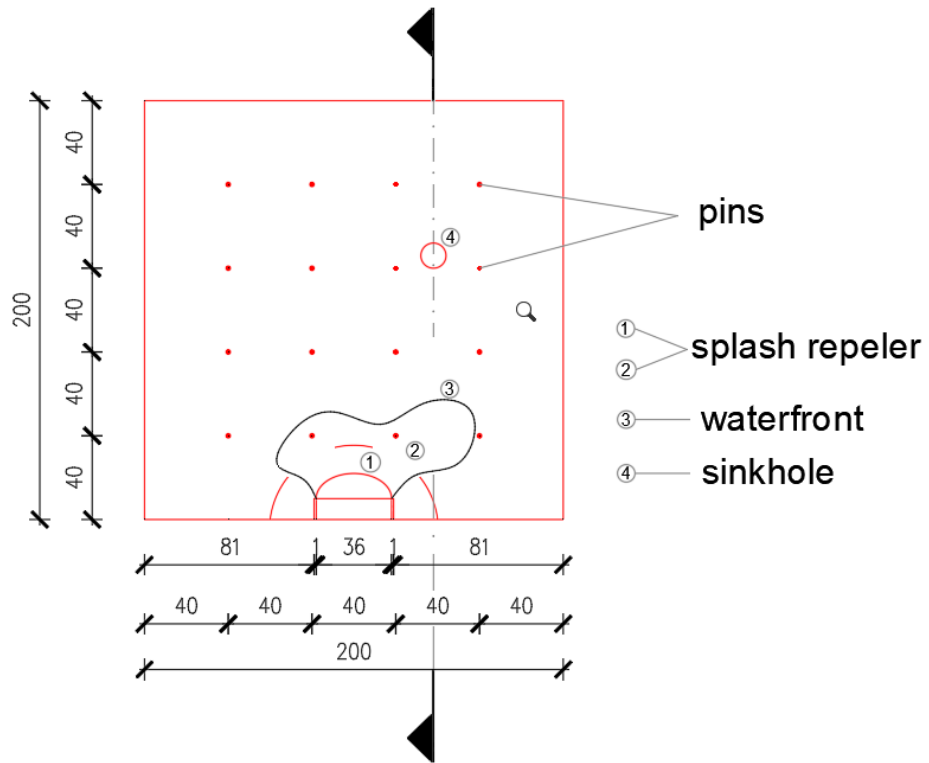
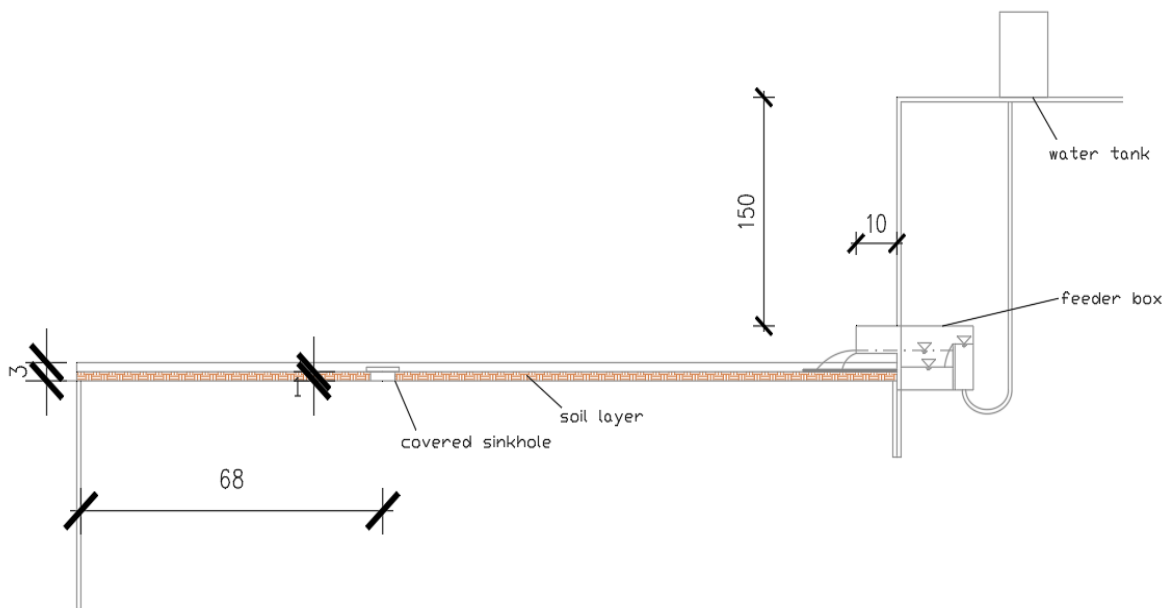*Figure.3.3 Layout of the soil flume during the flooding phase(M 1:100)*


Figure.3.4 Cross-section of the laboratory setup during flooding phase(M 1:100)

3.3.3 Sinkpoint detection using thermal tracers

The second phase of the experiment is a continuation, of the experimental trial described in the previous *Section 3.3.2*. Laboratory parameters described in *Section 3.3.1*, will be combined in a study case for each experimental trial involving sink point detection and altered after each experiment so various conditions are tested. Hence parameter combinations are made with one of: two values of thermal discharge rates, three types of sinkhole materials, and one to three designated positions of the sinkhole. From *Figure 3.5* it is shown that each sinkhole was dug up at a specific position in the soil plane, after which it is filled with granular material of varying permeability, as presented in *Figure 3.6* and *Figure 3.7*. The first experiments were done with combinations involving 1 sinkhole, and after that sinkholes were dug subsequently following the testing of each possible set of combinations involving one or more sinkholes. Positions of the sinkholes were chosen according to the movement of water recorded in *Section 3.3.2* so that they are placed at a distance(suggested in *Figure 3.5*) that favors a clear concentration of the thermal tracer, seen through the infrared image.
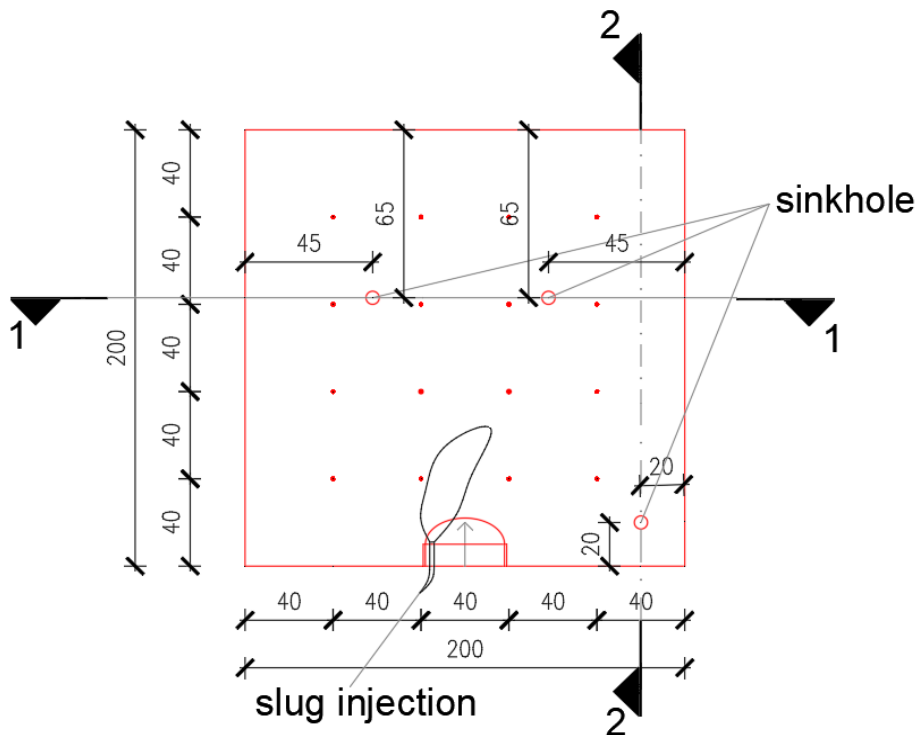
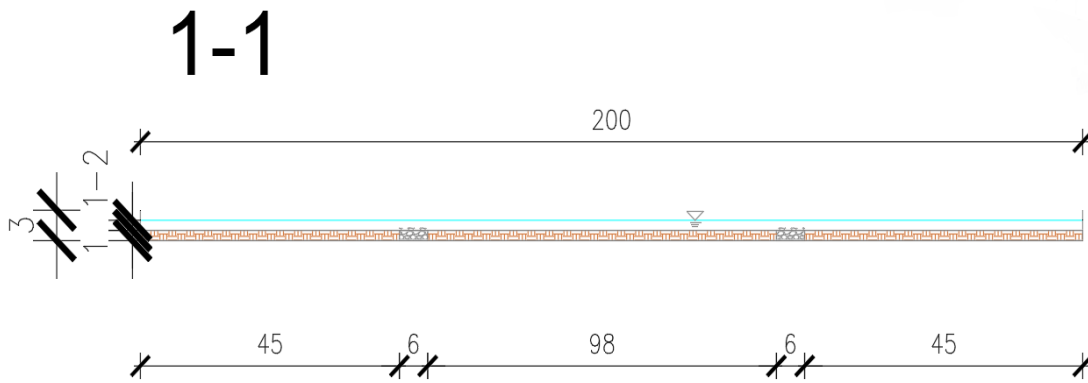*Figure.3.5 Layout of the soil flume with 3 sinkholes during the sink point detection phase (M 1:100)*

1-1

Figure.3.6 Horizontal cross-section through the 2 top sinkholes during the sink point detection phase (M 1:100)
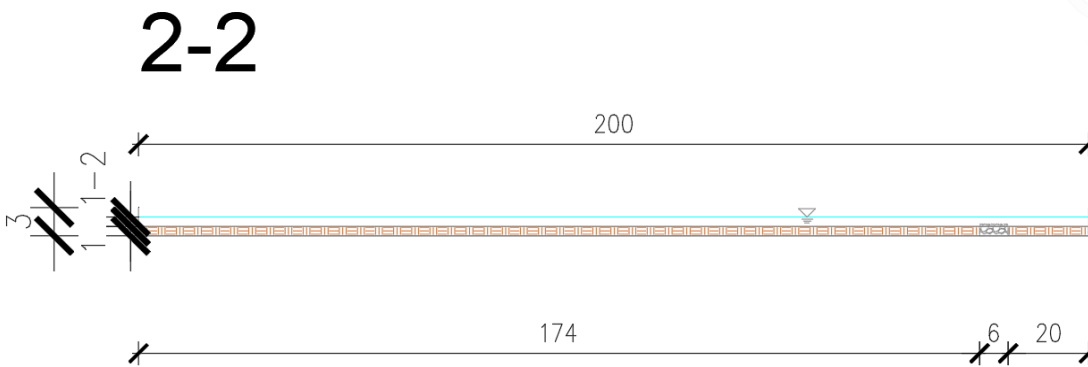
2-2

Figure.3.7 Horizontal cross-section through the 2 top sinkholes during the sink point detection phase (M 1:100)

Before applying the thermal tracer the discharge rate needs to be configurated through volumetric measuring. Several samples of hot water output into a flask were measured during a span of 10 seconds and then weighed to determine the discharge value. After which a comparison was done and two discharge rates: $Q_{D1}=0,025$ L/s and $Q_{D2}=0,035$ L/s, of the thermal tracer, were used in the experiments. To check if the frame of the infra-red camera is centralized so it captures the edges of the flume, we put 4 cups of hot water at each corner of the flume. Hot water was applied to the water bed created from flooding the flume, through a slug injection on the upstream end of the flume, as it can be seen on *Figure 3.5*. For the initial experiment, the lower discharge rate was used first, and then the higher value; this order was maintained during all experiments. The infra-red camera recorded the movement of the tracer leading edge until it reached the sink point (or points), as well as after the fact to reassure our claim.

4. ANALYSIS AND RESULTS

This chapter consists of an analysis and discussion of the results gathered from the experimental trials conducted in *Chapter.3.* and is divided into two sections. In the first section, results are presented through a temporal water movement sequence, as well as charts and maps signifying water-based properties and processes. The second section presents the results of the thermographic procedure for detecting the sink point in the soil flume, coupled with a summary of those results.

4.1 Flooding phase

The first phase of the experiment describes the shallow water system, by assessing the main aspects of water spread through the soil surface. Visual recordings and thermal images, serve as the basis for extracting quantitative and qualitative data. In the soil flume experiments, the validation of the data is dependent on the conditions and equipment used during the experiments[86]. Analysis of the flooding phase is performed from the moment water enters the system until we collect the last piece of data.

4.1.1 Area of water spread

The sequence in *Figure 4.1* represents the development of the waterfront from the time close to the beginning of the experiment until the flume surface is flooded. Visual cases of the water coverage were chosen based on the accumulation of water on the soil surface and the temporal difference between individual flooded areas. These factors accounted for the continuous spread of the waterfront which is shown through images that have an appropriate(scaled) temporal and spatial difference between the water-covered area.
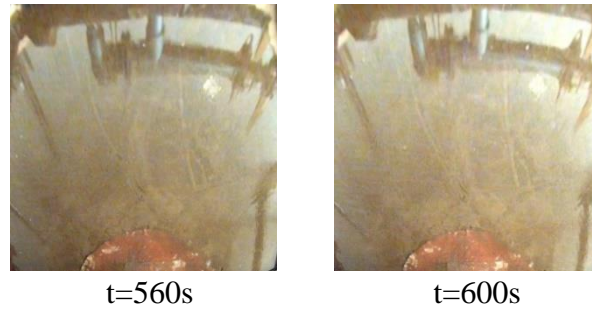

| t=0s | t=30s | t=60s | t=120s |

| t=180s | t=240s | t=360s | t=480s |

| t=560s | t=600s |
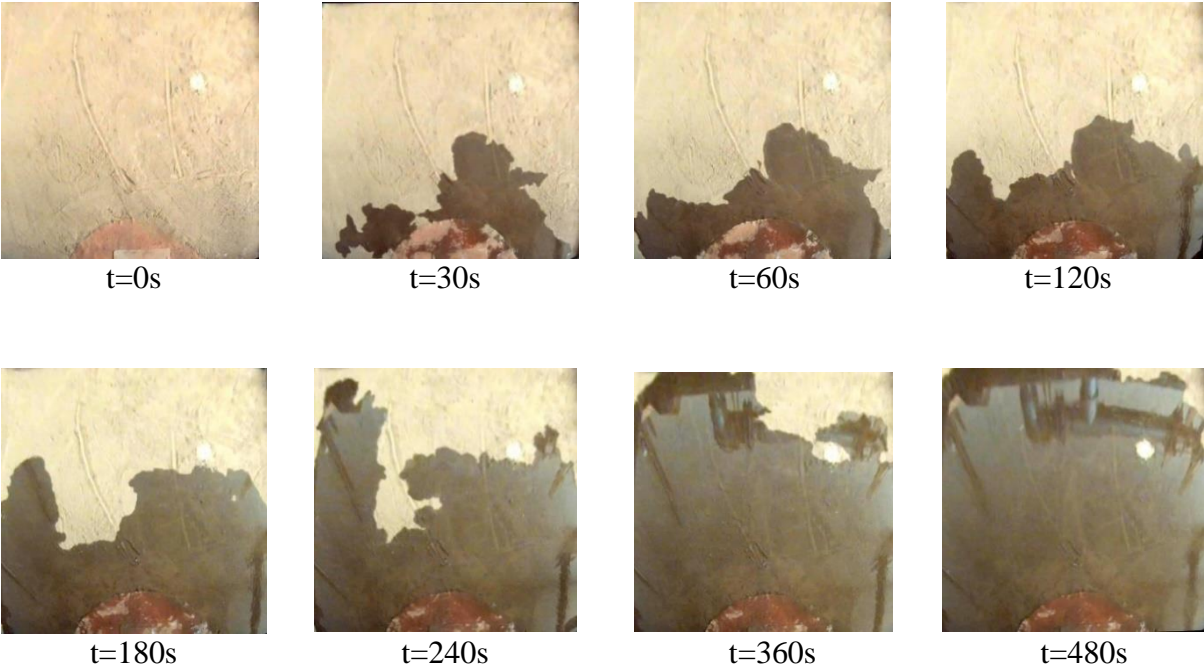
Figure.4.1 Top view of the water cover across the soil flume

At the beginning of the experiment, the velocity of the waterfront matches the discharge velocity, due to the negligible friction between the water layer and the smooth mat. Water exiting the feeder box at the upstream part moves primarily in the longitudinal direction towards the downstream part of the flume. Although at the beginning the flow was diverted laterally due to the uneven discharge of water from the feeder box flume until the discharge of water reaches a stable rate. In these beginning moments velocity of the waterfront approximately matches the discharge velocity. In the first 20 seconds, the waterfront progresses in all directions, as a cause of water being channelized through rills and other irregularities(slight depressions, fissures, furrows) on the soil surface throughout the area. During this time the velocity of the waterfront gradually decreases, due to friction caused by the heterogeneous surface roughness, with exceptions where the velocity increases due to the connection of the adjacent streams or streamlining. At the time point of 30 seconds, in   *Figure 4.3*, it can be observed that an exponential rise in flooded area and perimeter was realized, when comparing the values of this time increment to the ones following it. The high value of waterfront length results from irregular sheet flow across the flume and the rapid rise in the flooded area is due to the velocity of the waterfront slightly decreasing, with being a short distance away front the inflow point [91]. After the half-minute mark(30 seconds) the streams from all sides have connected and sheet flow can be observed for the whole water-covered area, as it is portrayed in *Figure 4.3*. with a decline in value on the waterfront length function. From the first 30 seconds until 120 seconds, the flooded area is growing at a uniform speed. Due to the slow infiltration rate, most of the water volume gets distributed on the surface, where ponding occurs in certain shallow areas[92]. During the time between 60 seconds and 120 seconds, the waterfront reaches the edges of the flume and starts spreading towards the downstream end of the flume as seen in *Figure 4.1*, at which time the development of the flooded perimeter is almost linear *Figure 4.3*. At the very edge of the flume, the velocity is 0 due to the no-slip condition, so the movement of the water is governed by the incoming flow and its reflection off the edge, which results in an increase in volume along the edge[26]. The rise in the flooded area is relatively linear for 4 minutes from 120 seconds until 360 seconds as depicted in *Figure 4.3*. During this time a peak in the flooded perimeter is achieved, due to the slight difference in elevation on one part of the flume surface, which covers up in time with the climb in water level. Once the water gets to the sinkhole it slowly starts to seep into the grainy structure. Because of the separate consistency of the sinkhole and soil, the water moves around the sinkhole and joins together with the waterfront from the opposite side which has already reached the upstream end of the flume(Figure 4.1). In *Figure 4.3*, until the 480th second, the waterfront progresses steadily, while the area rises in value and the perimeter decreases. From that time water at the bottom end reaches a considerable depth (close to 3 cm) and continues uniformly spreading towards the upstream right corner. The process of covering the last corner of the flume and the sinkhole takes 2 minutes, due to the seepage rate of the sinkhole and curved surface area along the right corner. This happens during the time interval of 480 to 600 seconds, where both the area and perimeter

graphs in Figure 4.3 achieve an approximately constant value. The experiment is finalized at 600 seconds, at which time the water has achieved a considerable depth of ~5cm. This makes for a good time frame when taking into account the erosive energy that a higher flow could distribute and the optimal flow for the outlet size[93]. Based on the basic infiltration rate for the loamy soil(20-30mm/h) and taking into account the length of the experiment, we can determine that the water didn't permeate enough of the soil profile to slow down the surface runoff through leaking
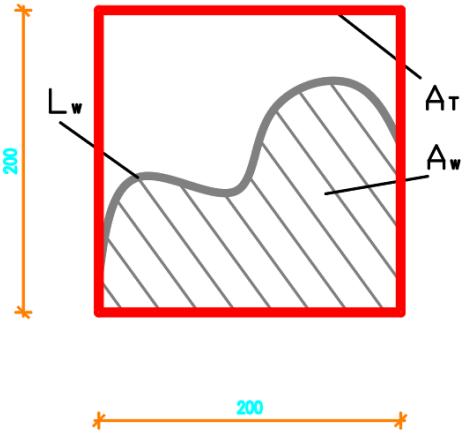

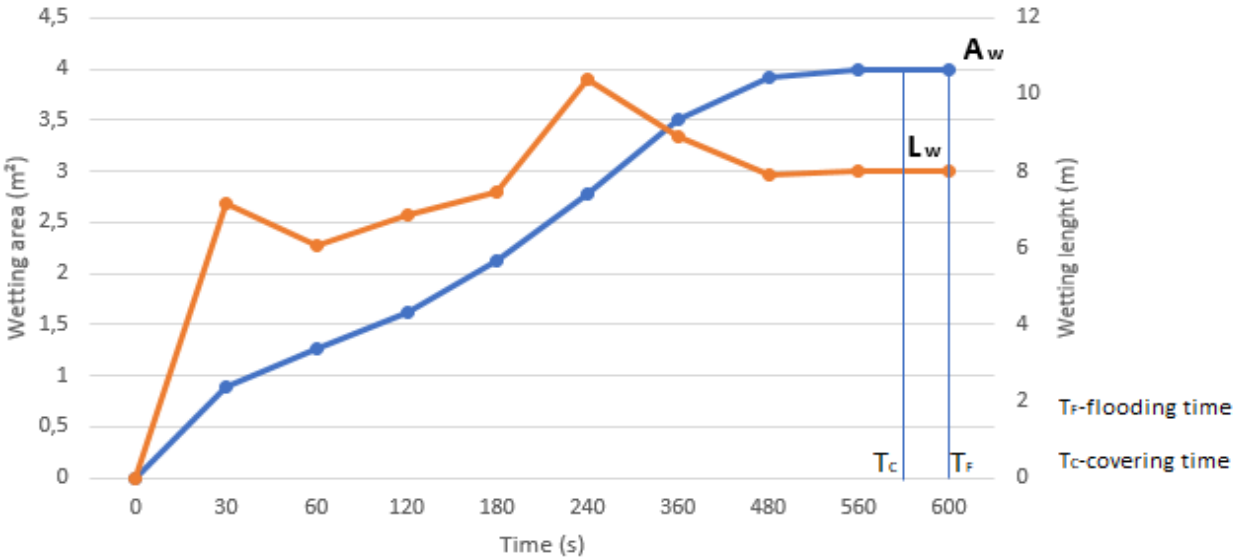*Figure.4.2 Illustrative sketch of the wetted area*

Figure.4.3 Progression curve of the wetting area (AW) and wetting length (LW), with a legend

4.1.2 Velocity field

Shallow overland flow velocities were defined through infrared thermographic observation and software analysis. The process of tracing the movement of the opaque plume was performed with both the dye tracer and the thermal tracer. Nevertheless, the thermal tracer contributed clearer results in comparison to the dye tracer, which suffered from the loss of transparency, as shown in *Figure 4.4*. The velocity of the thermal plume taken as an example, from *Figure 4.4,*

was calculated through the usual velocity equation(v=s/t), where the value Dx1 represents the distance between the leading edge at the time(t) and time(t+Dt), and value Dx2 represents the distance between the leading edge at the time(t) and time(t+2Dt). Each image was recorded in succession, with a 1second gap. At the point of injection, the thermal plumes spread through the water medium, because of the governing processes of convection and thermal diffusion. Following the movement of the thermal plume, heat energy is transferred and lost with time, because of the following overlapping processes: conduction, radiation, and evaporation[25,94]. Because the injection of the hot dye, happened a little while, after the waterfront crossed the pinned location, the movement of the thermal plume is very expressive. This is a result of heat energy entering the wetted soil really quickly(because of the shallow depth of the flooded area), because it has the same emissivity coefficient as water[77].
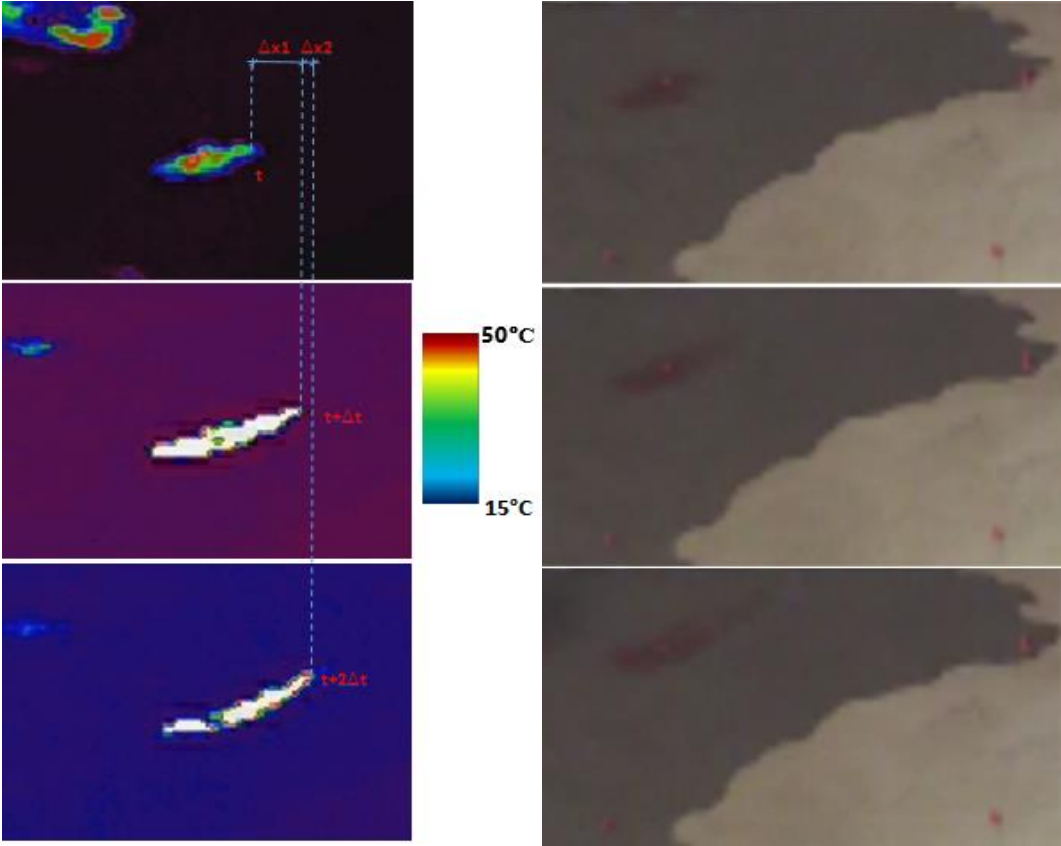

Figure 4.4 Side-by-side comparison of thermal(left side) and dye(right side) tracer's transport time

To understand the behavior of the water flow in the flooding phase, through the change in velocity value and direction at each tracer injection point, we have defined a velocity map *Figure 4.5*. The travel distance of every thermal plume, from its point of injection, was calculated through the use of software applications. Firstly for every tracer injection, three representative images were picked out, at time spots that show the development of the tracer mark, which were gathered through thermographic imaging. For every thermal plume, the displacement vector was constructed in AutoCad, by connecting the starting leading edge of the tracer(top picture- *Figure 4.4*) with a projected coordinate that defines the leading edge of the tracer after a noted period of time(bottom picture-*Figure 4.4*). The coordinates of the leading edge of both thermal plumes had to be defined in the same temperature range, as shown in

Figure 4.4. After the displacement vector has been appointed to the image, the correction of the vector image was done through CamScanner which provides a top view disposition, and it was imported into Gimp software for accurate scaling of the travel distances in regards to the actual flume geometry. Through this process and manual calculation, travel distance values were defined, as well as the velocity vector and its direction in relation to the flume edges.

The movement and energy distribution of the hot dye is dependent on the topographic, hydraulic, and thermal features of the surrounding, which are important in defining the velocity vectors in *Figure 4.5*. The velocity map was constructed by appointing the value and direction of the dominant velocity measured through thermal tracing at each point in the pinned area. Looking at *Figure 4.5*., we can see that the velocity experiences the highest values during the beginning stages of the flooding and throughout the left side of the flume. The reason for this is the higher rate of flow on the left side of the flume and also the nonconservative aspect of the thermal tracer, which contributes to lower thermal diffusion under higher values of flow rate [37]. Due to the volume of 20mL and temperature threshold of around 50°C, the thermal mark kept a higher temperature longer without dissipating and in these cases was more distinguishable on the infrared image than in the case where we recorded lower velocities[44,45]. At some injection points in *Figure 4.5*, the spread of the thermal mark is divided into two or three directions, due to the variations in the velocity profile at those points[26]. It is also important to point out that the injection of the tracer plays a big part in the formation of the velocity vectors. In the case of lower flow velocities at the injection point there is an initial disruption of the flow after the injection, and for higher values of velocity, the hot dye just inputs into the flow[45,77]. In cases where the convection and diffusion outmatch the flooding velocity, there is a lateral and longitudinal separation of the velocity vector. Significantly lower values of velocity are seen in the second row and the top row in *Figure 4.5*, as a consequence of a short traveling distance of the thermal mark in a larger time period, towards the waterfront(which expands slowly), or the edge of the flume. The thermal mark right on the tip or closer to the waterfront will have a higher concentration time, due to the hot water exchanging energy with the soil as it moves. After a couple of tracer injections, a cooling period is needed so that the flooded area achieves thermal equilibrium through a cooler temperature.
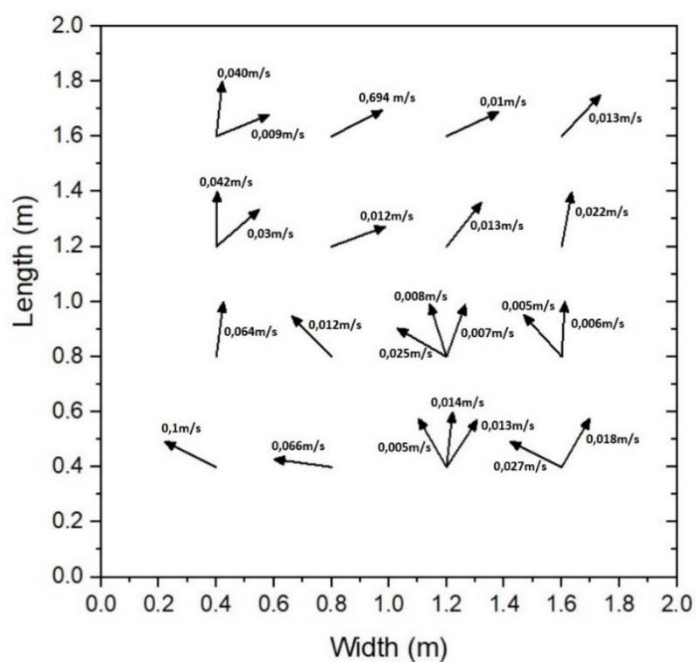
Slika 4.5 Velocity map

4.2 Sink point detection phase

Analysis of all of the experimental trials mentioned in the 3rd Chapter, which are determined through a combination of variable parameters, is too extensive for the purpose of this master's work. That is why we will be reviewing the cases that yielded the most favorable results during our analysis. All for the means of quantitatively and qualitatively describing the detecting process for all three displacements of the sinkhole in the soil flume. All of the experimental cases described ahead had a higher permeability of the sinkhole.

4.2.1 Detection analysis for the case of 1 sinkhole

The infrared thermal images in Figure 4.6 present the movement of the hot water towards the sinkhole, which consists of gravel-sized grains; in a required time frame, under a constant discharge Q_{D2}(mentioned in *Section 3.3.3*). Considering the first set of experiments was performed for only one sinkhole, we had 4 different cases to analyze. The case which contributed the most favorable results was the one in *Figure 4.6,* which involves a higher discharge rate and a higher permeability of the sinkhole.
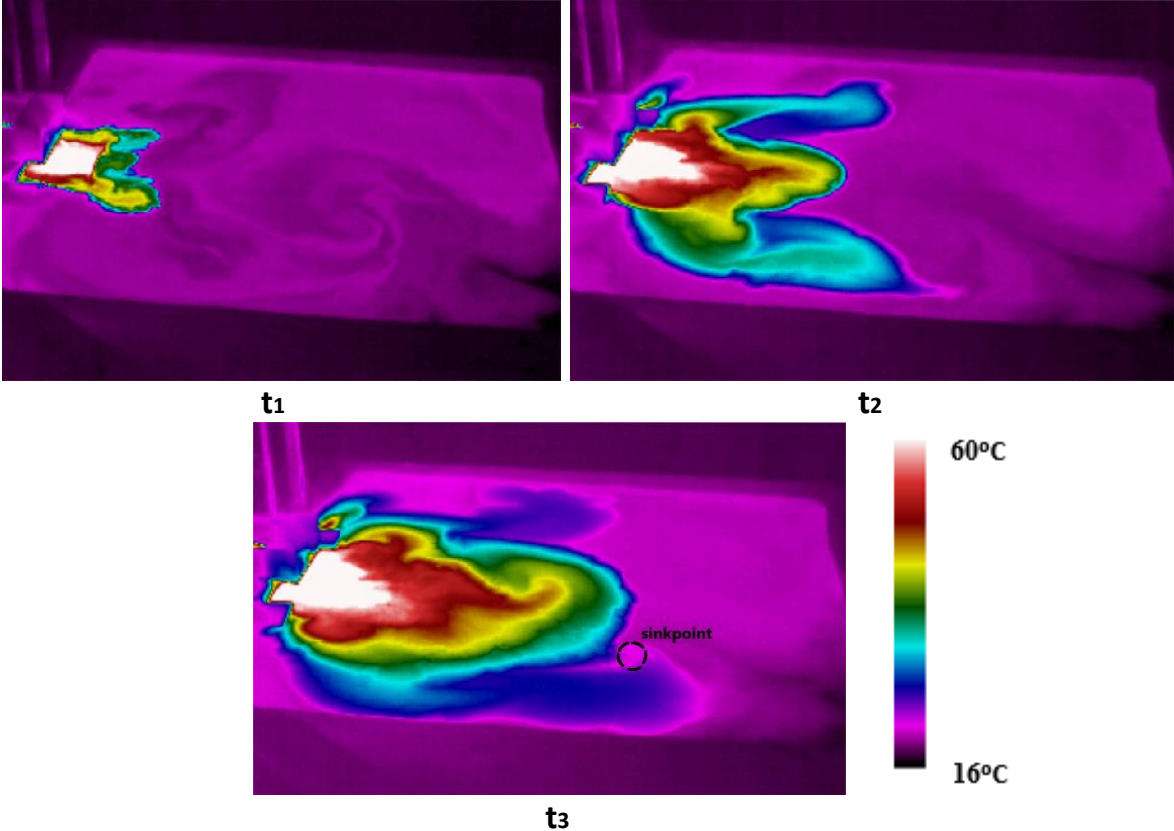
Figure 4.6 Tracking the movement of the thermal tracer toward the sinkhole

Before the slug injection of the hot water, the water retained on the soil surface after the flooding is drawn towards the constructed sinkhole which in this case exhibits a high permeability rate. The movement of water towards this point is a state of the fact that water moves from a position of higher hydrostatic pressure toward lower hydrostatic pressure[24]. This as well as gravity is one of the factors that have an influence on the direction in which

the leading edge thermal plume will spread, along with the discharge rate. Concerning the discharge rate in *Figure 4.6.*, during the beginning stage t_1 three breakthrough curves start forming on each side and the middle of the thermal plume; this formation is more distinct in the later stages t_2=58 sec and t_3=2,07 min. This is due to the high velocity under which the hot water flows and starts accumulating in the longitudinal direction. Although right after the initial intake of the hot water the flow direction slightly deviates, due to the splash on the flooded surface and it starts spreading on both sides of the central axis of the flume. Apart from the mentioned factors, the thermal properties of water also have an influence on the formation of the thermal plume. As it has already been mentioned due to the high discharge and attraction force towards the sinkpoint, we observe the development of the thermal mark, but these factors also contribute to a higher longitudinal hydrodynamic dispersion(convection+ diffusion) rate[42,96]. At the time t_1 in *Figure 4.6.,* this phenomenon isn't distinguishable because of: -the ponding of the hot water at the upstream end, - the high specific heat capacity of water(more time for heating and cooling), - a small time period for heat distribution in regards to the beginning of the experiment. The follow-up infrared image captured at time t_2 provides a more distinguishable form of the thermal plume. Due to the mixing properties and kinetic energy distribution, the developed breakthrough thermal curves at each side, cover a longer surface area although with a lower value of temperature in comparison to the middle thermal curve. The area around the central axis is maintained at a heightened temperature due to a constant high rate of discharge which concentrates the flow longitudinally[98]. The image captured at the time t_3 represents approximately the time of discovery of the sinkpoint, which is characterized by the elongation of the leading edge thermal plume towards that point and the decrease in temperature of the right breakthrough thermal curve around that point. To further analyze the thermal gradient, at each point on the flooded surface for the observed point in time t_3(Figure 4.6.), thermal graphs were constructed at determined cross-sections as depicted in *Figure 4.7*. According to *Figure 4.7.*, the highest values of temperature were achieved closest to the upstream end of the flume at the distance of 1-1,5m because of the already mentioned reasons. At the level with the sinkpoint temperature values are evenly matched on the left side of the flume and then experience an exponential climb from the middle towards the right side of the flume. The registered value of temperature at the sinkpoint is T=23,7°C in accordance with the elongated thermal mark captured in Figure 4.6. For the final cross-section, the temperature values around the flooded area mostly uniformly matched, with higher values than at the beginning of the experiment, due to the flooded area trying to achieve thermal equilibrium[25,98].
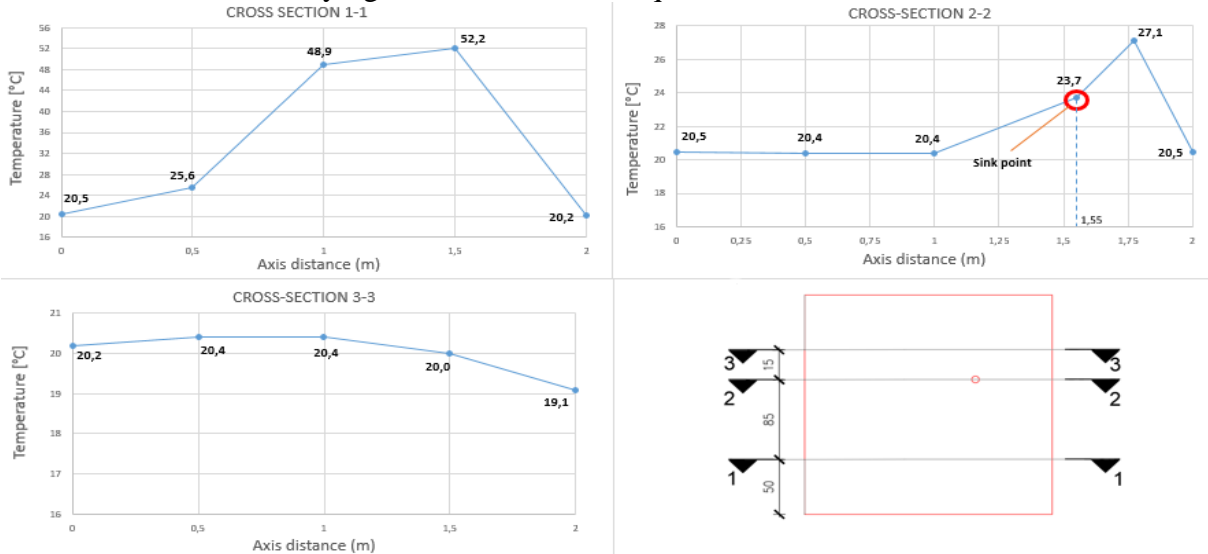

Figure 4.7 Temperature graph at each defined cross-section of the flooded surface

4.2.2 Detection analysis for the case of 2 sinkholes

The infrared thermal images in *Figure 4.9.*, present the movement of the hot water towards the sinkholes, which consist of gravel-sized grains; in a required time frame, under a constant discharge Q_{D1}(mentioned in *Section 3.3.3*). The second set of experiments was performed for two sinkholes, one symmetrical in regards to the previous one in *Section 4.2.1.*, which contributed to 6 different cases to analyze. The case which contributed the most favorable results(because of the quality response of the experimental method) was the one in *Figure 4.8.*, which involves a lower discharge rate and a higher permeability of the sinkholes.
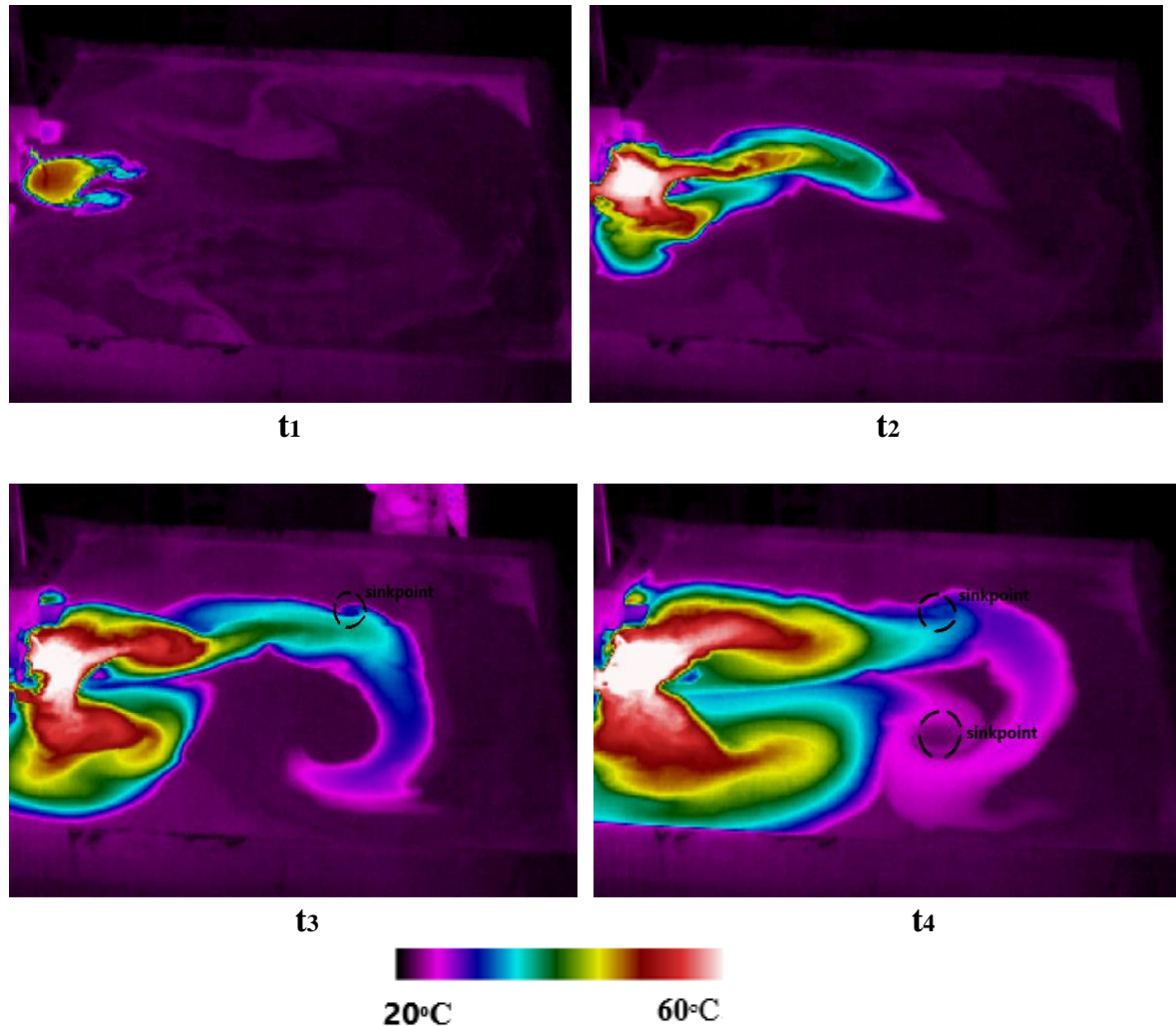
Figure 4.8 Tracking the movement of the thermal tracer toward the two sinkholes

In reference to the previous *Section 4.4.2.*, this experiment opens a new pathway for water to escape, hence enhancing the attraction force of the water towards the sinkhole. Because both sinkholes are of the same diameter and consistency, they achieve equilibrium in the seepage rate[24]. As we can see at time t1 in *Figure 4.8.*, under a slower discharge rate the thermal plume accumulates near the upstream end of the flume and two breakthrough curves are formed following the attraction force of the opposite sinkholes. Over time the lower discharge rates contribute mostly to the lateral spread of the thermal plume, all the while enhancing the longitudinal spread in both directions[97]. At time $t_2=39$ sec there is a clear distinction between the two breakthrough curves referenced by the high-temperature value, where the left

side has a more expanded reach than the right side. This is due to the more accessible pathway based on surface irregularities on the left side of the flume, which increases the flow toward that point(as it was seen in *Figure 4.1.*). The position of the left sinkhole is discovered at the time point t_3=1,25min, by the formation of a vortex in *Figure 4.8.* This happens as a result of the Coriolis effect when the leading edge thermal plume reaches the proximity of the sinkhole, at which point a singular swirl motion increases its momentum towards the center of the sinkhole[99,100]. In this case, we see another breakthrough curve forming from the thermal plume leading up to the left sinkhole, where under the swirling momentum a breakthrough curve is formed which gets diverted toward the right sinkhole led by the attraction force[98]. Finally at the time t_4=2,42min the right sinkhole has been detected, through the same means as the one opposite to it. Here the thermal plume leading edge from the bottom right side which has been slowly gaining speed during this time, merges with the one that came from the left side of the flume. When talking about heat distribution across the flume, since lower discharge values correlate with a higher lateral dispersion rate, at the time point of t_2 and t_3, it is noticeable that the temperature is mostly evenly distributed along the upstream section of the flume[42]. The exception here is the left breakthrough curve of the thermal plume, which experiences a higher temperature at a broader scale, due to the concentration of the flow on that side, as is seen in *Figure 4.8.* The temperature value of the sinkhole at the time spot t_3 in *Figure 4.8.* is T=30,5°C due to the thermal capacity on that route reaching a significant value quicker. To further analyze the thermal gradient, at each point on the flooded surface for the observed point in time t_4(*Figure 4.8.*), thermal graphs were constructed at determined cross-sections as depicted in *Figure 4.9.* According to *Figure 4.9.*, the highest values of temperature were achieved closest to the upstream end of the flume at the distance of 1-1,5m, because of the highlighted lateral spread from the beginning of the experiment, which contributed to the increase in temperature over time. At the cross-section in level with the sinkpoints, the temperature value on the left sinkpoint is higher than on the right sinkpoint. The reason for this is the difference in thermal gradient at each point where for the left sinkhole the temperature value around that area has reached a certain threshold T=31,7°C, and on the right sinkhole, the temperature T=22,4°C is kept stable under the swirling motion[103]. At the very last cross-section in *Figure 4.9.*, the temperature values are mostly different along the width of the flume, and this is due to the higher rate of mixing of the hot water with the room temperature water at the upstream end, as a result of swirling momentum.
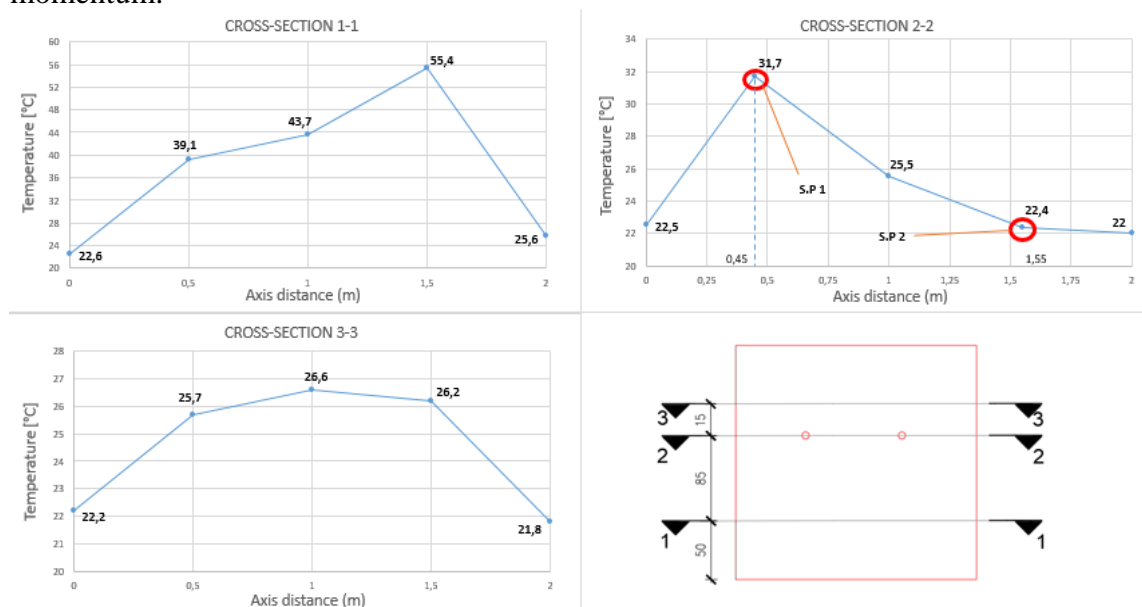

Figure 4.9 Temperature graph at each defined cross-section of the flooded surface

4.2.3 Detection analysis for the case of 3 sinkholes

The infrared thermal images in *Figure 4.10* present the movement of the hot water towards the sinkhole, which consists of gravel-sized grains; in a required time frame, under a constant discharge Q_{D2}(mentioned in *Section 3.3.3*). The third set of experiments was performed for three sinkholes, two sinkholes from the previous *Section 4.2.2.*, were kept at the same position with an additional sinkhole in the upstream right corner. This experimental formation contributed to 8 different cases to analyze. The case which contributed the most favorable results was the one in *Figure 4.10.*, which involves a higher discharge rate and a higher permeability of the sinkholes.
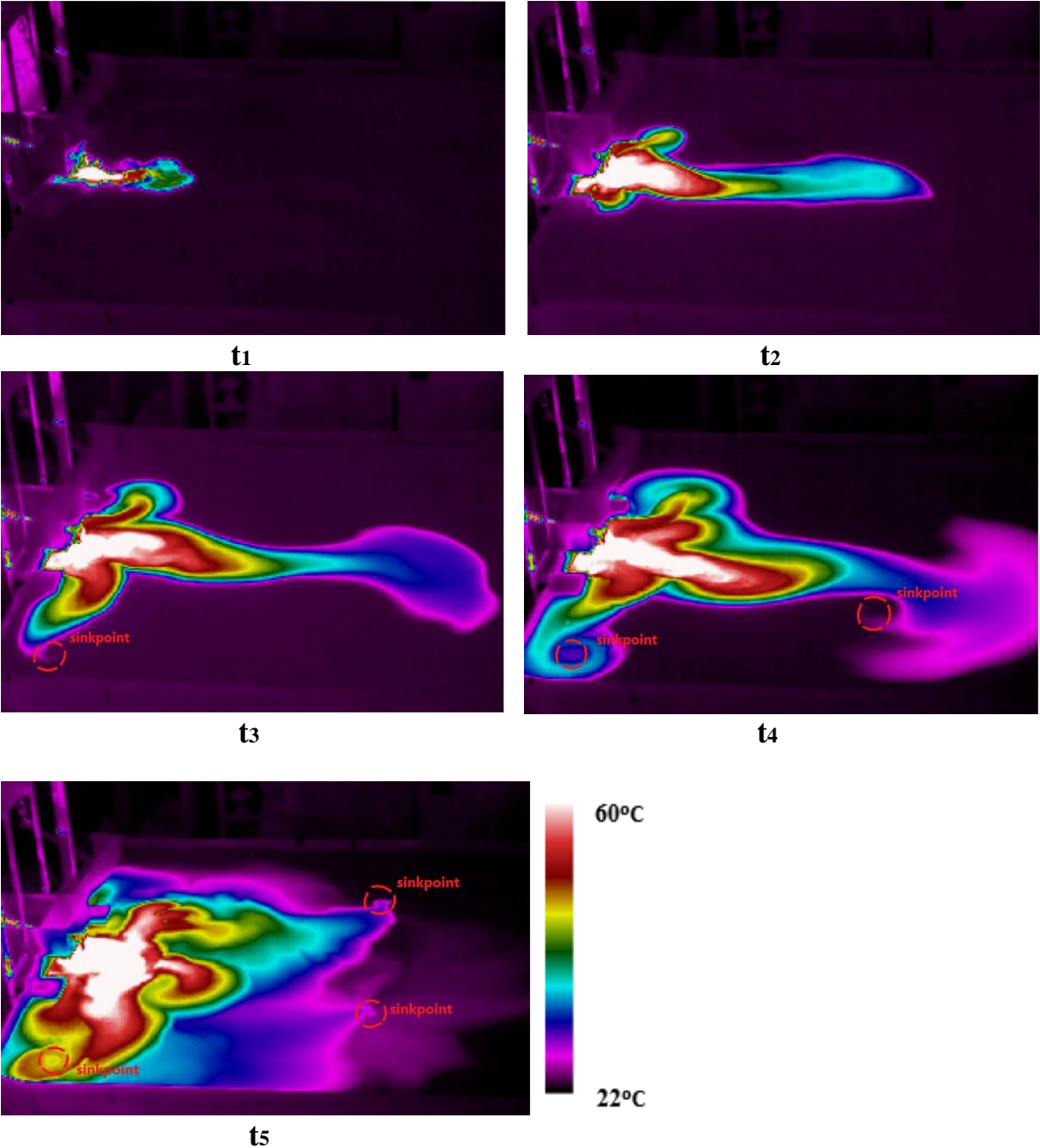
Figure 4.10 Tracking the movement of the thermal tracer toward the three sinkholes

The previously discussed phenomenon of water attraction(*Section 4.4.1-4.4.2*) is now enhanced by the presence of a third sinkhole[24]. The location was defined specifically near

the corner of the flume to test out the effectiveness of the lateral spread of the thermal tracer. The *Figure 4.10.* shows that in the beginning stage t_1 the thermal plume spreads mainly along the middle of the flume, with rifts among streamlines in the leading edge of the tracer due to the dispersion rate[42]. This continues on, for some time, as we can see at the time point $t_2=28$ sec, due to the increase in flow cultivated from the attraction forces of the downstream sinkholes and the high discharge rate. At this time we can also see a breakthrough curve forming on both sides of the thermal plume, which is on one side caused by the attractive force of the sinkhole, but also by the turbulence in the upstream end resulting from the high temperature. The detection of the first sinkhole occurs at $t_3=1,04$ min, and it is characterized by the elongation of the leading edge thermal plume, caused by the swirling around the sinkhole, recognized in later stages t_4, t_5. At this time, the thermal plume continues flowing down the middle, due to the attraction force of the symmetrical and identical, until it reaches the downstream end of the flume before the time t_4. A new sinkhole has been detected at the time point $t_4=1,57$ min, through a swirling motion around the sinkhole of the thermal curve which extended its reach from the middle and downstream part after reflecting off of the edge of the flume[95,96]. After that, the detection of the last sinkhole doesn't occur for quite some time, due to the flow of the thermal tracer being concentrated on the already established pathways. Finally, the detection is registered at the time $t_5=6,20$ minutes, as a result of temperature expansion into the more regions of lower temperature and the acting force of attraction towards that point creates a vortex[101]. The temperature gradient was mostly consistent with the flow of the thermal tracer throughout the experiment. In the beginning stages t_1 and t_2, due to the high velocity in the middle region, the high temperature is mostly kept near the upstream end and decreases with length. This is due to the primary mechanism of radiation and conduction, under which the tracer losses the temperature value, as well as the secondary mechanism of hydrodynamic dispersion which increases mixing with the surrounding water[25,98]. Only at the time point t_3 and t_4, there is a lateral expansion of the thermal plume on the upstream end, due to the accumulation of hot water at the outlet. Firstly the discovered sinkhole at the time t_3 has a temperature of T=25,2°C, after which the sinkhole discovered at time t_4 has a temperature of T=23,8°C. The thermal plume that was lead all the way across the length of the flume reflects off the edge of the flume and mixes with the downstream surrounding water. This increases the area and effectiveness of heat distribution due to the change in heat capacity value in that region. At the time t_5 the region of high temperature has expanded due to the mixing of hot water and connections among flows of hot water. The high temperature in the previous time t_4 has cooled off around the sinkhole with only a thermal link coming from the upstream region. From the image, at time t_5 it is also distinguishable that the left sinkhole was discovered by the extended thermal curve that was reflected off the bottom edge of the flume at the time t_4[95]. To further analyze the thermal gradient, at each point on the flooded surface for the observed point in time t_5(Figure 4.10.), thermal graphs were constructed at determined cross-sections as depicted in *Figure 4.11.* and *Figure 4.12*. Because of the large area of temperature distribution, thermal graphs were constructed for both the x and y directions of the crosssection. According to *Figure 4.11.* and *Figure 4.12.*, the highest values of temperature were achieved closest to the upstream end of the flume at the distance of 1-1,9m, because of the long time period needed to increase the temperature in that region exponentially. At this cross-section, the temperature value of the upstream sinkhole is T=48,6°C which is a maximum value in the longitudinal direction(Figure 4.12.), but not in the lateral direction(*Figure 4.11*). At the cross-section at the level with the top sinkpoints, the temperature value on the left sinkpoint is higher than on the right sinkpoint, as evident in *Figure 4.11.* The reason for this is the highlighted increase in temperature around the left sinkhole where the temperature is T=30,6°C, which we can see in Figure 4.10., due to the concentration of flow. On the right sinkhole, the temperature

T=27,5°C is lower than on the right one due to the cooling and withdrawal of flow in this region. Both temperature values don't present maximum values in the longitudinal direction, due to the prevailing high temperatures in the upstream region. At the very last cross-section in *Figure 4.9.*, the temperature values are mostly different along the middle-right width of the flume, due to the mentioned reflection of the bottom edge of the flume.
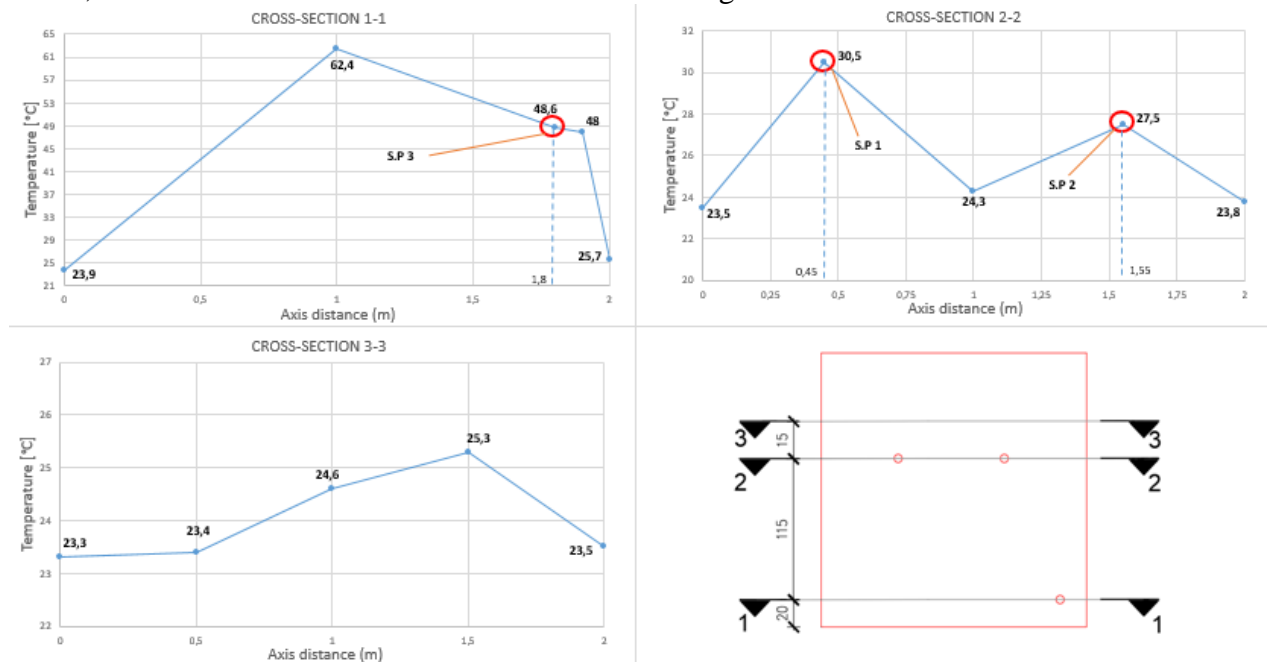

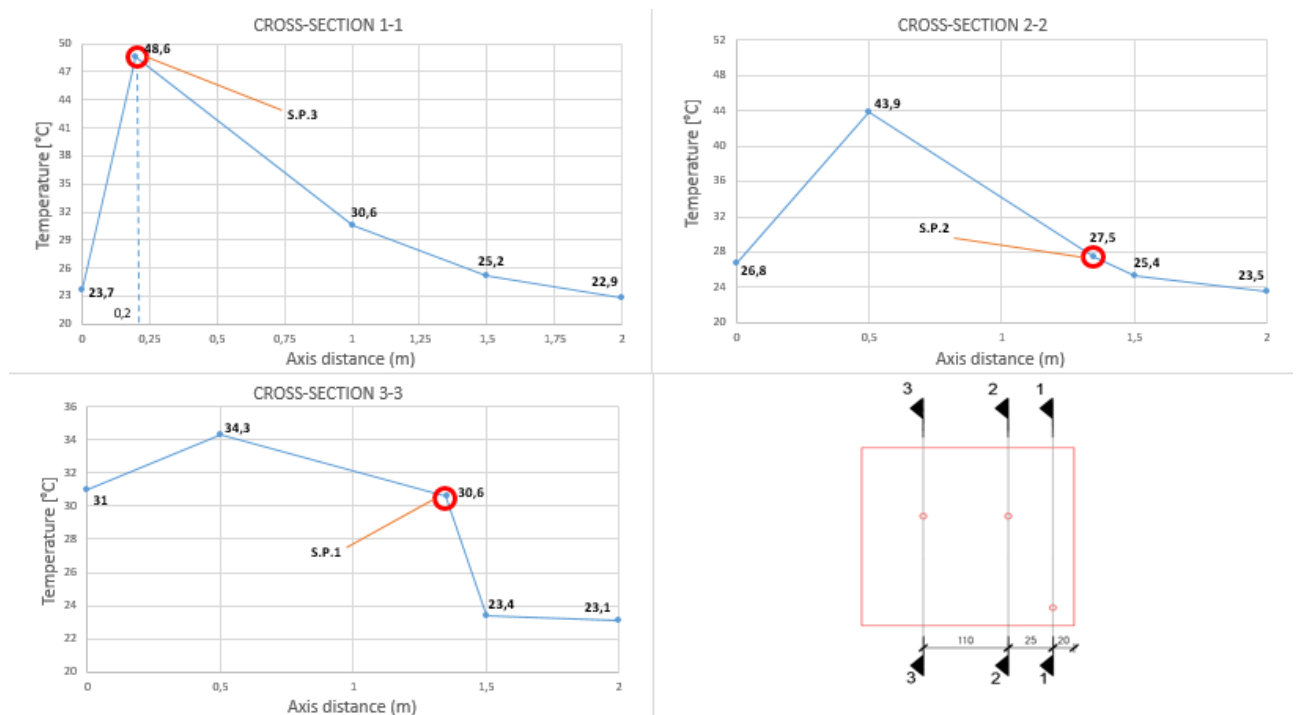*Figure 4.11 Temperature graph at each defined axial cross-section of the flooded surface*

Figure 4.12 Temperature graph at each defined ordinate cross-section of the flooded surface

4.2.4 Summary of results

Exper. order	Tracer discharge	Tracer mater.	Sinkhole position	Sinkhole filling	Detection	Detection time	Sinkhole temperature	Discharge
1	Q_m=0,025 L/s	Thermal	[single]	sand	yes	7,56min	29,6-31°C	0,0213L/s
2	Q_m=0,025 L/s	Thermal	[single]	gravel	yes	6,38min	30-30,8°C	0,0594L/s
3	Q_m=0,035 L/s	Thermal	[single]	sand	no		28,8-29,4°C	0,0126L/s
4	Q_m=0,035 L/s	Thermal	[single]	gravel	yes	2,29min	24-25,5°C	0,0715L/s
5	Q_m=0,025 L/s	Thermal	[L R]	sand	L-yes R-no	L=1,77min	L=26,5-27,2°C R=25,6-26,8°C	Q_L=0,024L/s Q_R=0,024L/s
6	Q_m=0,025 L/s	Thermal	[L R]	gravel	yes	L=2,21min R=3,04min	L=30,8-32°C R=22-23,2°C	Q_L=0,05L/s Q_R=0,028L/s
7	Q_m=0,025 L/s	Thermal	[L R]	L-sand R-gravel	yes	R=56sec	L=20-21°C R=25,5-27°C	Q_L=0,024L/s Q_R=0,08L/s
8	Q_m=0,035 L/s	Thermal	[L R]	sand	no		L=27,6-28,1°C R=26,1-27,2°C	Q_L=0,031L/s Q_R=0,028L/s
9	Q_m=0,035 L/s	Thermal	[L R]	gravel	yes	L=2,04min R=2,51min	L=27,4-28,8°C R=23,6-24,1°C	Q_L=0,04L/s Q_R=0,031L/s
10	Q_m=0,035 L/s	Thermal	[L R]	L-sand R-gravel	L-no R-yes	R=42sec	L=21,5-22,1°C R=23,4-24°C	Q_L=0,025L/s Q_R=0,032L/s
11	Q_m=0,025 L/s	Thermal	[L R B]	L-gravel R-gravel B-sand	L-yes R-yes B-yes	L=2,03min R=2,22min B=3,05min	L=29,4-30,1°C R=29,6-30°C B=23,8-24,6°C	Q_L=0,031L/s Q_R=0,027L/s Q_B=0,016L/s
12	Q_m=0,025 L/s	Thermal	[L R B]	gravel	L-yes R-yes B-yes	L=5,53min R=3,21min B=1,37in	L=27,9-28,6C R=25,2-26,5°C B=23,9-24,5°C	Q_L=0,025L/s Q_R=0,038L/s Q_B=0,040L/s
13	Q_m=0,025 L/s	Thermal	[L R B]	L-sand R-sand B-gravel	L-no R-yes B-yes	R=2,44min B=1,23min	L=21,3-22°C R=22,4-23,2°C B=24,6-25,6°C	Q_L=0,004L/s Q_R=0,012L/s Q_B=0,038L/s
14	Q_m=0,025 L/s	Thermal	[L R B]	sand	no		L=25,1-25,8°C R=27,2-27,9°C B=27,7-28,6°C	Q_L=0,002L/s Q_R=0,004L/s Q_B=0,006L/s
15	Q_m=0,035 L/s	Thermal	[L R B]	L-gravel R-gravel B-sand	L-yes R-yes B-no	L=1,21min R=1,21min	L=29,1-29,7°C R=29,4-30,4°C B=23,1-23,5°C	Q_L=0,024L/s Q_R=0,03L/s Q_B=0,011L/s
16	Q_m=0,035 L/s	Thermal	[L R B]	gravel	L-yes R-yes B-yes	L=6,25min R=2,06min B=1,1min	L=27,1-28,3°C R=24,8-25,7°C B=23,5-24,8°C	Q_L=0,023L/s Q_R=0,033L/s Q_B=0,042L/s
17	Q_m=0,035 L/s	Thermal	[L R B]	L-sand R-sand B-gravel	L-no R-yes B-yes	R=1,17min B=1,46min	L=21-22,5°C R=22,9-23,5°C B=23,8-25,2°C	Q_L=0,006L/s Q_R=0,016L/s Q_B=0,039L/s
18	Q_m=0,035 L/s	Thermal	[L R B]	sand	L-no R-no B-yes	B=15,05min	L=25,4-26,2°C R=28,6-30,4°C B=28,1-29,2°C	Q_L=0,003L/s Q_R=0,009L/s Q_B=0,007L/s

Table 4.1. Results of the analysis process of detecting the sinkhole through the use of a thermal tracer for all combinations of parameters

Table 4.1. presents all the key values of hydraulic tracing towards the sinkhole in a restricted spatially confined environment, gained from performing series of experiments, using variable parameters. Every column in *Table4.1.* refers to the geological, hydrological, thermal, and numerical parameters defining the conditions of each experimental trial which is numerically marked in each row. Apart from the parameters in *Table 4.1.* other important aspects that give insight into the behavior and processes in the experimental proceeding are: -topography – leading edge tracer velocity –flow direction –flow length –dispersion rate –thermal gradient[42,55]. Data measured manually or through a software program is placed in the last 4 columns of *Table 4.1.* The time of detection was registered at a point in time when the infrared image captured a specific event or change in the thermal pattern around the sinkhole, which varied from the constant movement. The temporal value of the detection is defined as a difference between the beginning of the recording of the infrared camera, which in some cases had a few seconds of delay in regards to the beginning of the experiment and the time of detection. Values of the sinkhole temperatures were defined as the maximum and minimum temperatures measured inside and following the diameter of the sinkhole, at the time when the initial temperature was registered. Discharge values in the last column of *Table 4.1* which account for the seepage volume from the sinkhole, were measured manually after the detection was registered. Not all of the experiments were carried out with the desired outcome, that saying, exactly for every set of experiments there was one for which the detection of the sinkhole wasn't registered. The detection process by itself was signified through an abrupt change in the continuity of movement or temperature(e.g. vortex creation, thermal regulation) around the sinkhole[99,101]. In *Table 4.1* there is a link between the first group of tests which were done with 1 sinkhole and the second group of tests performed with 2 sinkholes, in which both experimental sets were done with a higher tracer discharge Q_{D2}. Due to the low vacuum effect at the sinkhole position and the concentrated flow along the central axis of the flume, the sinkhole didn't invoke any response in regards to the thermal tracer flowing across or around its proximity, even after the dispersion of heat. In the case of the experiment with 3 sinkholes and a lower tracer discharge Q_{D1}, the thermal pattern didn't experience any major changes, with the leading edge of the thermal tracer only curving or going above the sinkholes. Due to the initial concentration of flow down the central axis, the process of dispersion is over time mostly focused laterally, with the region of high temperatures staying stagnant without no divergence, which allows for the detection of the sinkholes[97,98]. Looking at the data from *Table 4.1.* we can draw a relationship between the temperature of the sinkhole depending on the sinkhole material and the tracer discharge. Namely, this distinction is explained through *Figure 4.14.* , by which we can appoint 2 cases of study. In the case of the lower permeability(sand) and two tracer discharges, the higher Q_{D2} will produce higher temperature values at the sinkhole, than the lower discharge Q_{D1}. The reason for this is the extended flow length, due to the reflection of the thermal tracer of the downstream end of the flume or in the case of 1 sinkhole a more concentrated flow. This increases the efficiency of dispersion before and after the sinkhole and enables the intake of hot water on the route before and after the sinkhole due to the low vacuum(gravity+hydrostatic pressure) υL at that point[100]. Secondly, in the case of higher permeability and two tracer discharges, the lower Q_{D1} will produce higher temperature values at the sinkhole, than the higher Q_{D2}. The reason for this is the discontinuation of the flow length during the discharge Q_{D2} due to the higher vacuum υL at the sink point, which allows only a partial intake of hot water during the travel time of the tracer. While the discharge Q_{D1} maintains a continuous supply route towards the sink point.
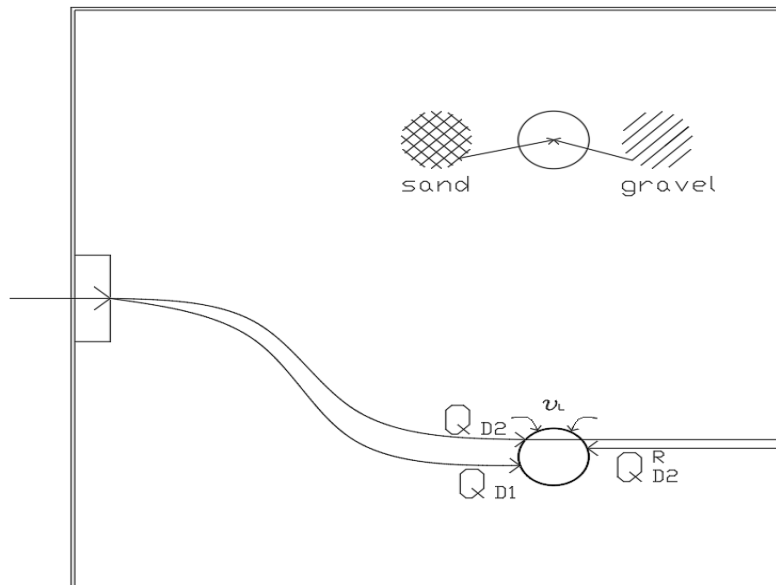
Figure 4.14. Demonstration of the tracer flow across the sinkhole under two different discharge rates and for two different sinkhole materials

The relation between the temperature at the sink point and the seepage discharge in *Table 4.1* is administered through the temperature difference at that point as well as the value of temperature. High values of temperatures, transfer more kinetic energy which advances the travel speed of water particles or momentum at the sink point[102]. This successive action contributes to the creation of a vortex at the sinkhole, under the Coriolis effect. As was already mentioned the temperature values at the sinkhole in *Table 4.1.* were included as a difference between the maximum and minimum values at that point. Hence, bigger differences in temperature contributed to higher drainage rates, due to the scale of the thermal gradient being increased which improves the thermal conductivity. Although these mentioned factors aren't the only ones affecting the discharge value at the sinkhole, they are important in influencing changes in flux around the sinkhole.

5. CONCLUSION

Water depletion scenarios are issues that have to be dealt with and mediated daily, especially in large water-holding sections such as retention basins, detention ponds, valley-dammed reservoirs, and agricultural lands. Therefore it is of crucial importance to understand the nature of water loss and allocate the place of potential leakage, seepage, and deep percolation. The problem of identifying areas of water loss is an ongoing issue in the scientific and engineering community that is increasingly gaining stride, through different methods, one of which is tracing using tracers. The involvement of this work in the problem at hand focuses on using thermal and dye tracing techniques to determine the sink point in large shallow reservoirs. To embody this real-life water-based system the area of testing was set up as a physical laboratory scale model. The aforementioned physical model consisted of a soil flume 2x2 m which was connected to a water supply system to simulate the shallow water flow through the solid surface. The objectives of the work were established around the qualitative and quantitative evaluation of the shallow water flow and thermal tracing through infrared thermography. Experiments were conducted in a sequence, where the goal of the first phase of experiments was to investigate the flooding of the soil surface. During the second phase of experiments, the goal was to examine and analyze the method of using a thermal tracer to detect the sinkhole. A significant and reliable figure of information was obtained by repeating the experiments in the case that the conditions weren't right or the images could not be processed properly. For the first phase of the experiment, the sandy loam soil of low permeability was used to match the surface of the large shallow reservoirs. Due to the topography of the surface, the discharge rate was adjusted to achieve laminar flow, which was necessary to enhance the clarity and precision of the recording. Under these conditions and considering the depth of the flume, positive results were achieved, that summarize the flow patterns, flooding time, and the velocity of the leading edge of water flow. Even though a double tracer was used to improve the efficiency of the experiment only the results of the thermal tracer were analyzed due to the low quality of recording of the dye tracer. Topographic features had a big influence on the movement of the water cover while the flooding was ongoing, and poin injections of the double tracer were used to determine the velocity vectors at each point on the flume surface. The results showed that in the early stages the water cover expanded mainly in the lateral direction with a simultaneous longitudinal expansion on the right side of the central axis. The value of the area and the wetting length of the water cover experienced a jump during the first two minutes and the middle of the experiment due to the uneven velocity at different points of the leading water edge. The fastest expansion of the water cover was registered on the left side of the central axis of the flume, due to the surface morphology on that part increasing the velocity to achieve concentrated flow. Sheet flow was mostly exhibited on the right side of the central axis before the sinkhole, as seen through the different values and directions of the velocity vectors at each point. One of the disadvantages of this experimental phase is the uneven expansion of the water cover which makes it difficult to inject the double tracer without compromising it through the connection of adjacent flows. In this case, it would be suggested to use a line outlet of water following the width of the

flume of 2 m, instead of the current central outlet which contributes to irregular flow patterns. For the second phase of the experiments, other different routes (colored, fluorescent, etc.) were considered, until the choice did not fall for the injection of thermal route, due to the existing infrared thermographic recording system. Each group of experiments was carried out on the basis of preliminary conditions defined by a combination of the default leakage rate, filling the sinkhole and the number of sinkholes. The results selected for the analysis are based on the opinion that the shown images clearly define changes in temperature and movement of the tracers that occur to the sinkhole. Each representative result for a certain number of sinkholes has given the opportunity to accurately describe the flow, the speed of dispersion, the thermal gradient and the flow length of the route. Experiments have produced more clearly or informative infrared images for the larger values of the flow and permeability of the sinkhole. Although this was not true for every experiment, because in the case of 2 sinkholes, and the greater flow of the tracer material, information that could be collected from thermal images were intricate, in the sense that many changes occurred at once. Many factors have influenced the movement of the thermal tracer, but to summarize them, it mainly depended on the flow rate and the level of dispersion. In the summary of the results, it was found that the earliest detection time was recorded in the case with 2 sinkholes. The reason for this was the increase in the speed of the leading edge of the tracer, influenced by the topographic features, the attraction forces towards the drainage cavity, the efficiency of the dispersion and the velocity of the route expression. The heat gradient was the most widespread in the case of lower permeability and lower drainage of the tracers with higher temperatures concentrated at a low distance from the outlet. For comparison, greater permeability, together with the higher flow of the traser leak, resulted in higher temperature values permeated along the length of the flow according to the point of permeability, but also with a limited thermal gradient over the surface of the square flume. The main reason for this was that the speed of dispersion, which was most successful for the lower flow of the tracer material along the route, due to the preservation of the volume (amount of heat) on the route in the event of a larger tracer leakage. The results for the flow of assessment from the sinkholes were quite relative given the number of sinkholes used for each experiment. In addition, comparisons can be made in each experimental group tested for 1 or more sinkholes or between groups. One of the most important features defined by these experiments is the dependence of the speed of depending on the temperature of the flow line to the sinkhole as well as the differences between temperature values at that point. In view of this in the analysis of the results, it can be observed that in certain cases, higher flow velocities of the tracer will not result in a higher rate of seepage discharge. In contrast to the smaller velocities of the tracer discharge, depending on the topographic characteristics and the distribution of heat, it will contribute to a higher rate of seepage discharge. Of course, other factors have influence like, the size of the grain in the drainage cavity, which limits the flow of water to a default value, depending on the maximum volume that can seep through it. In these cases, the higher velocity speed is not necessarily better because the velocity of hot water flows doesn't get drawn by the speed of suction of the sinkhole. The detecting technique, for determening the sinkpoint by using the thermal tracer, holds the advantage over other monitoring techniques (salt, fluorescent material and small density material), due to the clarity of

inspecting infrared shots as well as unlimited volume of thermal traser. However, due to the inexhaustible flow of thermal energy, the procedure itself can be very intrusative on the analysis, due to the chaotic nature, the spread of hot water. In addition, other drawbacks are that it does not allow at the same time to capture the real and infrared image, as well as the limited time of the performance of the procedure due to the constant balacing out of the environmental temperature. This could be facilitated by the use of more conservative tracers that allow for a larger spectrum of administration into the environment, as well as using physical tracers that are soluable in water, leaving a distinctive trace visible in the real scenario.

6. REFERENCES

1. Singh, V.P. Handbook of Applied Hydrology; McGraw-Hill Education: New York, NY, USA, 2017; 1440p.

2. Hamilton, S. (2014). hyter Loss. Water Intelligence Online, 13. doi:10.2166[CrossRef]

3. Water loss control, Julian Thornton Reinhard Sturm George Kunkel, P.E.(2008)

4. Kunkel Jr., G. A. (2016). M36 Water Audits and Loss Control Programs, Fourth Edition. doi:10.12999/awwa.m36ed4[CrossRef]

5.Hydrology and Floodplain Analysis: International Edition, 5th Edition, Philip B. Bedient; Wayne C. Huber; Baxter E. Vieux(2012)

6. Chow, V.T.; Maidment, D.R.; Mays, L.W. Applied Hydrology; McGraw-Hill: New York, NY, USA, 1988.

7. Leibundgut, C.; Maloszewski, P.; Külls, C. Tracers in Hydrology; Wiley-Blackwell: Hoboken, NJ, USA, 2009.

8. Khanna, M., & Malano, H. M. (2006). Modeling of basin irrigation systems: A review. Agricultural Water Management, 83(1-2), 87–99. doi:10.1016/j.agwat.2005.10.003[CrossRef]

9. Grigg, N. S. (2009). Total water management: leadership practices for a sustainable future. Water International, 34(2), 290–293. doi:10.1080/02508060902937512[CrossRef]

10. Abernethy, C. L. (2005). Financing river basin organizations. Irrigation and River Basin Management: Options for Governance and Institutions, 75–92. doi:10.1079/9780851996721.0075[CrossRef]

11. Irrigation and Water Resources Engineering, G.L.Asawa (2006)

12. Ward, F. A., & Pulido-Velazquez, M. (2008). Water conservation in irrigation can increase water use. Proceedings of the National Academy of Sciences, 105(47), 18215–18220. doi:10.1073/pnas.0805554105[CrossRef]

13. Yekti, M. I. (n.d.). Role of reservoir operation in sustainable water supply to Subak irrigation schemes in Yeh Ho River Basin. doi:10.18174/404538[CrossRef]

14. Huffman, R., Fangmeier, D., Elliot, W., & Workman, S. (2013). Soil and Water Conservation Engineering Seventh Edition. doi:10.13031/swce.2013[CrossRef]

15. Daus, M., Koberger, K., Koca, K., Beckers, F., Encinas Fernández, J., Weisbrod, B., … Wieprecht, S. (2021). Interdisciplinary Reservoir Management—A Tool for Sustainable Water Resources Management. Sustainability, 13(8), 4498. doi:10.3390/su13084498[CrossRef]

16. Finley, S. (Ed.). (2016). Sustainable water management in smallholder farming: theory and practice. doi:10.1079/9781780646862.0000[CrossRef]

17. Younos, T., & Parece, T. E. (Eds.). (2016). Sustainable Water Management in Urban Environments. The Handbook of Environmental Chemistry. doi:10.1007/978-3-319-29337-0[CrossRef]

18. Sustainable management of reservoirs and preservation of water quality, Şahnaz Tiğrek1, Özge Göbelez, and Tuce Aras (2009)

19. Votruba, L., & Broža, V. (1989). Preface- Water Management in Reservoirs, 7–8. doi:10.1016/s0167-5648(08)70627-0[CrossRef]

20. Steven C. Chapra, 1996, Surface water quality modeling, p.156

21. Shallow Water Hydrodynamics - Mathematical Theory and Numerical Solution for a Two-dimensional System of Shallow Water Equations. (1992). Elsevier Oceanography Series. doi:10.1016/s0422-9894(08)x7007-2[CrossRef]

22. Compensating for Wetland Losses Under the Clean Water Act. (2001). doi:10.17226/10134 [CrossRef]

23. Plate section. (2008). Earth Surface Processes, Landforms and Sediment Deposits. Bridge, John; Demicco, Robert ;doi:10.1017/cbo9780511805516.024 [CrossRef]

24. Fluid mechanics: fundamentals and applications / Yunus A. Çengel, John M. Cimbala(2004)

25. Free-Surface Flow, Environmental Fluid Mechanics, by Nikolaos D. Katopodes(2018)

26. Free-Surface Flow: Shallow water dynamics, Nikolaos D. Katopodes (2018)

27. P. Rowiński and A. Marion (eds.), Hydrodynamic and Mass Transport at Freshwater Aquatic Interfaces, GeoPlanet: Earth and Planetary Sciences(2018), doi:10.1007/978-3-319-27750-9 [CrossRef]

28. Azab, A. M. (2012). Integrating GIS, Remote Sensing, and Mathematical Modelling for Surface Water Quality Management in Irrigated Watersheds. doi:10.1201/9780367807191[CrossRef]

29. Physical and Chemical Processes of Water and Solute Transport/Retention in Soils, Volume 56; Hussein Magd Eldin Selim, Donald L. Sparks (2001)

30. Rainfall-Runoff Processes;David G. Tarboton(2003) https://hydrology.usu.edu/rrp/

31. Pozrikidis,, C., & Gartling,, D. (2002). Fluid Dynamics: Theory, Computation, and Numerical Simulation. Applied Mechanics Reviews, 55(3), B55–B55. doi:10.1115/1.1470683

32. A Practical Approach to Water Conservation for Commercial and Industrial Facilities. (2006). doi:10.1016/b978-1-85617-489-3.x5001-2 [CrossRef] .

33. Gomi, T., Sidle, R. C., Miyata, S., Kosugi, K., & Onda, Y. (2008). Dynamic runoff connectivity of overland flow on steep forested hillslopes: Scale effects and runoff transfer. Water Resources Research, 44(8). doi:10.1029/2007wr005894

34. Jain, M. K., Kothyari, U. C., & Ranga Raju, K. G. (2004). A GIS based distributed rainfall–runoff model. Journal of Hydrology, 299(1-2), 107–135. doi:10.1016/j.jhydrol.2004.04.024

35. Mujtaba, B.; de Lima, J.L.M.P. Laboratory testing of a new thermal tracer for infrared-based PTV technique for shallow overland flows. Catena 2018, 169, 69–79. [CrossRef]

36. Jodeau, M.; Hauet, A.; Paquier, A.; Le Coz, J.; Dramais, G. Application and evaluation of LS-PIV technique for the monitoring of river surface velocities in high flow conditions. Flow Meas. Instrum. 2008, 19, 117–127. [CrossRef]

37. Abrantes, J.; Moruzzi, R.; Silveira, A.; de Lima, J.L. Comparison of thermal, salt and dye tracing to estimate shallow flow velocities: Novel triple-tracer approach. J. Hydrol. 2018, 557, 362–377. [CrossRef]

38. Zhang, G.-H.; Luo, R.-T.; Cao, Y.; Shen, R.-C.; Zhang, X. Correction factor to dye-measured flow velocity under varying water and sediment discharges. J. Hydrol. 2010, 389, 205–213. [CrossRef]

39. Tauro, F.; Grimaldi, S.; Petroselli, A.; Rulli, M.C.; Porfiri, M. Fluorescent particle tracers in surface hydrology: A proof of concept in a semi-natural hillslope. Hydrol. Earth Syst. Sci. 2012, 16, 2973–2983. [CrossRef]

40. Tauro, F.; Pagano, C.; Porfiri, M.; Grimaldi, S. Tracing of shallow water flows through buoyant fluorescent particles. Flow Meas. Instrum. 2012, 26, 93–101. [CrossRef]

41. Lei, T.; Chuo, R.; Zhao, J.; Shi, X.; Liu, L. An improved method for shallow water flow velocity measurement with practical electrolyte inputs. J. Hydrol. 2010, 390, 45–56. [CrossRef]

42. Schuetz, T.; Weiler, M.; Lange, J.; Stoelzle, M. Two-dimensional assessment of solute transport in shallow waters with thermal imaging and heated water. Adv. Water Resour. 2012, 43, 67–75. [CrossRef]

43. Zhou, J.; Liu, G.; Meng, Y.; Xia, C.; Chen, K.; Chen, Y. Using stable isotopes as tracer to investigate hydrological condition and estimate water residence time in a plain region, Chengdu, China. Sci. Rep. 2021, 11, 2812. [CrossRef] [PubMed] Agronomy 2021, 11, 1444 15 of 15

44. de Lima, R.L.; Abrantes, J.R.; de Lima, J.L.; de Lima, M.I.P. Using thermal tracers to estimate flow velocities of shallow flows: Laboratory and field experiments. J. Hydrol. Hydromech. 2015, 63, 255–262. [CrossRef]

45. Abrantes, J.R.; Moruzzi, R.B.; de Lima, J.L.; Silveira, A.; Montenegro, A.A. Combining a thermal tracer with a transport model to estimate shallow flow velocities. Phys. Chem. Earth

Parts A B C 2019, 109, 59–69. [CrossRef]

46. Abrantes, J.R.C.B.; de Lima, J.L.M.P.; Montenegro, A.A.A. Performance of kinematic modelling of surface runoff for intermittent rainfall on soils covered with mulch. Rev. Bras. Eng. Agrícola E Ambient. 2015, 19, 166–172. [CrossRef]

47. De Lima, J. L. M. P., Zehsaz, S., de Lima, M. I. P., Isidoro, J. M. G. P., Jorge, R. G., & Martins, R. (2021). Using Quinine as a Fluorescent Tracer to Estimate Overland Flow Velocities on Bare Soil: Proof of Concept under Controlled Laboratory Conditions. Agronomy, 11(7), 1444.

48. de Lima, J.L.M.P.; Isidoro, J.M.G.P.; de Lima, M.I.P.; Singh, V.P. Longitudinal Hillslope Shape Effects on Runoff and Sediment Loss: Laboratory Flume Experiments. J. Environ. Eng. 2018, 144, 04017097. [CrossRef]

49. Popova, Z., & Kuncheva, R. (1996). Modeling in Water Losses Evaluation for Nonhomogeneous Furrow Set. Journal of Irrigation and Drainage Engineering, 122(1), 1–6. doi:10.1061/(asce)0733-9437(1996)122:1(1)

50. Wöhling, T., Singh, R., & Schmitz, G. H. (2004). Physically Based Modeling of Interacting Surface–Subsurface Flow During Furrow Irrigation Advance. Journal of Irrigation and Drainage Engineering, 130(5), 349–356. doi:10.1061/(asce)0733-9437(2004)130:5(349) [CrossRef]

51. Li, G.; Abrahams, A.D.; Atkinson, J.F. Correction factors in the determination of mean velocity of overland flow. Earth Surf. Process. Landf. 1996, 21, 509–515. [CrossRef]

52. Dunkerley, D. Estimating the mean speed of laminar overland flow using dye injection-uncertainty on rough surfaces. Earth Surf. Process. Landf. 2001, 26, 363–374. [CrossRef]

53. Th. van Genuchten, M., & Leij, F. (2001). Solute Transport. Soil Physics Companion, 189–248. doi:10.1201/9781420041651.ch6 [CrossRef]

54. Appels, W. M., Bogaart, P. W., & van der Zee, S. E. A. T. M. (2017). Feedbacks Between Shallow Groundwater Dynamics and Surface Topography on Runoff Generation in Flat Fields. Water Resources Research, 53(12), 10336–10353. doi:10.1002/2017wr020727[CrossRef]

55 Jirka, G. H. (2001). Large scale flow structures and mixing processes in shallow flows. Journal of Hydraulic Research, 39(6), 567–573. doi:10.1080/00221686.2001.9628285[CrossRef]

56. Fang, X., Thompson, D. B., Cleveland, T. G., & Pradhan, P. (2007). Variations of Time of Concentration Estimates Using NRCS Velocity Method. Journal of Irrigation and Drainage Engineering, 133(4), 314–322. doi:10.1061/(asce)0733-9437(2007)133:4(314) [CrossRef]

57. https://vdocument.in/embed/v1/table-of-contents-institute-for-t-chapter-2-stormwater-section-2a-1-general.html ;NRCS Velocity method;Design Manual

58. Overland flow;T.S. Steenhuis, ... M.T. Walter, in Encyclopedia of Soils in the Environment, 2005

59. Kampf, S. K., & Mirus, B. B. (2013). 9.3 Subsurface and Surface Flow Leading to Channel Initiation. Treatise on Geomorphology, 22–42. doi:10.1016/b978-0-12-374739-6.00228-1[CrossRef]

60. Using artificial tracers to study water losses of ephemeral floods in small arid streams; Jens Lange, Chris Leibundgut, Tamir Grodek, Judith Lekach(1998)

61. Dabiri, D., & Pecora, C. (2019). Particle tracking techniques. Particle Tracking Velocimetry. doi:10.1088/978-0-7503-2203-4ch5[CrossRef]

62. Vienken, T., Huber, E., Kreck, M., Huggenberger, P., & Dietrich, P. (2017). How to chase a tracer – combining conventional salt tracer testing and direct push electrical conductivity profiling for enhanced aquifer characterization. Advances in Water Resources, 99, 60–66. doi:10.1016/j.advwatres.2016.11.010[CrossRef]

63. Lam, M. Y., Ghidaoui, M. S., & Kolyshkin, A. A. (2019). Hydraulics of shallow shear flows: onset, development and practical relevance. Environmental Fluid Mechanics, 19(5),

1121–1142. doi:10.1007/s10652-019-09682-0[CrossRef]

64. Tauro, F., Aureli, M., Porfiri, M., & Grimaldi, S. (2010). Characterization of Buoyant Fluorescent Particles for Field Observations of Water Flows. Sensors, 10(12), 11512–11529. doi:10.3390/s101211512[CrossRef]

65.Slug injections using salt in Solution,Moore, R.D. (2004)

66. Lick, W. (2008). Sediment and Contaminant Transport in Surface Waters. doi:10.1201/9781420059885[CrossRef]

67. Soil wettability and wetting agents . . . our current knowledge of the problem, Leonard F. DeBano, Joseph F. Osborn. Jay S. Krammes, John Letey(1967)

68. Persson, M., Haridy, S., Olsson, J., & Wendt, J. (2005). Solute Transport Dynamics by High-Resolution Dye Tracer Experiments-Image Analysis and Time Moments. Vadose Zone Journal, 4(3), 856–865. doi:10.2136/vzj2004.0129[CrossRef]

69. Hydraulic Structures, Sheng-Hong Chen(2009)

70. Zeleňáková, M., Diaconu, D. C., & Haarstad, K. (2017). Urban Water Retention Measures. Procedia Engineering, 190, 419–426. doi:10.1016/j.proeng.2017.05.358

71. Characterization of Biochar and Its Effects on the Water Holding Capacity of Loamy Sand Soil: Comparison of Hemlock Biochar and Switchblade Grass Biochar Characteristics O.-Y. Yu, M. Harper, M. Hoepfl, D. Domermuth(2017)

72. Effect of Surface Morphology on the Ordered Water Layer at Room Temperature,Chunlei Wang, Bo Zhou, Peng Xiu, and Haiping Fang;The Journal of Physical Chemistry C 2011 115 (7), 3018-3024,DOI: 10.1021/jp108595d

73. Yang, Z. (2018). Quantitative Assessment of Groundwater and Surface Water Interactions in the Hailiutu River Basin, Erdos Plateau, China. doi:10.1201/9780429487385

74. https://chem.libretexts.org/@go/page/351246?pdf

75. Th. van Genuchten, M., & Leij, F. (2001). Solute Transport. Soil Physics Companion, 189–248. doi:10.1201/9781420041651.ch6

76. Field, M. S. (2010). Simulating Drainage from a Flooded Sinkhole. Acta Carsologica, 39(2). doi:10.3986/ac.v39i2.105

77. De Lima, J. L. M. P., Abrantes, J. R. C. B., Silva, V. P., & Montenegro, A. A. A. (2014). Prediction of skin surface soil permeability by infrared thermography: a soil flume experiment. Quantitative InfraRed Thermography Journal, 11(2), 161–169. doi:10.1080/17686733.2014.945325

78. Luxmoore, R. J., & Sharma, M. L. (1980). Runoff responses to soil heterogeneity: Experimental and simulation comparisons for two contrasting watersheds. Water Resources Research, 16(4), 675–684. doi:10.1029/wr016i004p00675

79. Shingubara, S., & Kawakubo, T. (1984). Formation of Vortices around a Sinkhole. Journal of the Physical Society of Japan, 53(3), 1026–1030. doi:10.1143/jpsj.53.1026

80. Rau, G.C. et al., 2014. Heat as a tracer to quantify water flow in near-surface sediments. Earth-Science Reviews, 129, pp.40–58. Available at: http://dx.doi.org/10.1016/j.earscirev.2013.10.015.

81.Bai, M., Xu, D., Zhang, S., & Li, Y. (2013). Spatial–temporal distribution characteristics of water-nitrogen and performance evaluation for basin irrigation with conventional fertilization and fertigation methods. Agricultural Water Management, 126, 75–84. doi:10.1016/j.agwat.2013.05.006

82. Recking, A., Piton, G., Montabonnet, L., Posi, S., & Evette, A. (2019). Design of fascines for riverbank protection in alpine rivers: Insight from flume experiments. Ecological Engineering, 138, 323–333. doi:10.1016/j.ecoleng.2019.07.019

83. Lewis, T. J., & Beck, A. E. (1977). Analysis of heat-flow data — detailed observations in many holes in a small area. Tectonophysics, 41(1-3), 41–59. doi:10.1016/0040-1951(77)90179-2

84. Mayor, Á. G., Bautista, S., Small, E. E., Dixon, M., & Bellot, J. (2008). Measurement of the connectivity of runoff source areas as determined by vegetation pattern and topography: A tool for assessing potential water and soil losses in drylands. Water Resources Research, 44(10). doi:10.1029/2007wr006367

85. Palanisamy, B. & Workman, S.R., 2015. Hydrologic Modeling of Flow through Sinkholes Located in Streambeds of Cane Run Stream, Kentucky. Journal of Hydrologic Engineering, 20(5). Available at: http://dx.doi.org/10.1061/(asce)he.1943-5584.0001060.

86. Minkina, W., & Dudzik, S. (2009). Infrared Thermography. doi:10.1002/9780470682234

87. Águas de Coimbra. Quality Control of Water Intended for Human Consumption Micippality of Coimbra-Boavista Supply Area—1st Semester 2020; Technical Report; Águas de Coimbra, Coimbra, Portugal, (2020)

88. de Lima J.L.M.P., Abrantes, J.R.C.B. (2014). Using a thermal tracer to estimate overland and rill flow velocities. Earth Surface Processes and Landforms volume 39 issue 10 on pages 1293 to 1300

89. Appels W. M., Bogaart P. W., & van der Zee S. E. A. T. M. (2017). Feedbacks Between Shallow Groundwater Dynamics and Surface Topography on Runoff Generation in Flat Fields. Water Resources Research volume 53 issue 12 on pages 10336 to 10353

90. Gang L., Abrahams A.D., Atkinson J.F., (1996). Correction factors in the determination of the mean velocity of overland flow. Earth Surface Processes and Landforms, volume 21 issue 6 on pages 509 to 515

91. John R. Davis. (1961). Estimating Rate of Advance for Irrigation Furrows. Transactions of the ASAE, 4(1), 0052–0054. doi:10.13031/2013.41007

92. Maheshwari, B. L., & McMahon, T. A. (1992). Modeling Shallow Overland Flow in Surface Irrigation. Journal of Irrigation and Drainage Engineering, 118(2), 201–217. doi:10.1061/(asce)0733-9437(1992)118:2(201)

93. Hillel, D. (1982). Advances in Irrigation-De Lima, J. L. M. P., Zehsaz, S., de Lima, M. I. P., Isidoro, J. M. G. P., Jorge, R. G., & Martins, R. (2021). Using Quinine as a Fluorescent Tracer to Estimate Overland Flow Velocities on Bare Soil: Proof of Concept under Controlled Laboratory Conditions. Agronomy, 11(7), 1444.

94. Vynnycky, M., & Maeno, N. (2012). Axisymmetric natural convection-driven evaporation of hot water and the Mpemba effect. International Journal of Heat and Mass Transfer

95. Pfister, L., McDonnell, J. J., Hissler, C., & Hoffmann, L. (2010). Ground-based thermal imagery as a simple, practical tool for mapping saturated area connectivity and dynamics. Hydrological Processes, 24(21), 3123–3132. https://doi.org/10.1002/hyp.7840

96. Dunckel, A. E., Cardenas, M. B., Sawyer, A. H., & Bennett, P. C. (2009). High-resolution in-situ thermal imaging of microbial mats at El Tatio Geyser, Chile shows coupling between community color and temperature. Geophysical Research Letters, 36(23). https://doi.org/10.1029/2009gl041366

97. Schuetz, T., & Weiler, M. (2011). Quantification of localized groundwater inflow into streams using ground-based infrared thermography. Geophysical Research Letters, 38(3), n/a-n/a. https://doi.org/10.1029/2010gl046198

98. Liang, D., Chen, J. M., Chong, K. J. Y., & McCorkell, C. (2012). Thermal imaging study of temperature fields in shallow flows. Measurement, 45(5), 1015–1022. https://doi.org/10.1016/j.measurement.2012.01.042

99. Pozrikidis, C. (2009). Fluid Dynamics. https://doi.org/10.1007/978-0-387-95871-2

100. Field, M. S. (2010). Simulating Drainage from a Flooded Sinkhole. Acta Carsologica, https://doi.org/10.3986/ac.v39i2.105

101. Shingubara, S., & Kawakubo, T. (1984). Formation of Vortices around a Sinkhole. Journal

of the Physical Society of Japan, 53(3), 1026–1030. https://doi.org/10.1143/jpsj.53.1026

102. Wu, X., Guo, Q., Cai, M., Zhu, Y., Zhang, J., & Dong, Z. (2020). Study on the influence of fracture flow on the temperature field of rock mass with high temperature. Case Studies in Thermal Engineering, 22, 100755. https://doi.org/10.1016/j.csite.2020.100755

103. Lewis, T. J., & Beck, A. E. (1977). Analysis of heat-flow data — detailed observations in many holes in a small area. Tectonophysics, 41(1–3), 41–59. https://doi.org/10.1016/0040-1951(77)90179-2